INTERPRETATION OF ARRAY PRODUCTION LOGGING MEASUREMENTS IN HORIZONTAL WELLS FOR FLOW PROFILE

A Thesis

by

LULU LIAO

Submitted to the Office of Graduate and Professional Studies of
Texas A&M University
in partial fulfillment of the requirements for the degree of

MASTER OF SCIENCE

Chair of Committee,	Ding Zhu
Committee Members,	A. Daniel Hill
	Yuefeng Sun
Head of Department,	A. Daniel Hill

December 2013

Major Subject: Petroleum Engineering

ABSTRACT

Interpretation of production logging in multi-phase flow wells is challenging, especially for highly deviated wells or horizontal wells. Flow regime-dependent flow conditions strongly affect the measurements of production logging tools. Segregation and possible back flow of denser phases result in misinterpretation of the inflow distribution. To assess the downhole flow conditions more accurately, logging tools have been developed to overcome the flow regime related issues. Multiple-sensor array tools measure the fluid properties at multiple locations around the cross-sectional area of the wellbore, providing a distributed measurement array that helps to relate the measurements to flow regime and translate the measurement to inflow distribution. This thesis present a methodology for using array data from production logging tools to interpret downhole flow conditions. The study uses an example logging tool that consists of 12 resistivity, 12 capacitance probes, and six spinners around the wellbore circumference. The method allows interpretation of phase volumetric flow rates in sub-divided cross-sectional areas based on sensor locations. The sub-divided area method divides the wellbore cross-sectional area into several layers depending on the number and arrangement of the sensors with each layer containing at least one sensor. Holdup

and velocity outputs from sensors in each wellbore area segment are combined to calculate the volumetric flow rates of each phase in each segment. These results yield a profile of flow of each phase from the high side to the low side of the wellbore, and the overall flow rates of each phase at every location along the well where the interpretation method is applied.

The results from different methods of interpreting production logging are compared in the thesis. Three Eagle Ford horizontal well examples are presented in the thesis; one has single sensor PLT measures, and the other two cases used a multiple sensor tool package. The examples illustrate differences of interpretation results by different methods, and recommend the procedures that yield better interpretation of multiple sensor array tools.

DEDICATION

To my parents and grandmother

ACKNOWLEDGEMENTS

I would like to thank my committee chair, Dr. Ding Zhu, and my committee members, Dr. Hill and Dr. Sun, for their guidance and support throughout this research. Thanks also to my dear friends Ouyang, Jingyuan and so on who make my life full of fun and make me brave to face difficulty in the past two years at Texas A&M University. I will always remember the days together with them.

Special thanks to my parents for their support and encouragement, I love them always.

Thanks to CSSA, who gives me a chance to develop myself in after-school jobs.

I appreciate all the schoolmates around me, which made me more mature and confident.

The places I have always been are important in my life. The Richardson Building of the Harold Vance Department of Petroleum Engineering, Office #714, is my working place. Plantation Oks apartment is my living place. I like all the places such as Student Recreational Center, Reed Building basketball court, Bryan Lake, Mug Walls, Azure, Cinemark, Road House, HEB and Chef Cao's.

Additionally, I would like to acknowledge the financial support from Shell Oil Co. as well as the facility support of the Harold Vance Department of Petroleum Engineering.

NOMENCLATURE

A_i Cross-section area of the wellbore, where i=1 to 5 denotes each segment, ft^2

A_j Cross-section area of all segments occupied by phase j, (gas, oil or water), ft^2

A_T Total cross-section area of pipe, ft^2

B_j Formation volume factor for phase j, (gas, oil or water)

b_d Constants that contain the threshold velocity to down run.

b_u Constants that contain the threshold velocity to up run.

d Casing ID, ft

f Spinner response, rps

f_d Spinner response for down run, rps

f_j Spinner responses, where j denotes the phase (gas, oil or water), rps

f_g Spinner response of gas section, rps

f_s Spinner response in static fluid, rps

f_u Spinner response for up run, rps

f_w Spinner response of water section, rps

$f_d^{'}$ Shifted down response, rps

$\overline{f_j}$ Average spinner response, where j denotes the phase (gas, oil or water), rps

$\overline{f_g}$ Average spinner response of gas section, rps

$\overline{f_w}$ Average spinner response of water section, rps

f_{100} Spinner response above all perforations, rps

Δf Difference between the up and the shifted down response, rps

h Vertical thickness of cross-section area, ft

m_j Conversion coefficient, where j denotes the phase (gas, oil or water), $\frac{ft}{\min}/rps$

m_n Spinner response slope for positive response, $\frac{ft}{\min}/rps$

m_g Conversion coefficient of gas, $\frac{ft}{\min}/rps$

m_p Spinner response slope for negative response, $\frac{ft}{\min}/rps$

m_w Conversion coefficient of water, $\frac{ft}{\min}/rps$

$q_{dh,j}$ Downhole volumetric flow rate, where j denotes the phase, $ft^3/\min$

q_i Phase flow rate, where I denotes the segment, $ft^3/\min$

q_j Total rate of each phase, where j denotes the phase (gas, oil or water), $ft^3/\min$

$q_{j,i}$ Total flow rate, $ft^3/\min$

r Casing radius, ft

v_e Effective velocity, $ft/\min$

v_f Fluid velocity, $ft/\min$

v_i Flow velocity, where i denotes the segment, $ft/\min$

v_j Flow velocity, where j denotes the phase, $ft/\min$

v_g Gas velocity, $ft / \min$

v_w Water velocity, $ft / \min$

v_t Threshold velocity, $ft / \min$

v_T Spinner tool velocity or cable speed, $ft / \min$

v_{Tu} Tool velocity for up run, $ft / \min$

v_{Td} Tool velocity for down run, $ft / \min$

$\overline{v_i}$ Average flow velocity, where i denotes the segment, $ft / \min$

$\overline{v_j}$ Average flow velocity, where j denotes the phase, $ft / \min$

$\overline{v_g}$ Average gas velocity, $ft / \min$

$\overline{v_w}$ Average water velocity, $ft / \min$

v_{100} Velocity above all perforations, $ft / \min$

$y_{j,i}$ Phase holdups, where i denotes the segment and j denotes the phase

TABLE OF CONTENTS

Page

LIST OF FIGURES

Page

Page

LIST OF TABLES

Page

1. INTRODUCTION

1.1 Problem Statement

Using production logging to determine the flow of oil, gas, and water phases is fundamental to understand production problems and to design remedial workovers.

But in highly deviated wells conventional production logging tools deliver less-than-optimal results because they were developed for vertical or near vertical wells. Downhole flow regimes in deviated boreholes can be complex and can include stratification, misting, and recirculation. Segregation, small changes in well inclination, and the flow regime influence the flow profile. Logging problems typically occur when conventional tools run in deviated wells encounter top-side bubbly flow, heavy phase recirculation, or stratified layers traveling at different speeds. Flow loop studies have also revealed the ineffectiveness of conventional logging tools in multiphase flows. Center measurements made by such tools are inadequate for describing complex flow because the most important information is located along the vertical diameter of the wellbore. Conventional tools have sensors spread out over long distances in the wellbore, making measurement of complex flow regimes even more difficult.

In order to better characterize the non-uniform phase distributions and velocity profiles that occur with multiple phases flowing in nominally horizontal wells, production logging tools have been developed that deploy arrays of sensors to sample flow properties at multiple locations in the well cross-section. The sensors used include small spinner flowmeters, to measure local velocities and capacitance, resistivity, and

optical reflectance probes to measure phase holdups. By combining these array measurements, it is possible to roughly map the distribution of phase flow rates as a function of position along the wellbore. Methodologies and models used in conventional logging interpretation cannot be used directly in the modern array tools because they are based on single-sensor tools. Developing new models and methodologies is essential for these new tools to be valuable.

1.2 Background and Literature Review

In the history of production logging, the temperature surveys to locate fluid entries in a wellbore, was first developed by Schlumberger et al. (1937). Early workers in fields found that the cooling of gas as it expands caused low temperature anomalies that indicated the entries of gas. Cool fluids also for injection wells were indications of permeable zones that remained after shut-in Millikan (1941). In the following years, Dale (1949) discussed the bottom hole flow surveys for determination of fluid and gas movements in wells. In Riordan (1951)'s work, the pressure was added to temperature production logging surveys to obtain more useful information about wellbore conditions. The types of fluid in the well could be identified by measuring the pressure gradient in the wells. By the mid-1960's other production logging tools had been developed to obtain further information about well conditions, particularly in multiple phase flow. Acoustic wave and capacitance technologies were applied in multiple phase flow (Riddle 1962).

As horizontal wells become increasingly common, the need to make measurements to optimise well health and manage the reservoir also increases. The development of the multiple array production suite (MAPS) started with the first capacitance array tool (CAT) in 1999 which consists 12 probes around the wellbore circumference to measure the phase holdup at different location. The resistance array tool (RAT) and spinner array tool (SAT) were then developed and tested for mechanical configuration of the CAT. Similar with CAT, resistance array tool has 12 probes and can be used to measure water holdup. spinner array tool only consist 6 small diameter sensors which help us to obtain an unimpeded view of the flow.

As new production logging tools became available, interpretation methods evolved for the more complex flow conditions being encountered.

Curtis (1967) present an approach applying in multiple-phase flow from vertical wells, in this approach the spinner flowmeter are calibrated based on the surface flow rate translated to the condition of downhole temperature and pressure.

Hill (1990) advanced a theory of the effective velocity and introduced three methods of spinner flowmeter interpretation, including single-pass method, two-pass method, and multi-pass method, respectively, which are important to the development of further models in multiphase flow at horizontal well.

The spinner flowmeter is an impeller that is place in the well to measure fluid velocity in the same manner that a turbine meter measures flow rate in the wellbore. Like a turbine meter, the force of the moving fluid causes the spinner to rotate. The rotational velocity of the spinner is assumed linearly proportional to fluid velocity, and

electronic means are incorporated into the tool to monitor rotational velocity and sometimes direction. A significant difference between a spinner flowmeter and a turbine meter is that the spinner impeller doesn't span the entire cross section of flow whereas the turbine meter impeller dose, with a small clearance between the impeller and pipe wall.

1.3 Full Bore Flowmeter Tool

The full bore flowmeter is a rotating-vane type velocity meter. As seen in **Fig. 1.1**, the vanes are maintained in a collapsed position within a protective centralized cage for passage through production pipe (Leach et al.,1974). They open up to the "full bore" configuration.

When running a spinner flowmeter log, we should decide whether the well conditions are such that a useful log can be expected. It is required that the well is flowing at a constant flow rate with sufficient flow rate, and good physical condition, and there should not be sand production (Hill, 1990). The interpretation fundamentals are summarized.

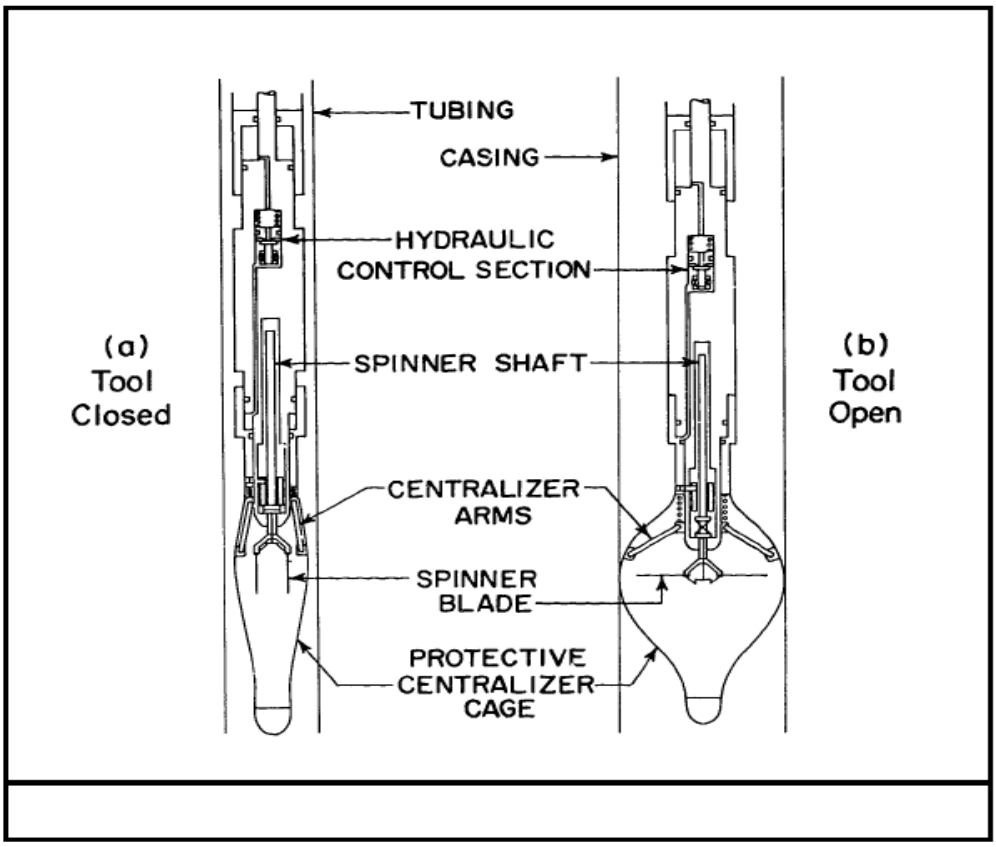

Fig. 1.1—Full bore flowmeter of Leach et al. (1974)

1.3.1 Single pass method

Single- pass interpretation is the simplest but least reliable method of spinner interpretation which uses a single logging run and is based on a linear spinner response to total flow rate. With this method, the highest spinner response (above all perforations) is as-signed 100% in-flow and the lowest spinner response is assumed to be in static fluid and thus is assigned 0% in-flow. At any point in between, the in-flow rate is assumed proportional to spinner response, as

$$v_f = v_{100}\left(\frac{f - f_s}{f_{100} - f_s}\right) \tag{1.1}$$

Thus, the fraction of total flow can be quickly calculated throughout the well.

1.3.2 Two-pass method

Another spinner flowmeter log interpreted technique developed by Peebler (1982) applying in fullbore flowmetr is the two-pass method. As its name implies, this method uses two logging runs, one up pass and one down pass, which are superimposed in a segment of zero fluid velocity (static column) to illustrate the flow profile. At the same cable speed, the two passes should overlie each other in no-flow segment if m_p and m_n are equal. Spinner should rotate in opposite directions throughout the well during the two runs when applying this method. We could obtain the equations for the spinner flowmeter response to the up and down runs as

$$f_u = m_p(v_f + v_{Tu}) + b_u \tag{1.2}$$

and

$$f_d = m_n(v_f + v_{Td}) + b_d \tag{1.3}$$

where f_u and f_d are spinner frequency responses to up and down runs, respectively, b_u and b_d are constants that contain the threshold velocity, v_{Tu} and v_{Td} are tool velocities for up and down runs.

The shifted down response is shown

$$f'_d = m_p v_{Tu} - m_n v_f + b_u \tag{1.4}$$

and fluid velocity is

$$v_f = \frac{\Delta f}{m_p + m_n} \tag{1.5}$$

where $\Delta f = f_u - f'_d$ is the difference between the up and the shifted down response.

1.3.3 Multi-pass method

The multi-pass or in-situ calibration method is the most accurate technique of spinner-flowmeter evaluation because the spinner response characteristics are determined under in-situ conditions (Peebler, 1982). As the name implies, multiple passes in a well at different tool speeds and directions are needed when applying the method. Stable well conditions must exist during all the logging passes for the multi-pass method to be applied.

Plot the spinner response (res/sec) versus cable speed (feet/min), calculated the slope, m_p and m_n, for response line. At station 1 where we only have the positive spinner responses, the threshold velocity, v_t is 0, we can calculate the v_f at station 1 by applying equation

$$v_f = \frac{f_0}{m_p} + v_t \tag{1.6}$$

Convert the fluid velocities to volumetric flow rate, we have

$$q = BA_w v_f \tag{1.7}$$

where q is volumetric flow rate, A_w is cross-sectional area, B is velocity profile correction factor, and v_f is fluid velocity from the multi-pass interpretation.

1.4 New Production Logging Tools

The working principle of the new production logging method is to measure the velocities and holdup of three phases in multiphase flow production well. The gas, oil, and water holdup are determined by the resistivity array tool (RAT) and capacitance

array tool (CAT), while the velocity of each phase flow is recorded by spinner array tool (SAT). A picture of CAT and RAT is shown in **Fig. 1.2**. The spinner array tool shares a similar structure with the capacitance or resistivity array tools as shown in **Fig. 1.3**. The main difference is that it incorporates six sensors, equally spaced around the periphery of the tool. This is different than the CAT and RAT which consist of 12 bowspring mounted sensors that open outwards from tool body to the casing.

Fig. 1.2—General views of capacitance array tool and resistivity array tool

Fig. 1.3—General view of spinner array tool

1.4.1 Capacitance array tool (CAT)

Capacitance array tool has a set of 12 miniature sensors mounted on the inside of a set of collapsible bowsprings and measure the capacitance of the surrounding fluid close to the well casing (**Fig. 1.4**). All 12 values are transmitted to surface or into a

memory section. The arms are placed alternately on a large or smaller radius size in the pipe which gives a global view of fluid phase distribution. CAT uses the similar principle of operation with traditional water-holdup tools. The biggest difference is that the capacitance sensors are arranged into 12 locations around the pipe which would help us have a better understanding of gas, oil and water holdup in the whole cross section. Qualitatively, water produces the lowest frequencies, oil produces higher frequencies, and gas produces the highest frequencies, almost triple of the water frequencies.

1.4.2 Resistivity array tool (RAT)

Resistivity array tool incorporates 12 micro resistance sensors, equally spaced around the periphery of the tool axis. This design would help us monitor all variation in fluid type of cross section. The application of array allows the RAT tool to be fitted up and down the well. Phase segregation happens in many wells, even in vertical wells with little deviation (Zett et al. 2011); the lighter phases migrate to the high side of the well, the heavier phase to the low side. Generally speaking, water has the lowest resistivity signal, oil has a higher resistivity signal and gas has the highest resistivity signal. A RAT log can generate the fluid phase distribution over the cross-section of a wellbore.

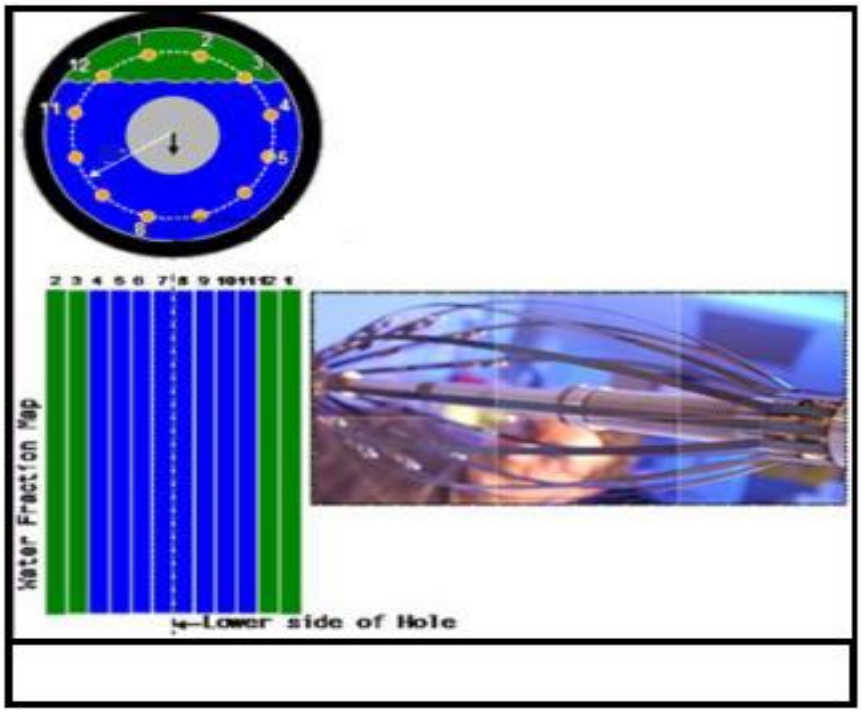

Fig. 1.4—Borehole tool position and holdup map of RAT of Al-Belowi A. R et al. (2010)

1.4.3 Spinner array tool (SAT)

Spinner array tool characters 6 miniature turbines arranged in array arms, enabling various local fluid velocities to be measured at 60 degree intervals around the wellbore. In a highly deviated or horizontal well, phase segregation occurs. The lighter phases flow to the high side of the wellbore, and the heavier phases migrate to the bottom of the well. In such a situation, the traditional centralized spinner flowmeter cannot provide quantitative estimates of the individual phase velocities. The introduction of spinner array tools gives us a chance to detect the different velocities of each phase that occurs in the wellbore.

Because the SAT data only shows the spinner response, we need.to translate the data to real velocity data. The critical work is to find an appropriate coefficient, m_p, between the spinner response and the real velocity. For a horizontal well at the heel, we locate a measuring station as our last station, then, with the surface gas, oil and water production, we can to calculate the m_{pg}, m_{po} and m_{pw} for three phases. Of course, we should consider the gas, oil and water holdup condition of each station. **Fig. 1.5** shows the map of SAT, RAT and CAT correlated with each other at same vertical position. Combining these three tools' measurement, we could obtain the phase velocity and phase holdup at same location.

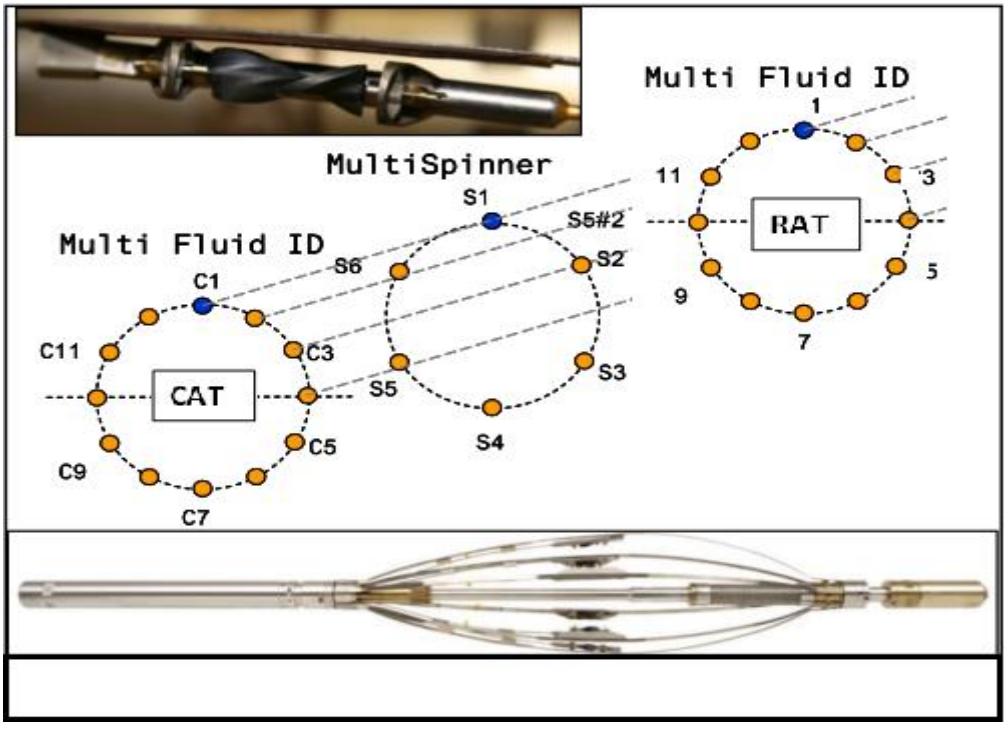

Fig. 1.5—Spinner flowmeter array aligned to holdup tools of Al-Belowi A R et al. (2010)

1.5 Objectives of Study

In this work, an analytical method will be developed for interpreting flow rates of multiple phases from array tool measurements in nominally horizontal wells. The method calibrates the spinner array response to ensure consistency with the total production rates of all phases from the well. The method also insures that the interpreted flow profile is consistent with the total production of all phases measured at surface conditions.

The developed log interpretation method is applied to three Eagle Ford production wells. All three wells are hydraulically fractured with multiple stages and each of them was producing oil, water, and gas during the period that fracture fluid was still being recovered from the well. The results from different methods of interpreting production logging are compared in the thesis. One has single sensor PLT measures, and the other two wells used a multiple sensor tool package for production logging. The examples illustrate differences of interpretation result by different methods, and recommend the procedures that yield better interpretation of multiple sensor array tools. The interpreted flow profiles are helpful in understanding the distribution of created hydraulic fractures and their productivities.

2. METHODOLOGY OF NEW PRODUCTION LOGGING TOOLS

2.1 Data Screening and Processing

In this study, three kinds of data sets will be interpreted for downhole flow profile and they are spinner flowmeter array tool, resistivity array tool and capacitance array tool, respectively. As mentioned before, combine these three production logging tools, we could observe the velocity of each phase and fluid properties from different portion of cross-section area of a wellbore.

The data needs to be processed before being applied to the interpretation. Because there is a large amount of logging data from a logging procedure, we should only select the data close to the area we are interested in. In this study, the interested area is the ones around the fractures. Of 15 total data stations along horizontal section of well, 10 points were selected at each fracture location, averaging 10 values of each zone we could get one more accurate value at this location.

Additionally, because that the tool rotation always happens during logging procedure, the sensor #1 may not at the top section, as **Fig. 2.1 b**) shows, and we believe that the top section of pipe often produce lighter phase and the bottom section produce denser phase as shown in **Fig. 2.1 a**), we assume sensor # 1 has highest value of SAT data and RAT data. Contrarily, sensor # 4 has lowest value of SAT and RAT data. **Fig. 2.1 c**) shows the correction position of each sensor around wellbore translated from **Fig. 2.1 b**).

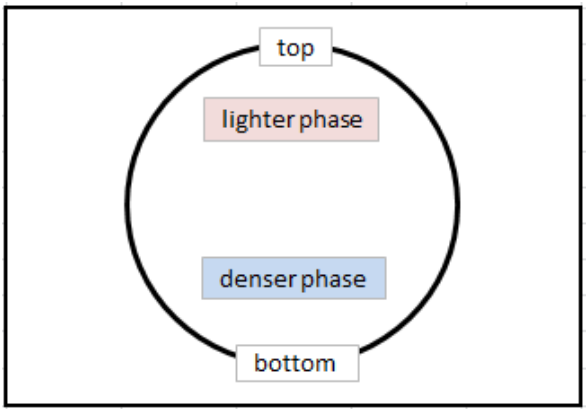

a) Before running spinner array tool

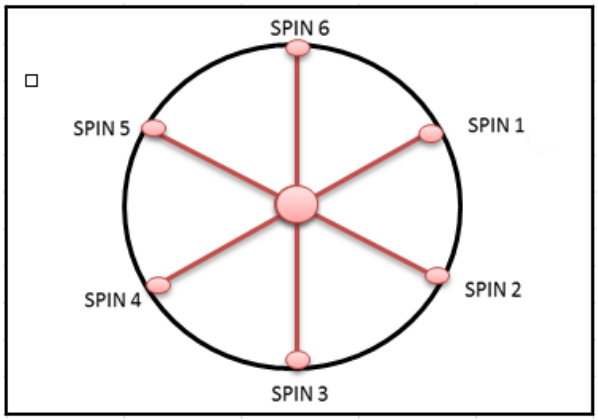

b) During running spinner array tool

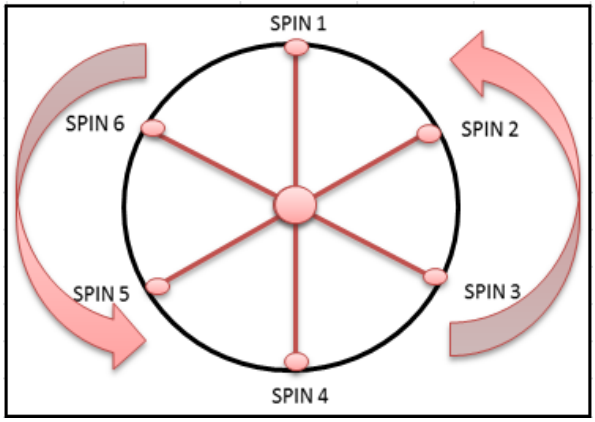

c) Rotate for interpretation

Fig. 2.1—Rotating sensor location for interpretation

2.2 Array Tool Geometry Configuration

Consider an array production logging tool that has sensors distributed around a nominally horizontal well as shown in the cross-sectional view in **Fig. 2.2**. The sensors at the same vertical location should be detecting the similar phase holdup and velocity values that are similar.

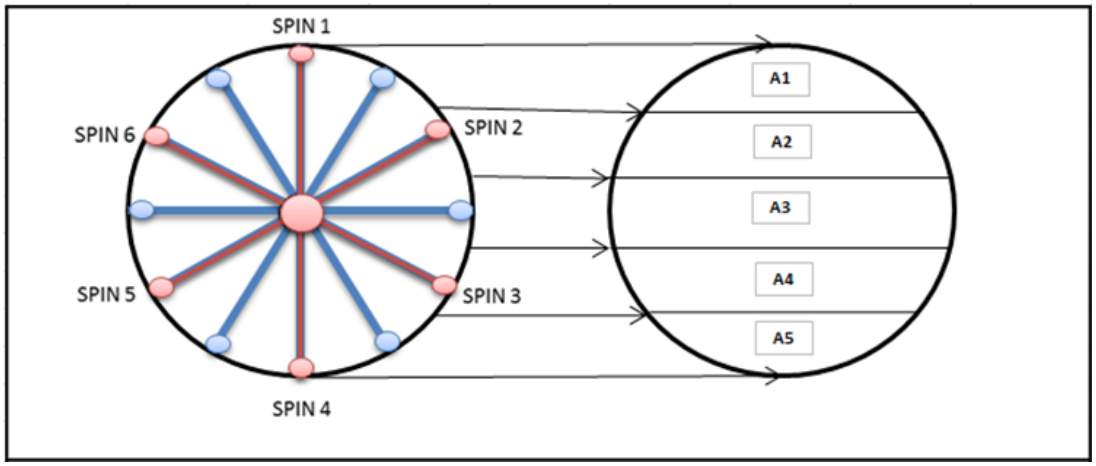

Fig. 2.2—Array tool configuration

We divide the wellbore cross-sectional area into five symmetric segments, denoted as A1, A2, A3, A4, and A5, each section has a vertical thickness. If the casing ID is d, then the thickness of the section is 1/5 of d. The areas of each of the segments are:

$$A_1 = A_5 = \frac{\arccos\left(\frac{r-h}{r}\right)}{180^\circ} A_t - (r-h)\sqrt{r^2-(r-h)^2} \tag{2.1}$$

$$A_2 = A_4 = \frac{\arccos(\frac{r-2h}{r}) - \arccos(\frac{r-h}{r})}{180°} A_t - [(r-2h)\sqrt{r^2-(r-2h)^2} - (r-h)\sqrt{r^2-(r-h)^2}]$$

(2.2)

$$A_3 = \{1 - \frac{\arccos[(r-2h)/r]}{90^\circ}\} A_t + 2(r-2h)\sqrt{r^2-(r-2h)^2}$$

(2.3)

When h is the same for all segments, these equations can be simplified to

$$A_1 = A_5 = 0.142 A_t \tag{2.4}$$

$$A_2 = A_4 = 0.231 A_t \tag{2.5}$$

$$A_3 = 0.253 A_t \tag{2.6}$$

In each segment, we average the responses from any multiple sensors present in that segment. From the arrayed spinner flowmeters in any segment, we obtain an average velocity, $\overline{v_i}$, where i denotes the segment. From any interpretation holdup measurements, we obtain phase holdups, $y_{j,i}$, where j denotes the phase (gas, oil, or water). Then the phase flow rate in a segment is

$$q_i = \overline{v}_j y_{j.i} A_i \tag{2.7}$$

The total rate of each phase at any location along the well is

$$q_j = \sum_{i=1}^{5} q_{j,i} \tag{2.8}$$

A simplified interpretation procedure that can be selected based on a qualitative evaluation of the production log data is to assume that each segment contains only a single phase. For this case, the flow rates of each phase are interpreted as

$$q_{j,i} = \sum v_i A_i \text{ for segments containing phase } j \tag{2.9}$$

2.3 Phase Distribution Determination

To determine whether a wellbore segment was occupied by hydrocarbon or water, a cut-off value is used to the average RAT response for that segment. Lower RAT readings correspond to water and higher readings to hydrocarbons. 0.52 is used to be the cut-off. If the section has a RAT value higher than 0.52, it contains only hydrocarbon, if the RAT value lower than 0.52, it contains only contains water.

2.4 Calibration of Spinner Flowmeter Responses

In order to insure consistency with the known total production of each phase from a well at the surface, the array spinner flowmeters are calibrated based on the surface flow rate translated to downhole temperature and pressure conditions. This approach is similar to that presented by Curtis (1967) for interpretation of multiple phases from vertical wells.

The spinner calibration is performed for data from a station at the heel of a horizontal well. First, the known surface flow rates flow of each phase, q_j, are converted to downhole volumetric rates, $q_{dh,j}$ by

$$q_{dh,j} = q_j B_j \tag{2.10}$$

where B_j is the formation volume factor for phase j. Note that if the flowing pressure at the heel is greater than the dew-point pressure for a gas-condensate well, or is greater than the bubble point pressure for a crude oil/gas well, the only phases in this well at downhole condition will be hydrocarbon and water. The mean velocity of a phase at the heel location is then

$$\overline{v_j} = \frac{q_{dh,j}}{A_j} \tag{2.11}$$

where A_j is the area of all segments occupied by phase j. We calibrate the array spinner by averaging the spinner responses, $\overline{f_j}$, occurring in all segments occupied by phase j, and then calculating the spinner response characteristics. According to conventional spinner flowmeter interpretation procedures (Hill, 1990), we assume that the spinner response is a linear function of the local effective velocity, v_e the vector sum of fluid and tool motion.

$$v_e = \overline{v_j} + v_T \tag{2.12}$$

where v_T is tool speed. Then,

$$m_j = \frac{v_e}{\overline{f_j}} \tag{2.13}$$

To interpret the array spinner responses in the rest of the well, we use the following equation in any segment occupied by phase j:

$$v_j = m_j \overline{f_j} - v_T \tag{2.14}$$

For example, assume that at the heel of the well, holdup measurements show that the bottom two segments of the well cross-section are occupied by water. Then,

$$\overline{v_w} = \frac{q_{dh,w}}{A_4 + A_5} \tag{2.15}$$

And the array spinner response to water at the heel, $\overline{f_w}$, is the average of all spinners located in segments 4 and 5. Then

$$m_w = \frac{\overline{v_w} + v_T}{\overline{f_w}} \tag{2.16}$$

And throughout the rest of the well, we calculate water velocities in segments occupied by water by

$$v_w = m_w \overline{f}_w - v_T \tag{2.17}$$

3. FIELD CASE STUDY

3.1 Interpretation of Well 1

3.1.1 Introduction of Well 1

The first example is a horizontal well with 15 stages along the horizontal section from 9000 feet to 13700 feet, each stage include 4 perforations centralization production logging data as shown in **Fig. 3.1**. The localized fluid density, dielectric and gas holdup reading over three intervals (1930, 2240, and 2875 FT MD) indicated a water sumps located in the low area of the horizontal section and do not have significant contribution to the total flow .

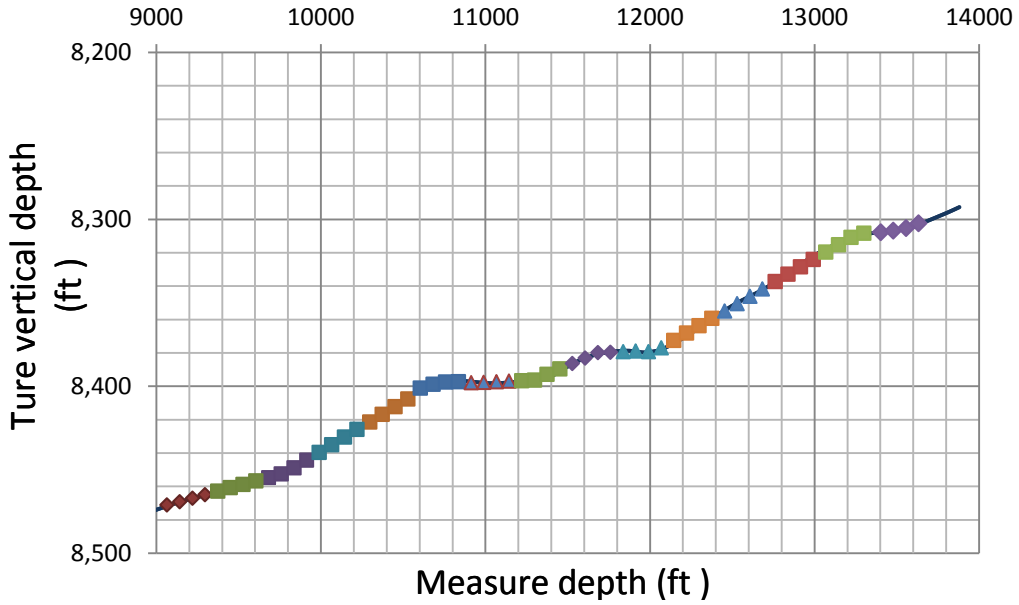

Fig. 3.1—Well trajectory with perforations of Well 1

In **Table 3.1**, we could see that Well 1 was producing 1600 standard cubic feet per day of gas, 180 standard barrel per day of oil and 160 standard barrel per day of water.

TABLE 3.1 SURFACE PRODUCTION DATA OF WELL 1

Fluid	Flow Rate
Gas	1600 [Mscf/D]
Oil	180 [STB/D]
Water	160 [STB/D]

Table 3.2 shows the fluid properties of Well 1, average properties are used at average temperature of $240°F$, the average pressure of 4632 psi. The average formation volume factor of gas and water ae 0r.0044 and 1.08, respectively.

TABLE 3.2 FLUID PROPERTIES OF WELL 1

Stage	*Depth, ft*	T_{wf}, ^oF	P_{wf}, *psi*	B_{water}	B_{gas}
1	NA	242	4632	1.59	0.00443
2	4318	240	4633	1.36	0.00443
3	4010	241	4635	1.08	0.00442
4	3702	241	4634	1.08	0.00441
5	3394	241	4633	1.08	0.00442
6	3080	241	4632	1.23	0.00442
7	2778	240	4631	1.19	0.00442
8	2470	240	4631	1.15	0.00442
9	2162	240	4630	1.11	0.00441
10	1849	240	4633	1.08	0.00441
11	1546	239	4631	1.10	0.00440
12	1238	239	4633	1.11	0.00440
13	930	239	4639	1.08	0.00440
14	622	239	4634	1.08	0.00440
15	314	239	4633	1.08	0.00440

3.1.2 Application of multi-pass method

For multi-pass method, we use 2 up passes and 2 down passes, we picked up 16 stations where have constant and reasonable values of LSPD & SP (LSPD is cable speed and SP is spinner flowmeter responses) among hundreds of thousands raw data. Because lacking data from station 11 to station 16, we only calculate the velocity from station 1 to station 10. Information is shown in **Fig. 3.2**. Ploting the spinner response (res/sec) vs. cable speed (feet/min), we could calculated the slope, m_p or m_n, for response line. At station 1 where only have the positive spinner response, the threshold velocity, v_t is 0. Calculate v_f at station 1 by applying equation 1.6. Convert the fluid velocities to volumetric flow rates with equation 1.7, where q is volumetric flow rate, Aw is cross-sectional area, B is velocity profile correction factor, and v_f is fluid velocity from the multi-pass interpretation.

station 1	
x	y
-61.2	-0.338
-45.723	0.134
19.95	5.05
31.2	6.58

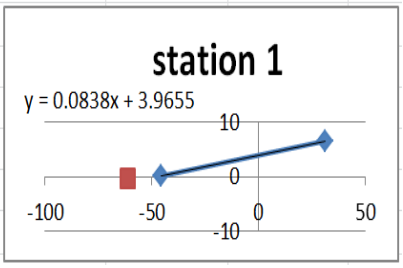

Fig. 3.2—Multi-pass example at station 1. $m_p = 0.0838$, $f_0 = 3.9655$.

Because the threshold velocity is found by taking the difference between two curve-fitted lines, it is very sensitive to any errors or fluctuations in the spinner response.

If the well flow rate is not stable or if two-phase flow effects cause a noisy spinner response, the threshold velocity cannot be accurately determined. In this situation, the threshold velocity may be obtained by logging in the downhole or with the well shut in. In a gas production well, however, this technique will most likely yield the threshold velocity in liquid, which is typically significantly different from that in gas. However the threshold velocity is obtained, it should be compared with the threshold velocity predicted by the tool supplier; if it is significantly higher than expected, the spinner is fouled with debris or the bearings are not adjusted properly.

Fig. 3.3 shows the calculated values of m_p and f_0 in other 9 stations:

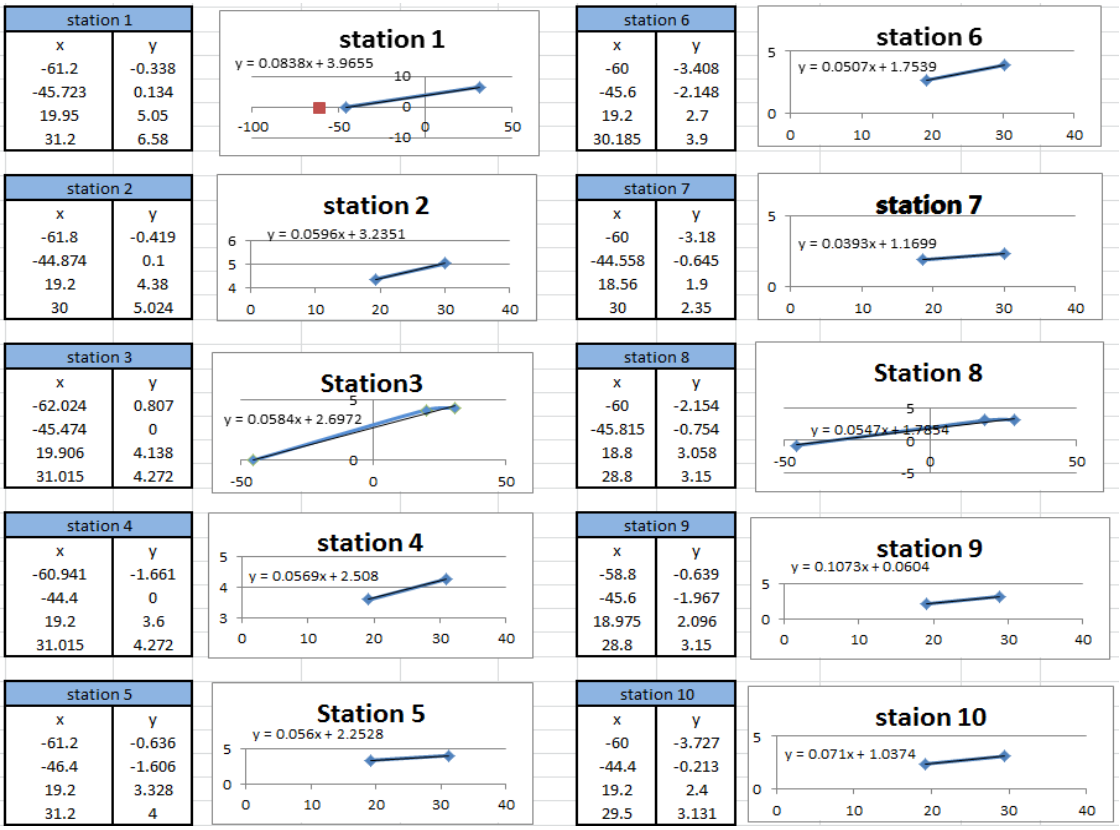

Fig. 3.3—Station 1- station 10 data, multi-pass method

Finally, the response slopes for all other stations are determined in a similar fashion and the results are given in **Fig. 3.4**.

Table - Spinner flowmeter interpretation

station	mp	fo	depth	Vf	Vbar	q	Total Flow	Flow Entering
	(rev/sec)/(ft/min)	(rev/sec)	(ft)	(ft/min)	(ft/min)	(Mcf/D)	(%)	(%)
Station 1	0.0838	3.9655	46	55.017		5.431705	100	1.339224262
Station 2	0.0596	3.2351	300	54.2802		5.358962	98.660776	14.71412379
Station 3	0.0584	2.6972	650	46.18493		4.559734	83.946652	7.460229413
Station 4	0.0596	2.508	947	42.08054		4.154517	76.486423	3.366169373
Station 5	0.056	2.2528	1259	40.22857		3.971676	73.120253	10.24207576
Station 6	0.0507	1.7539	1575	34.59369		3.415357	62.878177	-4.334586347
Station 7	0.0393	1.1699	1897	36.97845		3.650799	67.212764	7.885915083
Station 8	0.0547	1.7854	2194	32.63985		3.222459	59.326849	35.65615203
Station 9	0.1073	0.0604	2488	13.02291		1.285722	23.670697	-2.887034556
Station 10	0.071	1.0374	2796	14.61127		1.442538	26.557731	26.5577312
Station 11	Lack data							
Station 12								
Station 13								
Station 14								
Station 15								
Station 16								

Aw	0.118949097	cuft
B	velocity profile correction factor, 0.83	

Fig. 3.4—Spinner flowmeter interpretation

Fig. 3.5 shows the gas production rate percent of each station from 50 feet to 3000 feet.

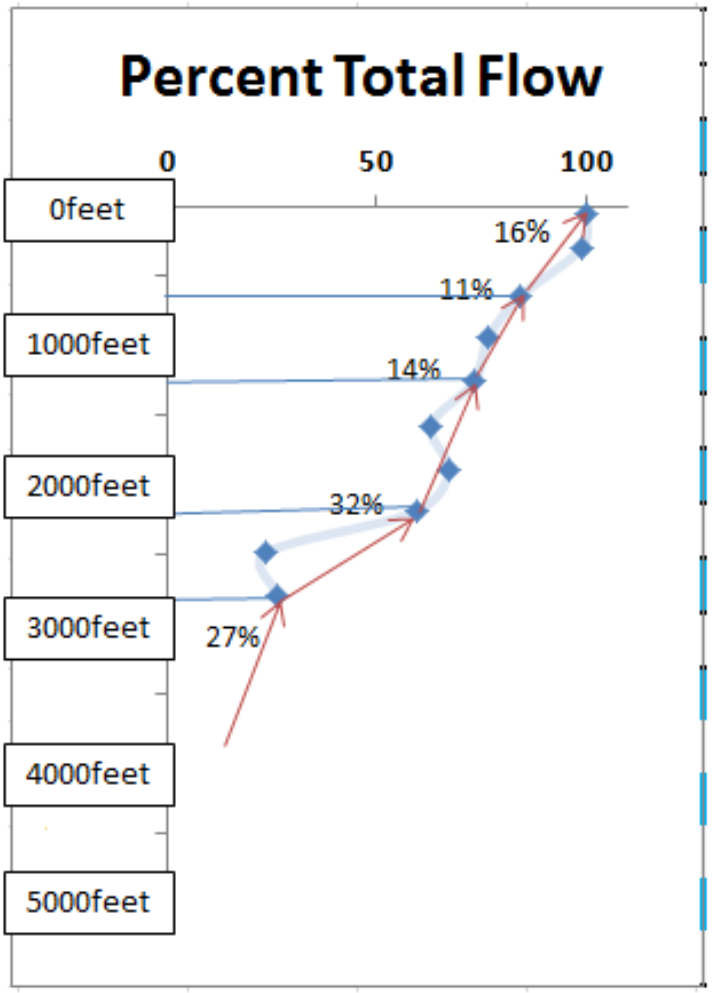

Fig. 3.5—Interpretation in multi-pass method

3.1.3 Application of commercial software interpretation

Fig. 3.6 shows production centralized logging data of well 1 including Gamma raw, cable speed, spinner flowmeter response temperature, pressure, and so on.

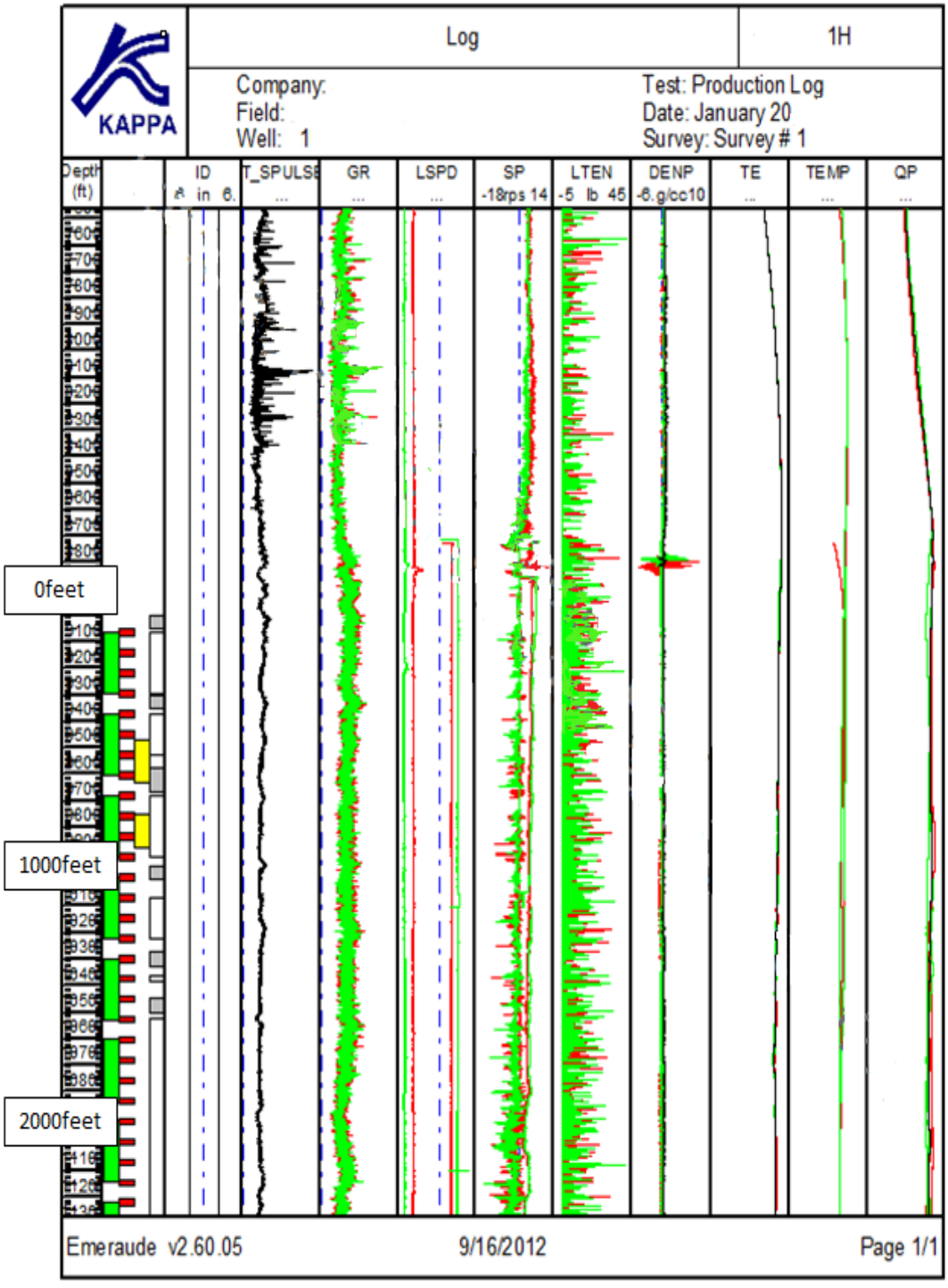

Fig. 3.6—Raw production data survey during well was flowing

Based on general observation of PLT data in horizontal wells taken using array tools, it was found that the fluid flow was stratified with the lighter fluid flowing at the top and the heavier fluids flowing at the bottom. The following can be encountered during logging.

1. With the single probe tools, there is no information on tool position inside the wellbore. If the tool is reading the liquid phase or the gas phase it could be caused by the tool position inside the wellbores, and the tool position could change from one location to another. This causes the inaccuracy in calculating fluid velocity in the horizontal section of the well.
2. Going from toe to heel in a toe-up horizontal well, the light fluid flowed at lower rate while the heavier fluid flowed at higher velocity and vice versa.
3. Temperature reduction is expected to be caused by gas entry into the wellbore experiencing gas expansion, and also gas flowing from smaller cross section area (larger volume of water in the pipe) into a larger cross section area (smaller water volume in the pipe) experiencing gas expansion
4. Temperature increase is expected to be caused by liquid entry into the wellbore and higher percentage of liquid at a particular depth such as water sump or other low areas in the pipe

From **Fig. 3.7**, the depth of well 1, spinner flowmeter response, temperature, and distribution of phases are shown. The red point marked in the plot shows higher spinner reading due to suspected higher liquid content in the pipe section which causes lower flow area for the gas. The blue point shows low spinner reading in the water sump.

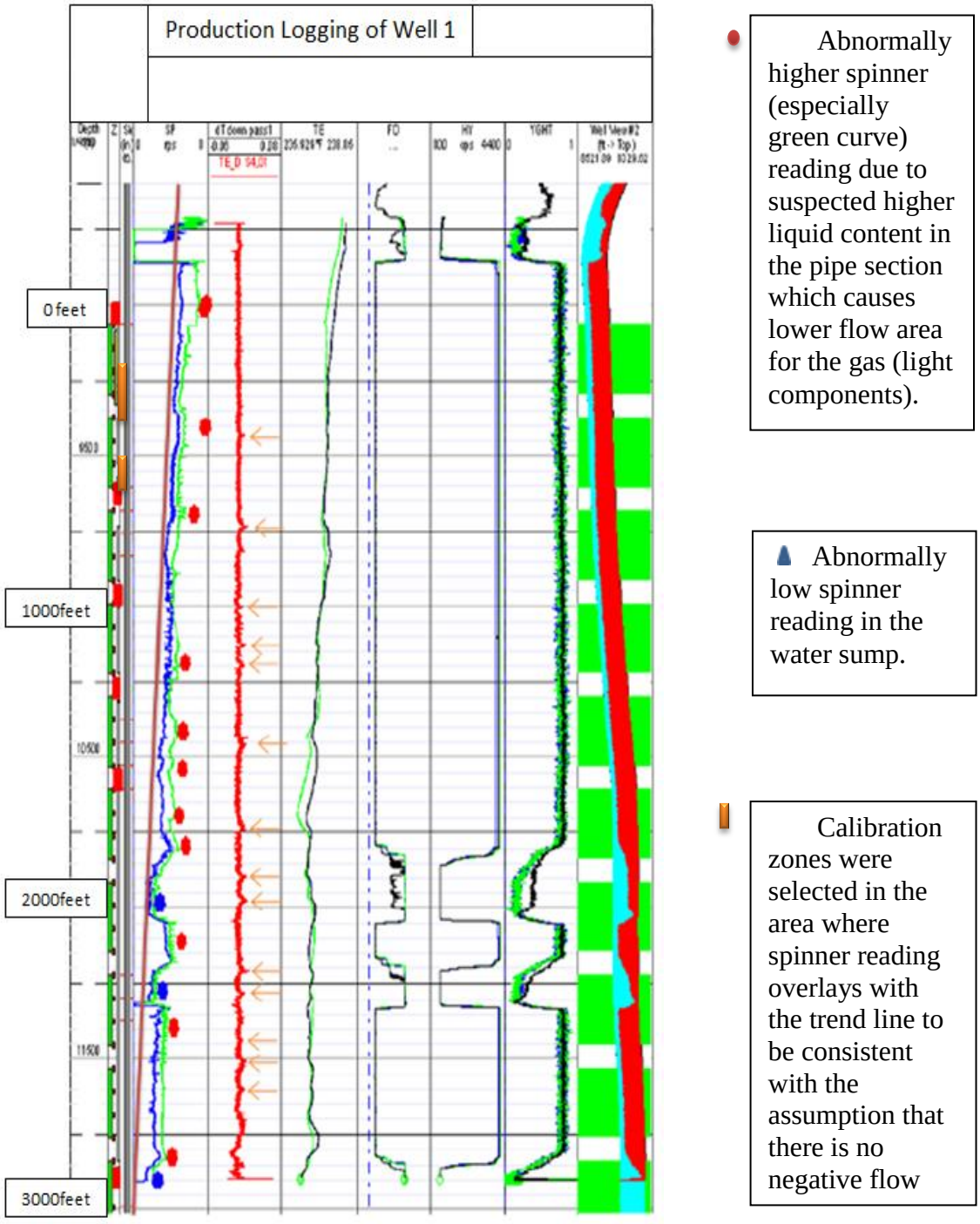

Fig. 3.7—Raw data showing fluctuations in spinner reading

5. Comparison with commercial interpretation tools. Emeraude software package was used in this study to compare with the result of the new method. In this section, the comparison will be presented.

   Two zones are used to calibrate including zone 1 from 469.34 feet to 635.18 feet and zone 2 from 752.86feet to 881.25feet. Because we have stationary measurements, we should then use Calibration Model 2 (Kappa Emeraude software). The PVT data used in the interpretation is list in **Table 3.3.**

TABLE 3.3 PVT DATA OF WELL 1

Fluid type	Condensate with water		**In separator conditions**	
The salinity (total dissolved solids in ppm)	1.2×10^5		Gas gravity	0.63
Temperature ($^\circ F$)	$90^\circ F$		GOR (cf/bbl)	8255
Dew point pressure (psia)	4290		Pressure (psia)	1632
Liquid gravity (sp.gr)	0.782		**In tank conditions**	
Thermal properties of gas ($1bm/^\circ F$)	0.26		Gas gravity	1.33
Thermal properties of oil ($1bm/^\circ F$)	0.49		GOR (cf/bbl)	5
Dew point temperature ($^\circ F$)	212			

The data below 3000ft is not good which contents to much noisy and we only interpret through station 6 to station 15. **Fig. 3.8** shows the volumetric rate of three phases of well 1, where red part represents gas production rate, green part represents oil production rate, and blue part represents water, respectively. We could see that most of

hydrocarbon comes from the zone between 1600 feet and 2600 feet and the zone near the heel.

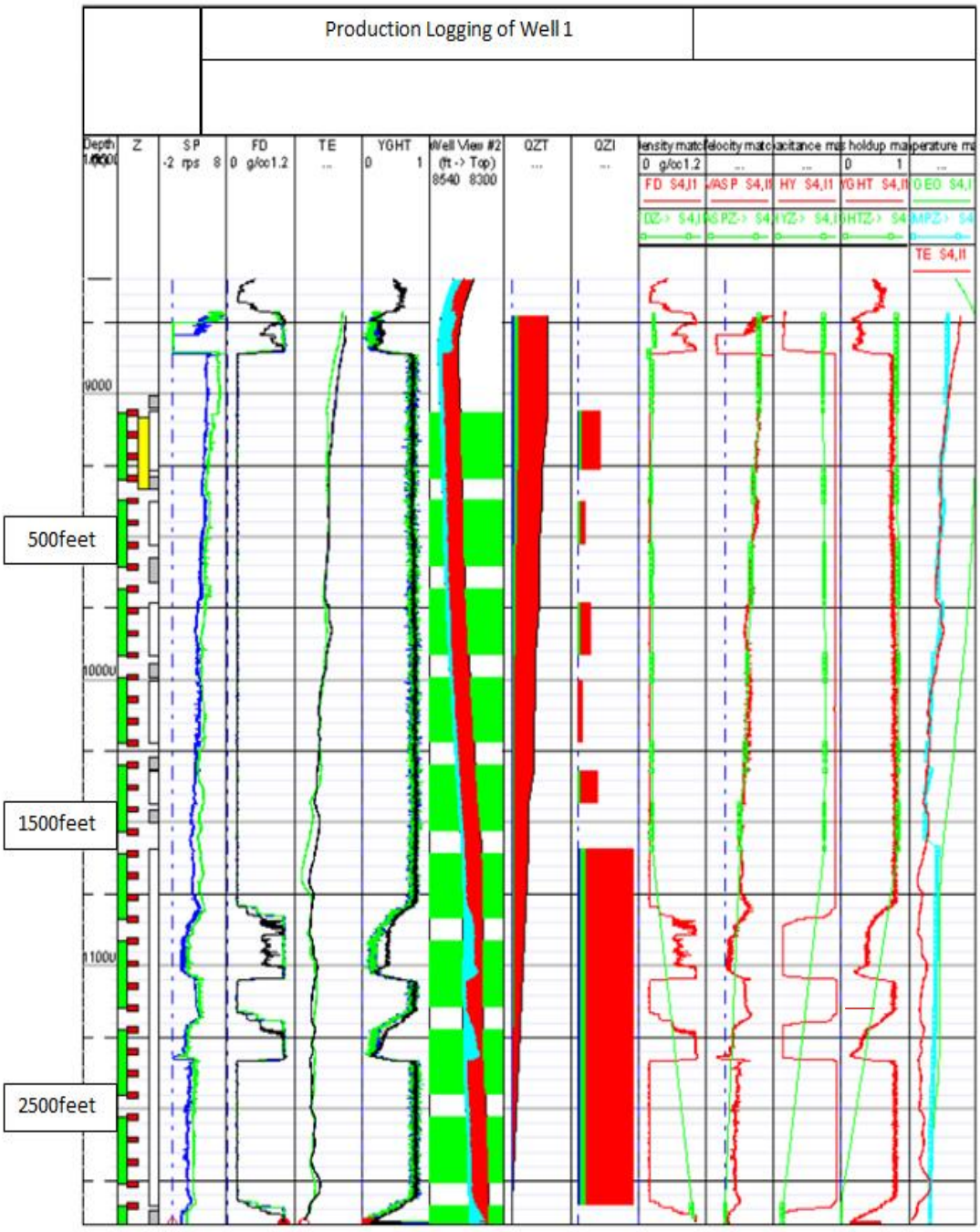

Fig. 3.8—Production rate of Well 1 in Emeraude

3.1.4 Comparison results between multi-pass method and commercial software

Applying multi-pass method, we assume this well only produce gas. So there we only consider about the production rate of gas. Compare new method and commercial software. In **Fig. 3.9**, light blue curve represents multi-pass method, green and orange curves represent results from Emeraude, and dark blue represents result from Plato.

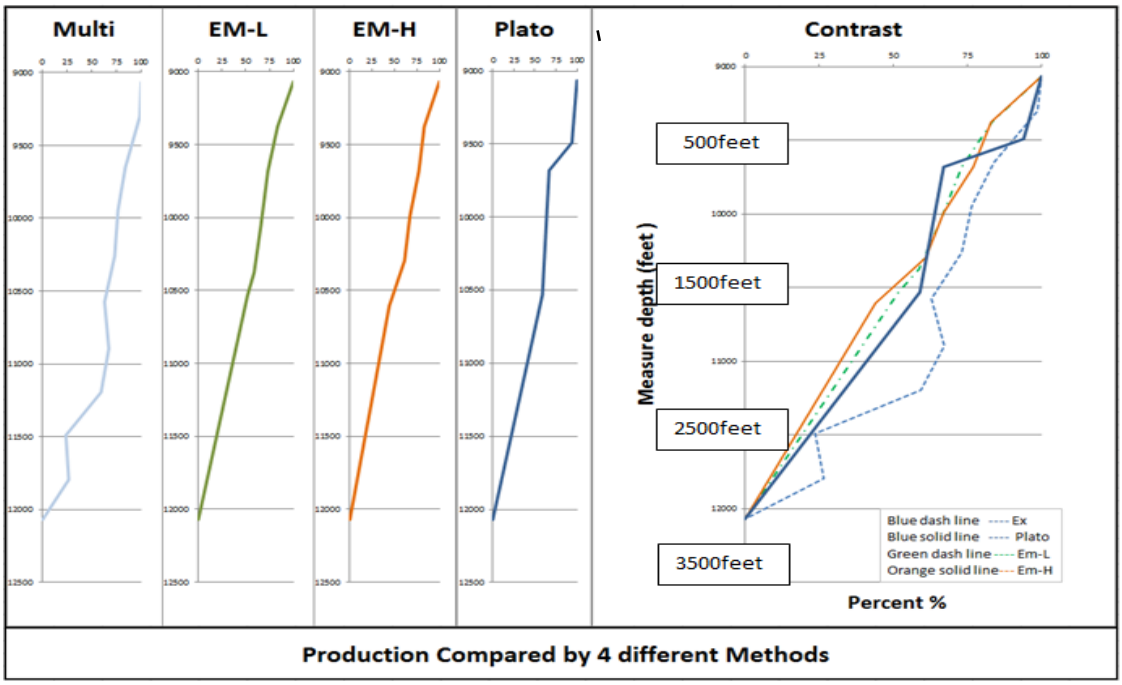

Fig. 3.9—Comparison result between multi-pass method and commercial software

From plot we could see that there is difference between single pass method and commercial software's result. Even on the locations of depth 12000ft and 10700ft,

negative production rate occurred. Combine with well trajectory, this kind of abnormal rate may cause by the liquid loading.

3.2 Interpretation of Well 2

3.2.1 Introduction of Well 2

The second example is a horizontal well with 15 stages of fracturing with the objective of estimating the rate contribution and fluid type from each perforation. The wellbore is about 5000 feet long in horizontal section. The well trajectory is shown in **Fig. 3.10**.

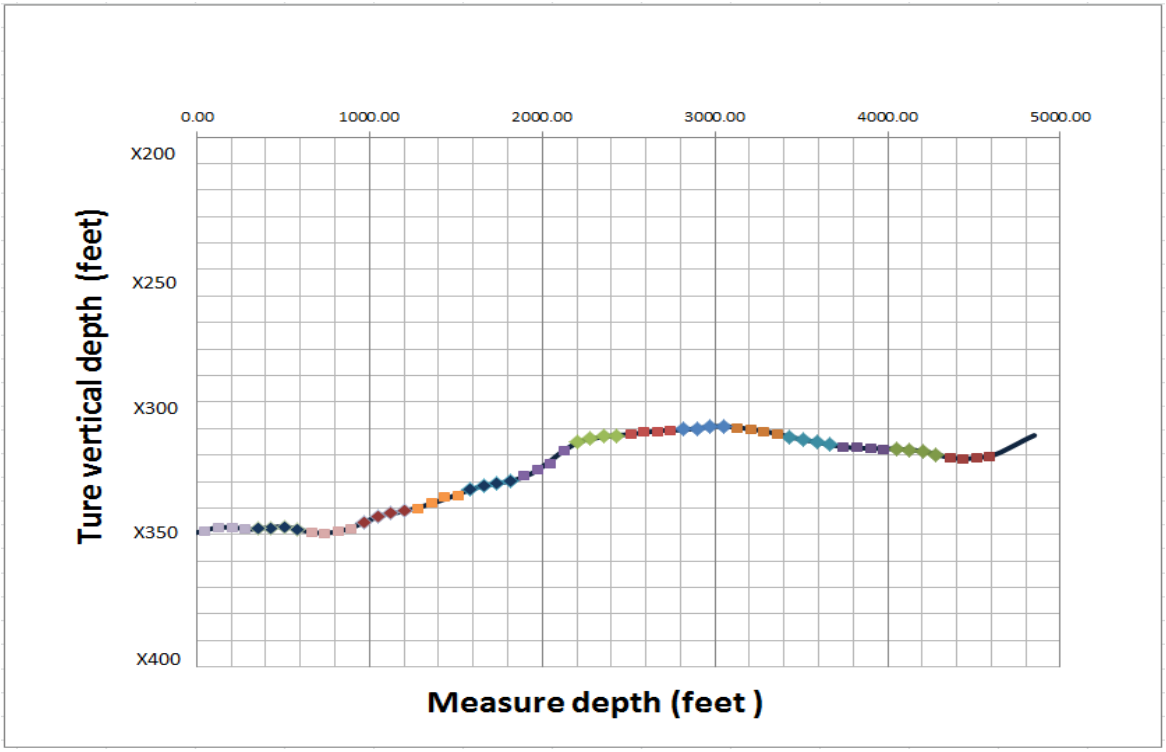

Fig. 3.10—Well trajectory with perforations of Well 2

Table 3.4 listed the flow rates of different phases at the surface in Well 2 was producing 1700 standard cubic feet per day of gas, 125 standard barrel per day of oil and 60 standard barrel per day of water.

TABLE 3.4 SURFACE PRODUCTION DATA OF WELL 2

Fluid	Flow Rate
Gas	1700 [Mscf/D]
Oil	125 [STB/D]
Water	60 [STB/D]

Table 3.5 shows the fluid properties of this well, and the average temperature is $240°F$, the average pressure is 4632 psi, and the average formation volume factor of gas and water are 0.0044 and 1.08, respectively.

TABLE 3.5 FLUID PROPERTIES OF WELL 2

Stage	*Depth, ft*	T_{wf} ,°F	P_{wf} , *psi*	B_{water}	B_{gas}
1	NA	242	4632	1.59	0.00443
2	4318	240	4633	1.36	0.00443
3	4010	241	4635	1.08	0.00442
4	3702	241	4634	1.08	0.00441
5	3394	241	4633	1.08	0.00442
6	3080	241	4632	1.23	0.00442
7	2778	240	4631	1.19	0.00442
8	2470	240	4631	1.15	0.00442
9	2162	240	4630	1.11	0.00441
10	1849	240	4633	1.08	0.00441
11	1546	239	4631	1.10	0.00440
12	1238	239	4633	1.11	0.00440
13	930	239	4639	1.08	0.00440
14	622	239	4634	1.08	0.00440
15	314	239	4633	1.08	0.00440

3.2.2 Application of single pass method

The spinner tools must be checked for proper operation before logging, the well conditions must be suitable for using a spinner flow meter, and the log must be run correctly. Usually, we have more accurately data from down pass, Because it has the operating direction with the production fluid's which would make down pass more sensitive to the flow. In well 2, we have 3 down passes at speed 30 feet/min and 3 up passes at 30, 60, and 90 feet/min (**Figs. A.1 to A.6**). As plot shows, we found that up passes have so much noisy and down passes have better measured data but they were ran by the same speed. We cannot use multi-pass method in such situation.

In the following example only the centralized full bore spinner (CFB) data (no SAT, RAT and CAT data) is used to establish the gas production.

The following assumptions were applied to interpretation:

- Well 2 only produce gas
- CFB data can represent the whole part of cross-section
- We only use down passes' data

Firstly, we interpret centralized full bore spinner by single-pass method. With this method, the highest spinner response (above all perforations) is assigned 100% flow and the lowest spinner response is assumed to be in static fluid and thus is assigned 0% flow. However, single-pass method is not very reliable. In order to obtain a good result, SAT (spinner array tool) can be used. The method used SAT data would be introduced in the following part of new method.

Example (down 1): in this situation we only use CFB plot and assume this is a

100% gas production well. We picked point A @.5ft as our 100% flow reference point on Fig. 3.11, there are 15 stages I assumed @4315ft, 4006ft, 3705ft, 3395ft, 3085ft, 2775ft, 2465ft, 2165ft. 1855ft, 1545ft, 1245ft, 935ft, 625ft, 315ft and 5ft, respectively. By single-pass method, we can obtain the flow rate as following:

From equation 1.1, we could calculate the flow rate percent at depth 4315 feet:

$$\frac{v_x}{v_{100}} = \frac{f - f_s}{f_{100} - f_s} = \frac{7.3280 - 0}{1.5177 - 0} = \frac{7.3280}{1.5177} = 0.207 = 20.7\%$$

Then we get the production rate of gas in well 2 along the horizontal section:

@4315ft: produce 20.7% @4005ft: produce 17.8%

@3705ft: produce 18.5% @3395ft: produce 27.7%

@3085ft: produce 30.5% @2775ft: produce 30.2%

@2465ft: produce 51.3% @2165ft: produce 55.8%

@1855ft: produce 65.5% @1545ft: produce 68.3%

@1245ft: produce 71.8% @935ft: produce 64.7%

@625ft: produce 70.9% @315ft: produce 90.3%

@5ft: produce 100.0%

Finally, we should re-find 100% flow reference point and the result is shown in **Fig. 3.11:**

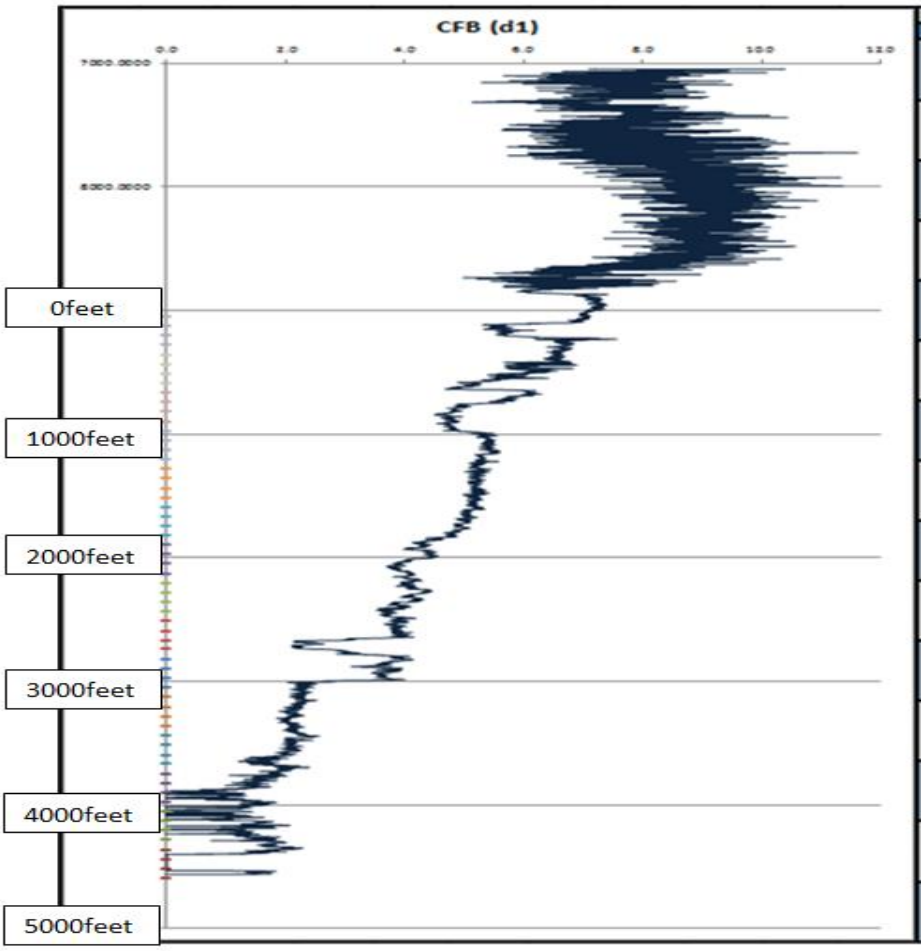

Fig. 3.11—Production profile calculation by single pass method

3.2.3 Application of new method

As we know if the actual pressure is higher than the dew point pressure is lower than the actual pressure, there is no oil presents. So in the following method we just consider about gas and water phase.

Using the methodology mentioned before, if the sectional RAT value is higher than 0.52, then the section is indicating gas. Otherwise it produces water. Because on

this principle, we first assign all sections a fluid type. There are 15 stations, and each one is divided into 5 sections. The fluid distribution is shown in **Fig. 3.12**.

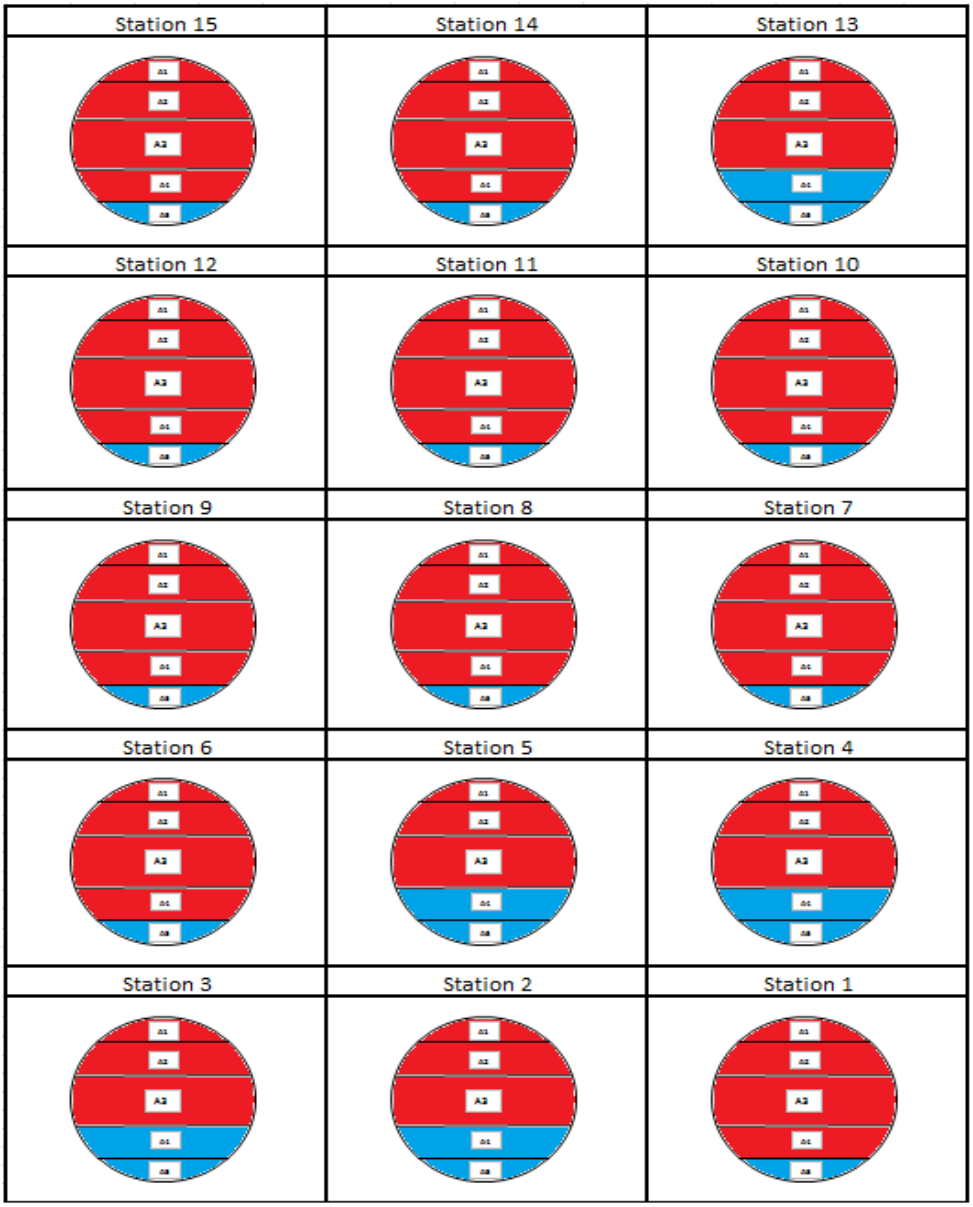

Fig. 3.12—Distribution of 2 phases at 15 stations of Well 2

The first step is to translate standard production rate into actual production rate at 9005 feet.

$$q_{g,act} = \frac{1.7\times10^{6}\,Mscf\times B_g}{24days\times60hours} = \frac{1.7\times10^{6}\times0.0044}{24\times60} = 5.101\,ft^3/\min \tag{3.1}$$

$$q_{o,act} = \frac{136BOPD\times B_o\times5.615}{24days\times60hours} = \frac{136\times1.08\times5.615}{24\times60} = 0.564\,ft^3/\min \tag{3.2}$$

$$q_{w,act} = \frac{62BWPD\times B_w\times5.615}{24days\times60hours} = \frac{62\times1.04\times5.615}{24\times60} = 0.247\,ft^3/\min \tag{3.3}$$

Note that because the pressure in horizontal part of Well 2 is higher than the dew point pressure, the well only produce gas between 0 feet and 4500 feet. We assume that 2 phases exist in the wellbore.

$$q_{g+o} = 5.101\,ft^3/\min + 0.564\,ft^3/\min = 5.665\,ft^3/\min \tag{3.4}$$

To determine the distribution of 2 phases, we use RAT data. In this station, A_1, A_2, A_3, and A_4 produce gas, and A_5 produces water, as shown in **Fig. 3.13**.

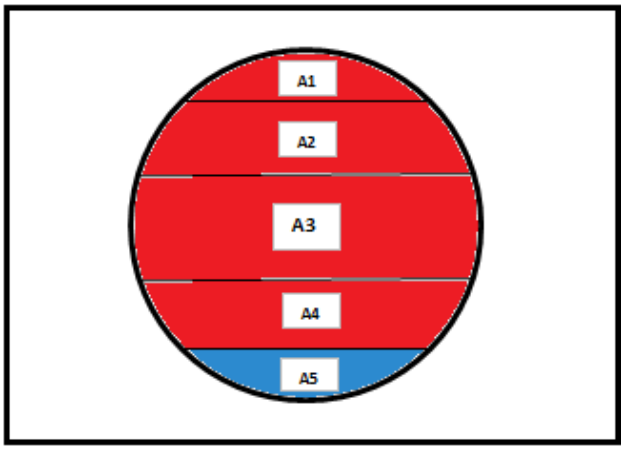

Fig. 3.13—Distribution of 2 phases at 5 feet of Well 2

The total areas which produce gas is

$$A_{g+o} = A_1 + A_2 + A_3 + A_4 = 0.010806 + 2 \times 0.029291 + 0.038756 = 0.108144\, ft^3 / \min$$

And then the gas velocity is

$$v_{g+o} = \frac{q_{g+o,act}}{A_{g+o}} = \frac{5.665\, ft^3 / \min}{0.108144\, ft^2} = 52.38\, ft / \min \tag{3.5}$$

The spinner response correlates with SPIN01, SPIN02, SPIN03, SPIN05 and SPIN06 the reading at sensor #1 to sensor #6. **Table A.1** shows the value of each sensor.

$$f_{g+o} = 0.2 \times (SPIN03 + SPIN05) + 0.2 \times (SPIN02 + SPIN06) + 0.2 \times SPIN01$$

$$= 0.2 \times (3.8278 + 4.1065) + 0.2 \times (4.2925 + 4.2581) + 0.2 \times 4.2189$$

$$= 4.141 rps \tag{3.6}$$

Thus we can get the velocity conversion coefficient m_{pg} from the heel station,

$$m_{pg+0} = \frac{v_{g+0}}{f_{g+0}} = \frac{52.38\, ft / \min}{4.141 rps} = 12.65 \tag{3.7}$$

For water production at this station, we have:

$$A_w = A_5 = 0.010806\, ft^2 \tag{3.8}$$

and

$$v_w = \frac{q_{w,act}}{A_w} = \frac{0.247\, ft^3 / \min}{0.010806\, ft^2} = 22.86\, ft / \min \tag{3.9}$$

The spinner response only correlates with SPIN04

$$f_w = SPIN04 = 4.0181 rps \tag{3.10}$$

Thus we can get the velocity conversion coefficient m_{pw} from the heel station,

$$m_{pw} = \frac{v_w}{f_w} = \frac{22.86\,ft/\min}{4.0181 rps} = 5.689 \tag{3.11}$$

Finally, we can calculate each station's spinner response of 2 phases.

$$v_{(g+o)i} = m_{p(g+o)} f_{(g+o)i} = 12.65 f_{(g+o)i} \tag{3.12}$$

$$v_{wi} = m_{pw} f_{wi} = 5.689 f_{wi} \tag{3.13}$$

Table 3.6 shows different value $f_{(g+o)i}$ of each section in 15 stations.

TABLE 3.6 SPINNER RESPONSES AT DIFFERENT SECTIONS OF 15 STATIONS OF WELL 2

STATION	DEPT feet	P1	P2	P3 (rps)	P4	P5
station 1	4315	1.2613	1.1436	0.9924	0.8413	0.8637
station 2	4005	1.1082	1.0435	0.9214	0.7994	0.7653
station 3	3705	1.4277	1.2844	1.1140	0.9436	0.9482
station 4	3395	2.0280	1.6141	1.3657	1.1174	0.9890
station 5	3085	2.3098	1.7885	1.4350	1.0815	1.0397
station 6	2775	2.8929	1.9397	1.6490	1.3583	1.3743
station 7	2465	2.2307	2.2870	2.0448	1.8027	1.8183
station 8	2165	2.4438	2.4522	2.2065	1.9609	2.5568
station 9	1855	2.8275	2.8941	2.5939	2.2937	2.6756
station 10	1545	3.1500	3.2009	2.8558	2.5107	3.0086
station 11	1245	3.2361	3.1820	2.8906	2.5991	2.9762
station 12	935	2.9174	2.9300	2.7213	2.5126	2.8746
station 13	625	7.4574	3.1780	2.2928	1.4077	0.0000
station 14	315	4.1344	4.0348	3.8057	3.5766	3.2916
station 15	5	4.2189	4.2753	4.1212	3.9672	4.0181

Then we can get the volumetric rate of gas and water shown in **Fig. 3.14** under downhole conditions, where red curve represents gas production rate and blue curve

represents water production rate. **Fig. 3.15** presents the profiles of gas, oil, and water at surface condition translated from the downhole condition, with the oil rates being calculated by assuming a constant GOR and a single hydrocarbon phase (gas) at downhole temperature and pressure.

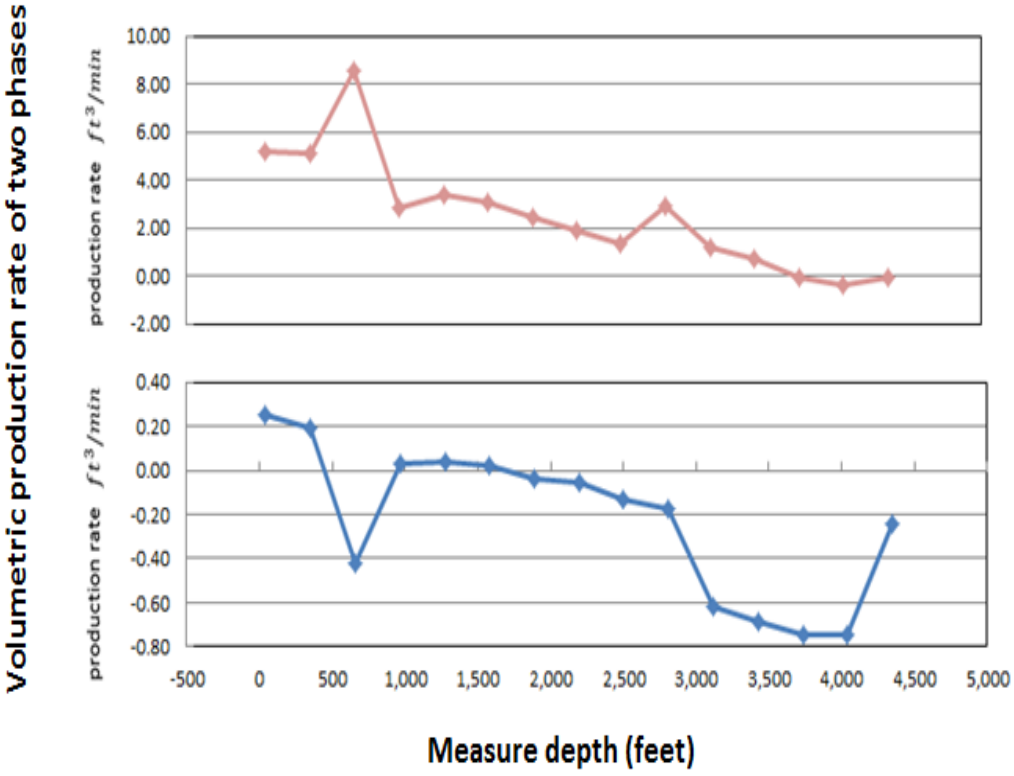

Fig. 3.14—Volumetric production rate of Well 2 under downhole conditions

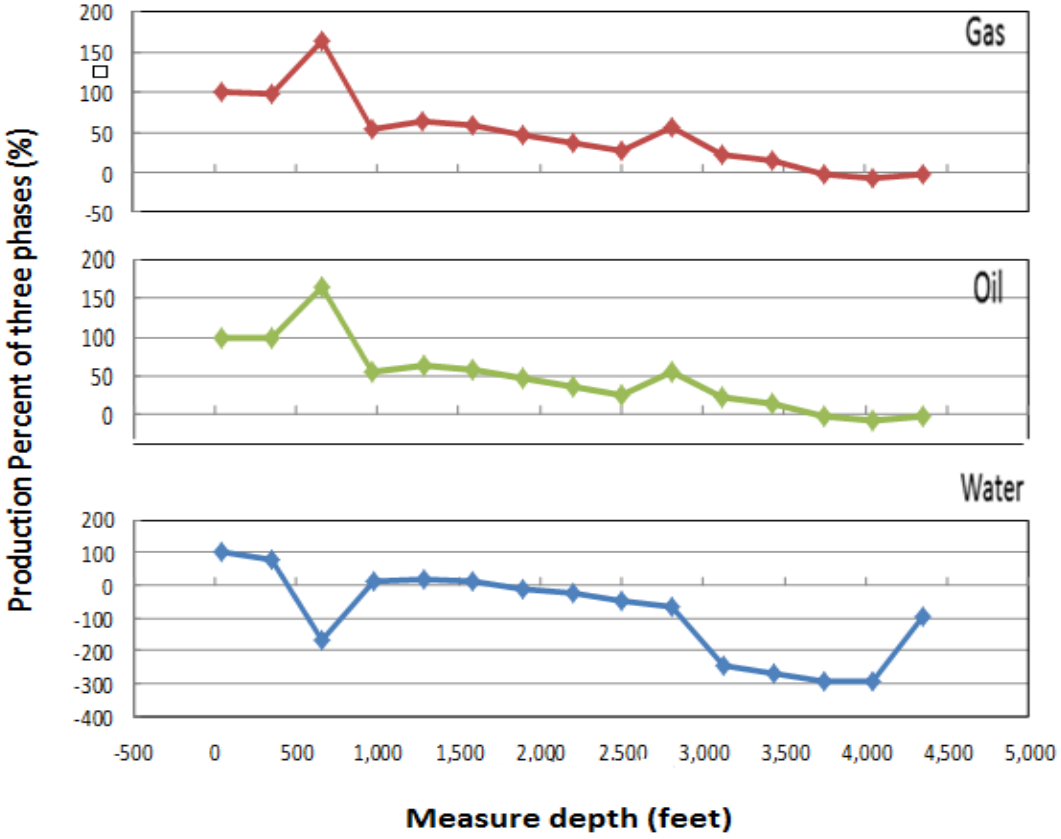

Fig. 3.15—Percent production rate of Well 2 at surface conditions

3.2.4 Application of commercial software interpretation

In this section, we use the commercial software package to interpret log data for Well 2, and then we compare results with new method. **Fig. 3.16** through **Fig. 3.21** show raw log data for centralized tool, capacitance array tool (CAT) (a) & (b), resistivity array tool (RAT) (a) & (b) and spinner array tool (SAT) given by these multiple probe tools.

In the creation of image views from CAT data, the data from string number 12 is ignored because all of the values given by the probe shows higher values than the maximum of the tool measurement range. In addition, the CAT data is calibrated by

normalizing them between 0 and 1 with a minimum and a maximum value of the measurement.

The original log data have several spikes which are caused by measurement error, and these are masked by tool (these are colored in gray on the data plots). In the following interpretation, these spikes are ignored.

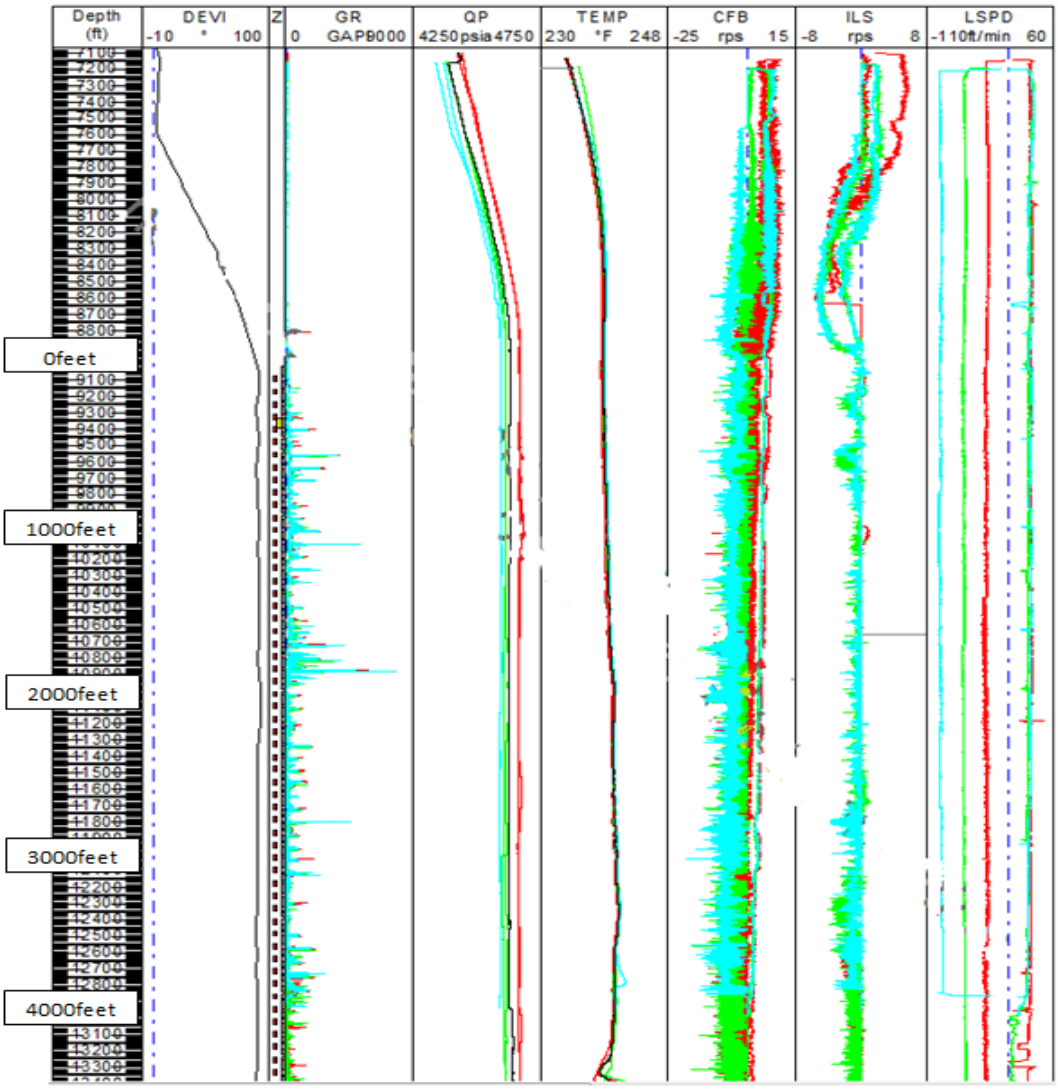

Fig. 3.16—Raw log data for centralized tools of Well 2

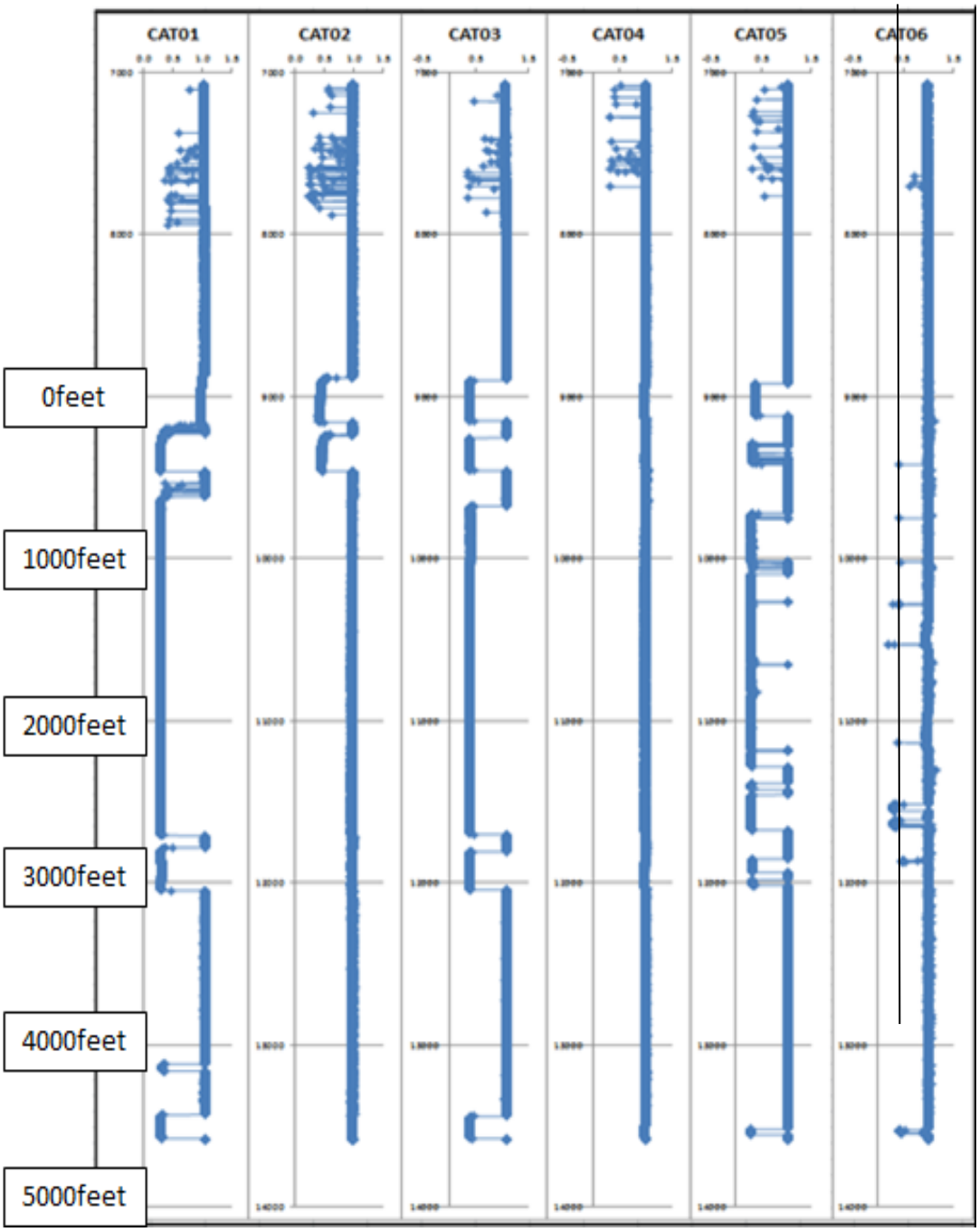

Fig. 3.17—Raw log data for capacitance array tool of Well 2 (CAT01-CAT06)

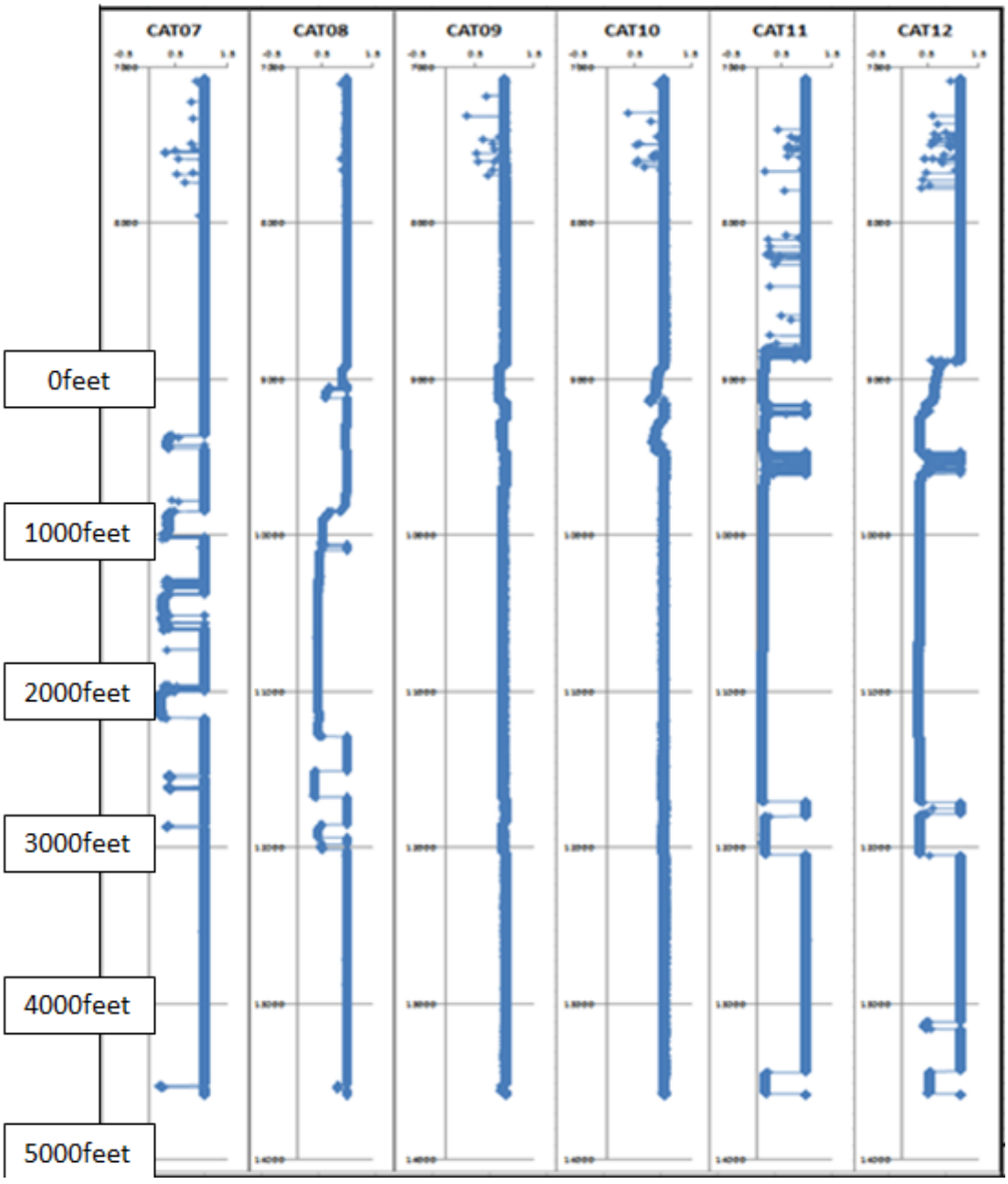

Fig. 3.18—Raw log data for capacitance array tool of Well 2 (CAT07-CAT12)

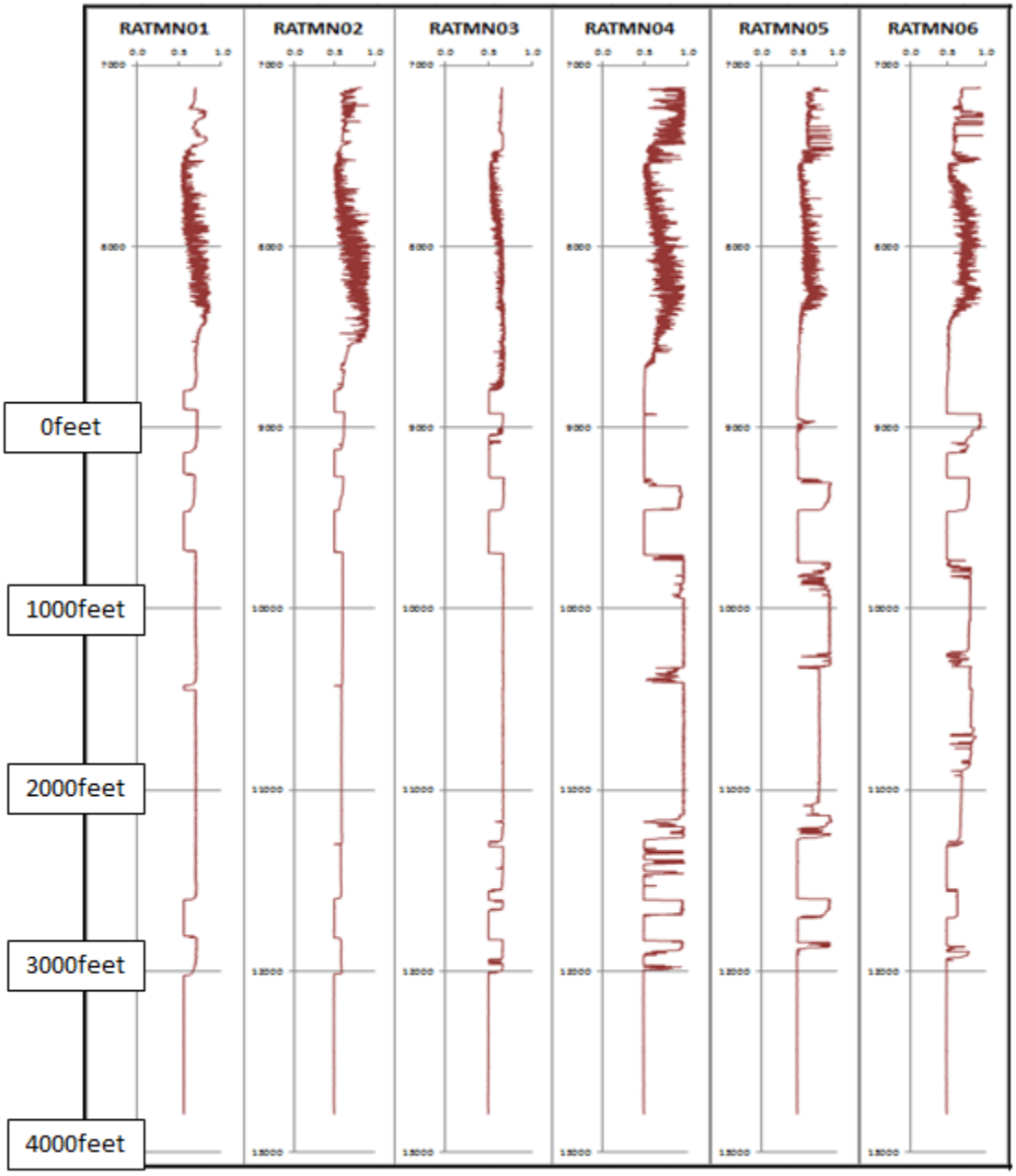

Fig. 3.19—Raw log data for resistivity array tool of Well 2 (RAT01-RAT06)

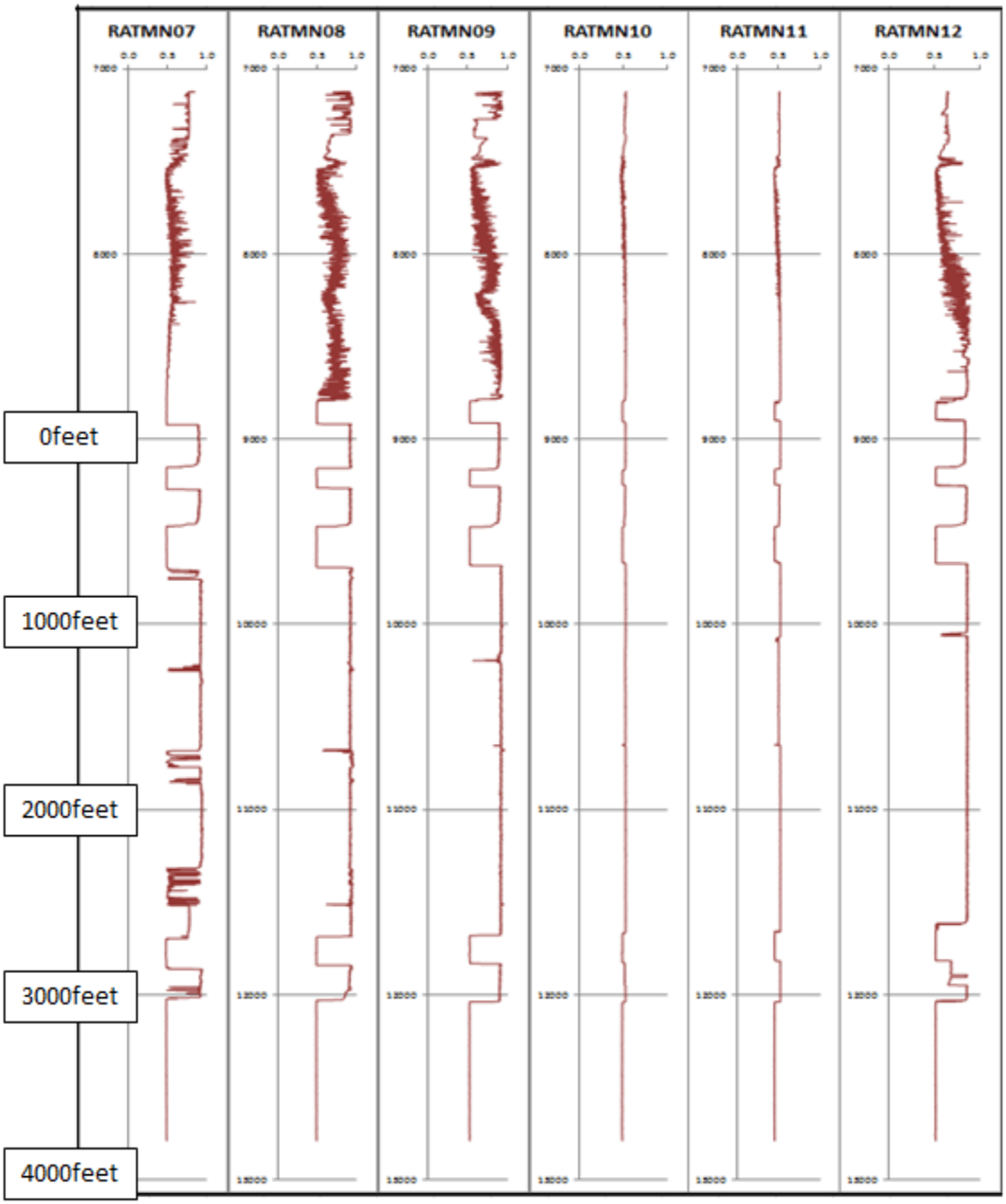

Fig. 3.20—Raw log data for resistivity array tool of Well 2 (RAT07-RAT12)

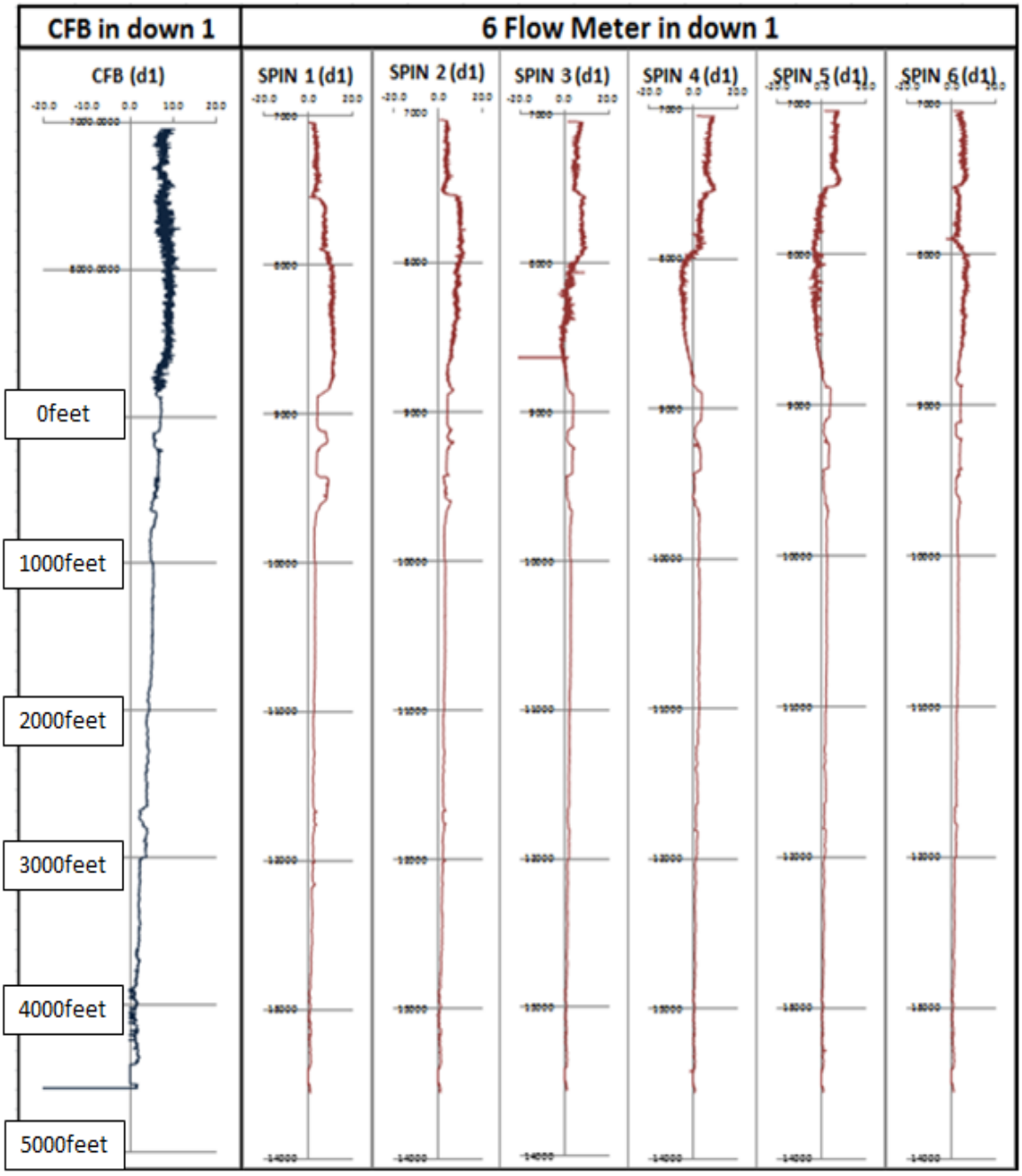

Fig. 3.21—Raw log data for spinner array tool of Well 2

According to production history, we knows that initial gas-liquid ratio (one-month average from Sep 4, 2011 to Oct 4, 2011) is higher than 10,000 scf/STB. The petroleum fluid is assumed to be gas condensate (McCain, et al. 2011). Therefore, the fluid type in Emeraude is set to gas condensate (dew point fluid) with water.

In order to process multiple probe tools' data, some PVT properties need to be specified to estimate the downhole condition, and these PVT properties are also used for interpretations of flow rate distribution along the wellbore and surface production rate. And also, the apparent velocities calculated based on spinner responses can be used as the tool constraints of the multiple probe tool processing.

In the inflow rate determination, we mainly match the data from multiple probe tools with the simulation results given by a certain set of inflow rate distribution. In the data matching, we used the velocity profile given by SAT, the gas and water holdups given by RAT and CAT, and gas rate distribution. Because the water rate data shows much higher amount of water (around 1600 STB/d at some locations) than the value at surface production (60 STB/d), it is not used for the inflow rate determination. The generated inflow distributions are shown in **Fig. 3.22**. In the estimation of inflow profiles, the surface production rate is used as the constraint of the problem.

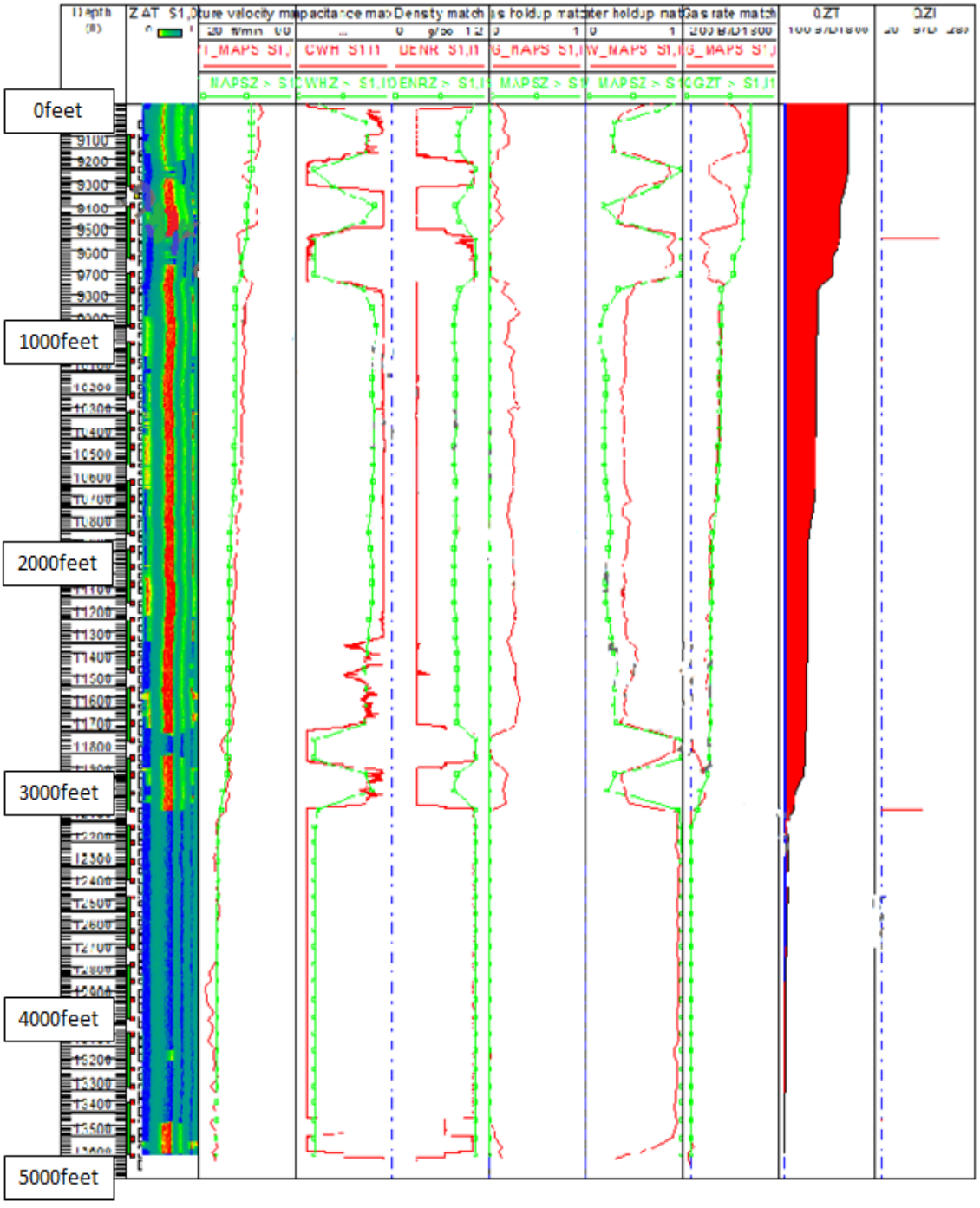

Fig. 3.22—Inflow rate prediction using multiple probe tools (Water sumps and temperature derivatives)

3.2.5 Comparison with results from new method

The following three plots show the production rate of gas, oil, and water. The dish line represents the result form company, the solid line represents the result from Emeraude and the points are results from new method.

The following plots presents the profiles of gas, oil, and water at surface condition translated from the downhole condition, with the oil rates being calculated by assuming a constant GOR and a single hydrocarbon phase (gas) at downhole temperature and pressure. The abnormal point at about 700 feet is caused by this point being a local trough and should be ignored.

Fig. 3.23 and **Fig. 3.24** are gas and oil flow profile show little production from the last two or three fractured intervals near the toe, then fairly uniform inflow over much of the well. About half of the total gas or oil inflow is interpreted to be entering from the first 1000 feet of wellbore from the heel.

Fig. 3.25 The interpreted water flow profile is more problematic. It is likely caused by inclination effects. The general trend of the water flow profile looks reasonable except for the anomalous values at 700 feet and at the station nearest the toe. However, the interpreted flow rates are actually negative, indicating backflow, from about 1800 feet from the heel all the way to the toe of the well.

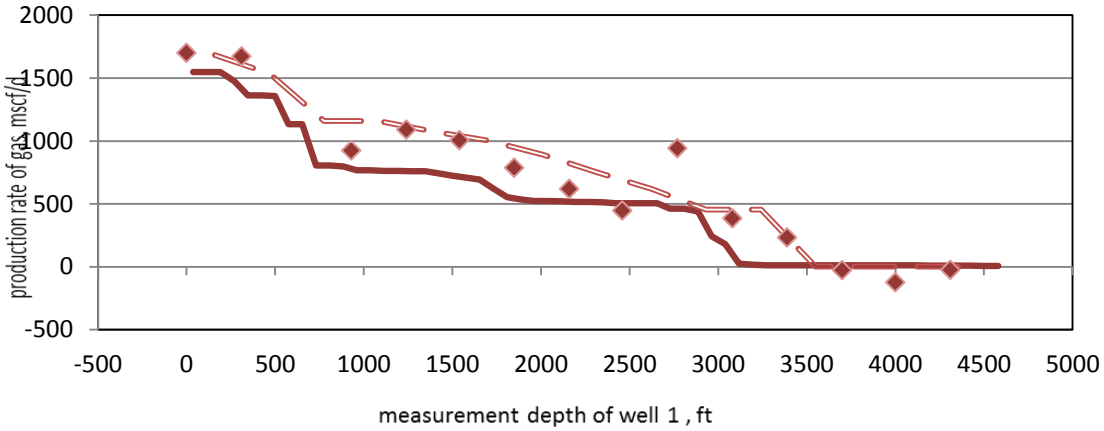

Fig. 3.23—Gas production rate in Well 2

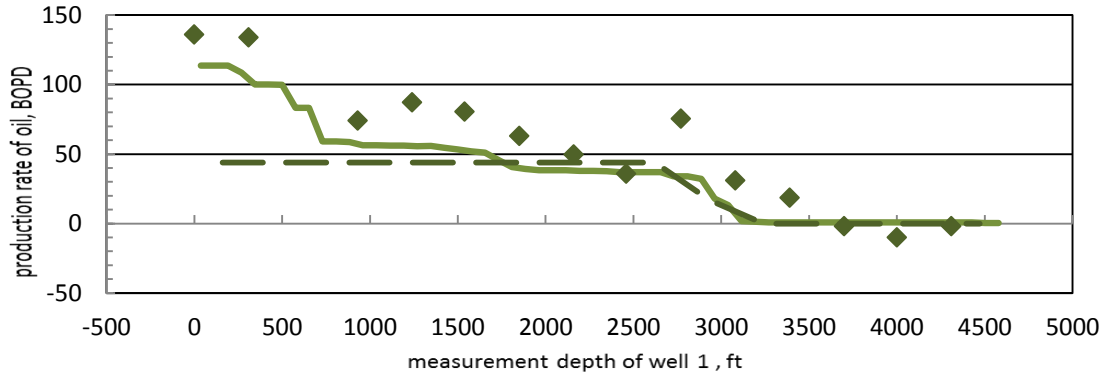

Fig. 3.24—Oil production rate in Well 2

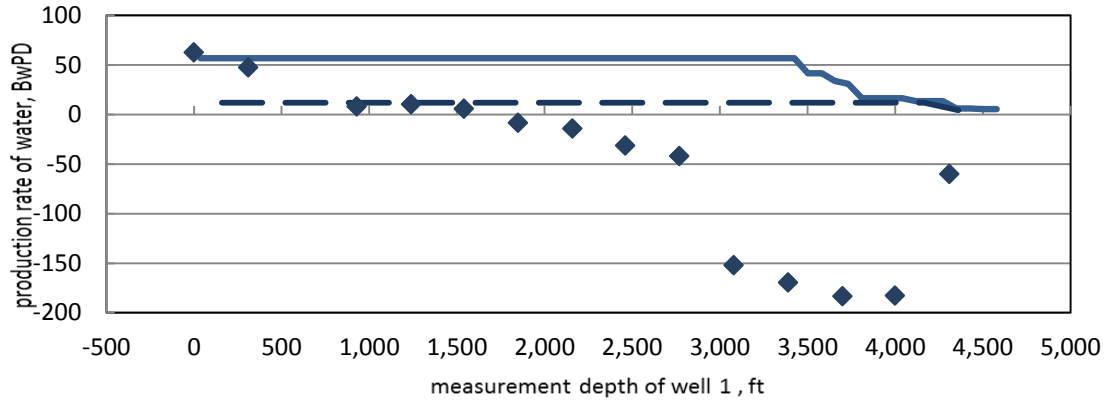

Fig. 3.25—Water production rate in Well 2

3.3 Interpretation of Well 3

3.3.1 Introduction of Well 3

The third example is a horizontal well with 15 stages of fracturing with the objective of estimating the rate contribution and fluid type from each perforation. The wellbore is about 5600 feet long in horizontal section. The well trajectory is shown in **Fig. 3.26**.

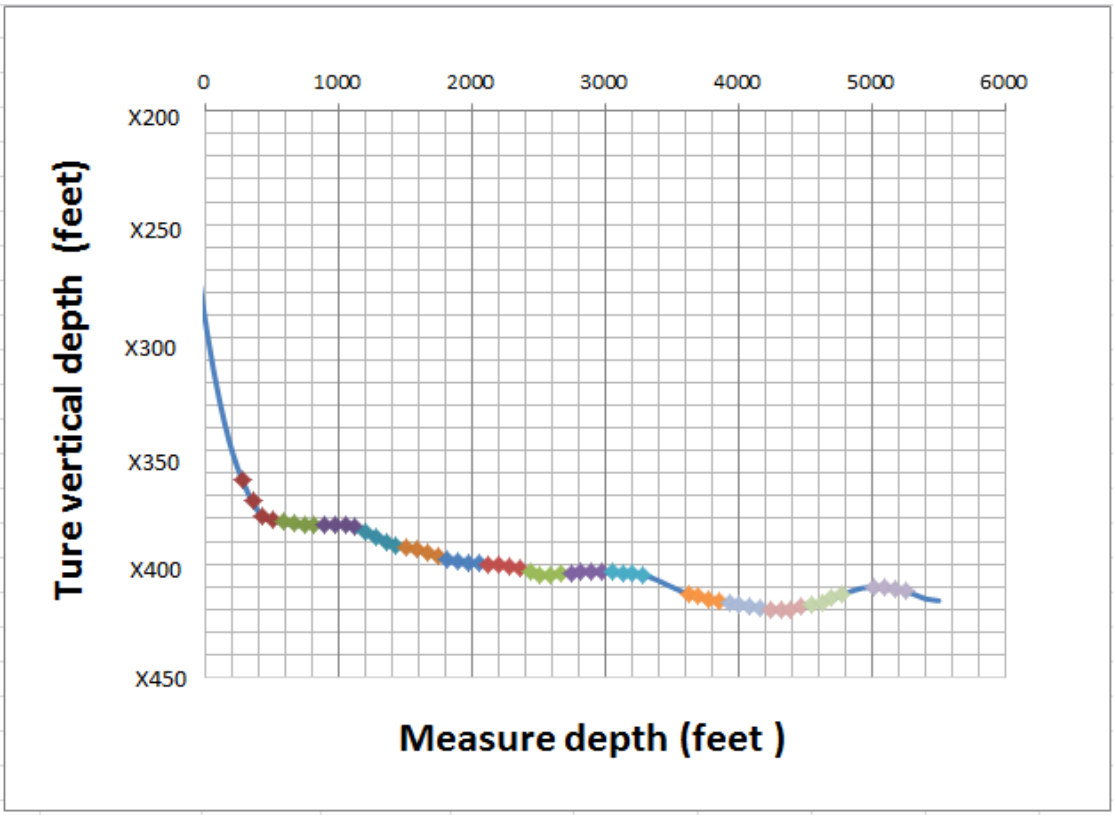

Fig. 3.26—Well trajectory with perforations of Well 3

Table 3.7 shows that Well 3 was producing 1900 standard cubic feet per day of gas, 170 standard barrel per day of oil and 40 standard barrel per day of water.

TABLE 3.7 SURFACE PRODUCTION DATA OF WELL 3

Fluid	Flow Rate
Gas	1900 [Mscf/D]
Oil	130 [STB/D]
Water	30 [STB/D]

Table 3.8 shows the fluid properties in Well 3, there we mainly use the average temperature is 240 F, the average pressure is 4632 psi, the average formation volume factor of gas and water are 0.0044 and 1.08, respectively.

TABLE 3.8 FLUID PROPERTIES OF WELL 3

Stage	*Depth, ft*	T_{wf}, *F*	P_{wf}, *psi*	B_{water}	B_{gas}
1	NA	242	4632	1.59	0.00443
2	4318	240	4633	1.36	0.00443
3	4010	241	4635	1.08	0.00442
4	3702	241	4634	1.08	0.00441
5	3394	241	4633	1.08	0.00442
6	3080	241	4632	1.23	0.00442
7	2778	240	4631	1.19	0.00442
8	2470	240	4631	1.15	0.00442
9	2162	240	4630	1.11	0.00441
10	1849	240	4633	1.08	0.00441
11	1546	239	4631	1.10	0.00440
12	1238	239	4633	1.11	0.00440
13	930	239	4639	1.08	0.00440
14	622	239	4634	1.08	0.00440
15	314	239	4633	1.08	0.00440

3.3.2 Application of new method

As we know if the dew point pressure is higher than the actual pressure, there will be oil and gas production in the well. So in the following method we should consider three phase, gas, oil, and water. **Fig. 3.27** shows the fluid distributions at 15 stations. Similar to the example before, each station is divided into 5 sections, and the oil gas, and water in the section is determined by the RAT and CAT values. Firstly, if the RAT value is smaller than 0.73 and CAT value is larger than 1.04, the section is producing water, if the CAT value is larger than 1.00 and also small than 1.04, then we assign oil. Finally, the rest parts all produce gas.

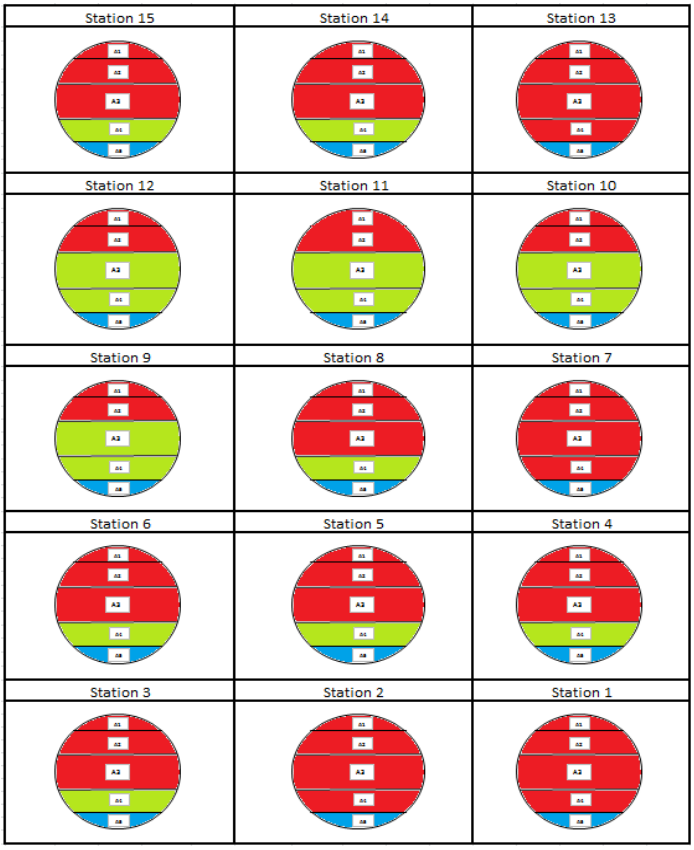

Fig. 3.27—Distribution of 3 phases at 15 stations of Well 3

We first translate standard production rate into actual production rate at 50 feet.

$$q_{g,act} = \frac{1.9\times10^{6}\,Mscf\times B_g}{24days\times60hours} = \frac{1.9\times10^{6}\times0.0044}{24\times60} = 6.993\,ft^3/\min \tag{3.14}$$

$$q_{o,act} = \frac{130BOPD\times B_o\times5.615}{24days\times60hours} = \frac{130\times1.08\times5.615}{24\times60} = 0.563\,ft^3/\min \tag{3.15}$$

$$q_{w,act} = \frac{30BWPD\times B_w\times5.615}{24days\times60hours} = \frac{30\times1.04\times5.615}{24\times60} = 0.123\,ft^3/\min \tag{3.16}$$

Then we determine the distribution of 3 phases by interpreting RAT and CAT data. The distribution of 3 phases at heel station is shown in **Fig. 3.28**.

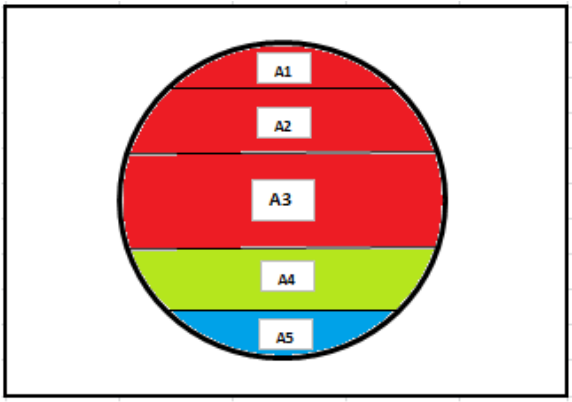

Fig. 3.28—Distribution of 3 phases at 50 feet of Well 3

Gas Area Division

$$A_g = A_1 + A_2 + A_3 = 0.010806 + 0.029291 + 0.038756 = 0.078853\,ft^2$$

$$v_g = \frac{q_{g.act}}{A_g} = \frac{6.993\,ft^3/\min}{0.078853\,ft^2} = 88.68\,ft/\min \tag{3.17}$$

The spinner response correlates with SPIN01, SPIN02, SPIN03, SPIN05 and SPIN06. SPIN06, the reading at sensor #1 to sensor #6, **Table A.2** shows the value of each sensor.

$$f_{g+o} = 0.1\times(SPIN03 + SPIN05) + 0.2\times(SPIN02 + SPIN06) + 0.3\times SPIN01$$

$$= 0.1\times(1.7286 + 1.6116) + 0.2\times(4.4216 + 2.9603) + 0.3\times 8.1662$$

$$= 4.42727 rps \tag{3.18}$$

Then we can get the velocity conversion coefficient m_{pg} from the heel station,

$$m_{pg} = \frac{v_g}{f_g} = \frac{88.68\, ft/\min}{4.42727 rps} = 20.03 \tag{3.19}$$

Oil production section is A_4 ($0.02921\, ft^2$), so

$$v_o = \frac{q_{o,qct}}{A_o} = \frac{0.563\, ft^3/\min}{0.02921\, ft^2} = 19.22\, ft/\min \tag{3.20}$$

The spinner response correlates with SPIN03 and SPIN05.

$$f_o = 0.5\times(SPIN03 + SPIN05) = 0.5\times(1.8278 + 1.6065) = 1.6701 rps \tag{3.21}$$

Then we can get the velocity conversion coefficient m_{po} from the heel station

$$m_{po} = \frac{v_o}{f_o} = \frac{19.22\, ft/\min}{1.6701 rps} \tag{3.22}$$

For water production, the area is A_5 ($0.010806\, ft^2$), thus,

$$v_w = \frac{q_{w.act}}{A_w} = 11.39\, ft/\min \tag{3.23}$$

The spinner response correlates with SPIN03 and SPIN05.

$$f_w = SPIN04 = 1.3511 rps \tag{3.24}$$

We get velocity conversion coefficient m_{pw} from the heel station,

$$m_{pw} = \frac{v_w}{f_w} = \frac{11.39\, ft/\min}{1.3511 rps} = 8.44 \tag{3.25}$$

Finally, we calculate spinner response of 3 phases at each station

$$v_{gi} = m_{pg} f_{gi} = 20.03 f_{gi} \tag{3.26}$$

$$v_{oi} = m_{po} f_{oi} = 11.51 f_{oi} \tag{3.27}$$

$$v_{wi} = m_{pw} f_{wi} = 8.44 f_{wi} \tag{3.28}$$

Table 3.9 shows different value $f_{(g+o)i}$ of each section in 15 stations of Well 3.

TABLE 3.9 SPINNER RESPONSES AT DIFFERENT SECTIONS OF 15 STATIONS OF WELL 3

STATION	DEPT feet	P1	P2	P3 (rps)	P4	P5
station 1	4990	0.8634	0.7360	0.6647	0.5935	0.0509
station 2	4490	1.4621	1.1098	1.0485	0.9871	0.8011
station 3	4200	1.7858	1.2675	1.1978	1.1282	1.0402
station 4	3900	1.6152	1.3693	1.2902	1.2111	1.1390
station 5	3500	2.4337	1.1686	0.9769	0.7853	0.6524
station 6	3000	3.2152	1.7715	1.4729	1.1742	1.0773
station 7	2700	2.1670	1.8634	1.8105	1.7577	1.3680
station 8	2400	4.3333	1.8239	1.2120	0.6002	0.2708
station 9	2100	6.1312	2.1223	1.5096	0.8968	0.8323
station 10	1800	5.8354	1.9077	1.5162	1.1248	1.0967
station 11	1500	6.9238	2.9424	1.8487	0.7551	0.5375
station 12	1190	7.3157	2.7276	1.8726	1.0177	0.2650
station 13	850	3.4516	3.5418	3.3614	3.1811	2.9395
station 14	550	8.1662	3.6910	2.6805	1.6701	1.3511
station 15	270	11.1967	5.7150	2.9657	0.2165	-1.3257

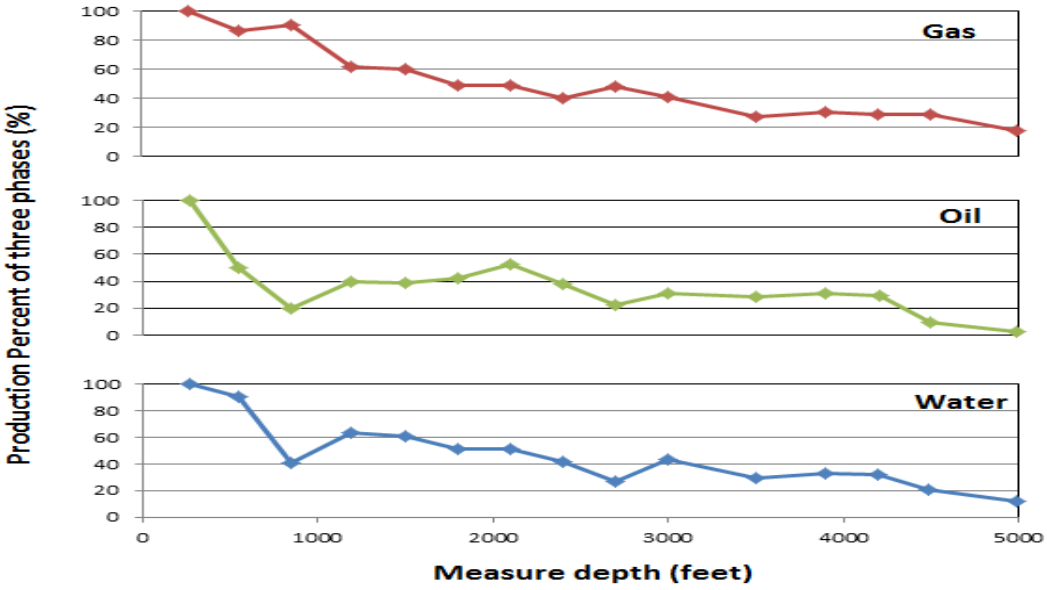

Fig. 3.29—Percent production rate of three phases of Well 3 at surface conditions

The interpreted volumetric rate profiles of gas, oil and water in actual volumetric flow rate at surface condition are shown in **Fig. 3.29**. The gas flow profile shows most half of the total gas inflow is interpreted to be entering from station 13 to station 15 near the heel. The oil and water flow profiles not looks good, that caused by the low production rate and well inclination effects.

3.3.3 Application of commercial software interpretation

Fig.3.30 through **Fig.3.35** show raw log data for centralized tool, capacitance array tool (CAT), resistivity array tool (RAT) and spinner array tool (SAT) and image views given by these multiple probe tools.

In the creation of image views from CAT data, the data from string number 12 is

ignored because all of the values given by the probe shows higher values than the maximum of the tool measurement range. In addition, the CAT data is calibrated by normalizing them between 0 and 1 with minimum and maximum value of the measurement.

The original log data have several spikes which are measurement noises. These are masked by tool (these are colored in gray in the data plots). In the following interpretation, these spikes are ignored.

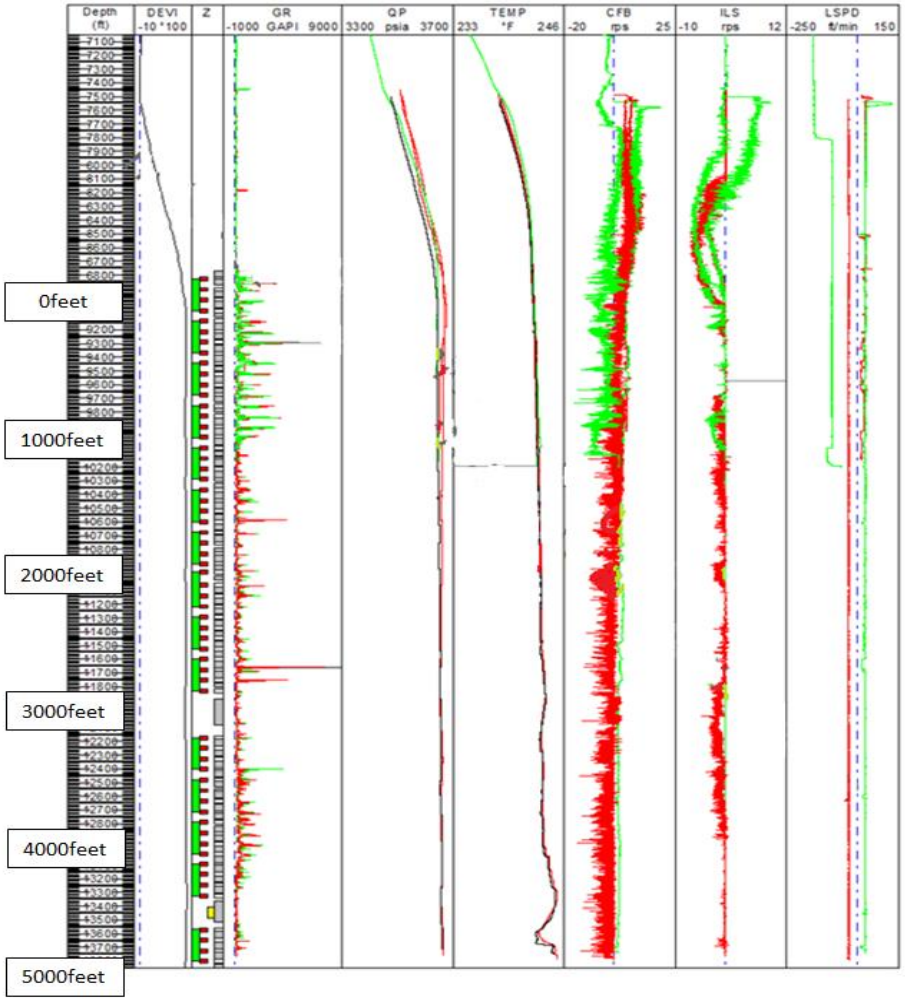

Fig. 3.30—Raw log data for centralized tools of Well 3

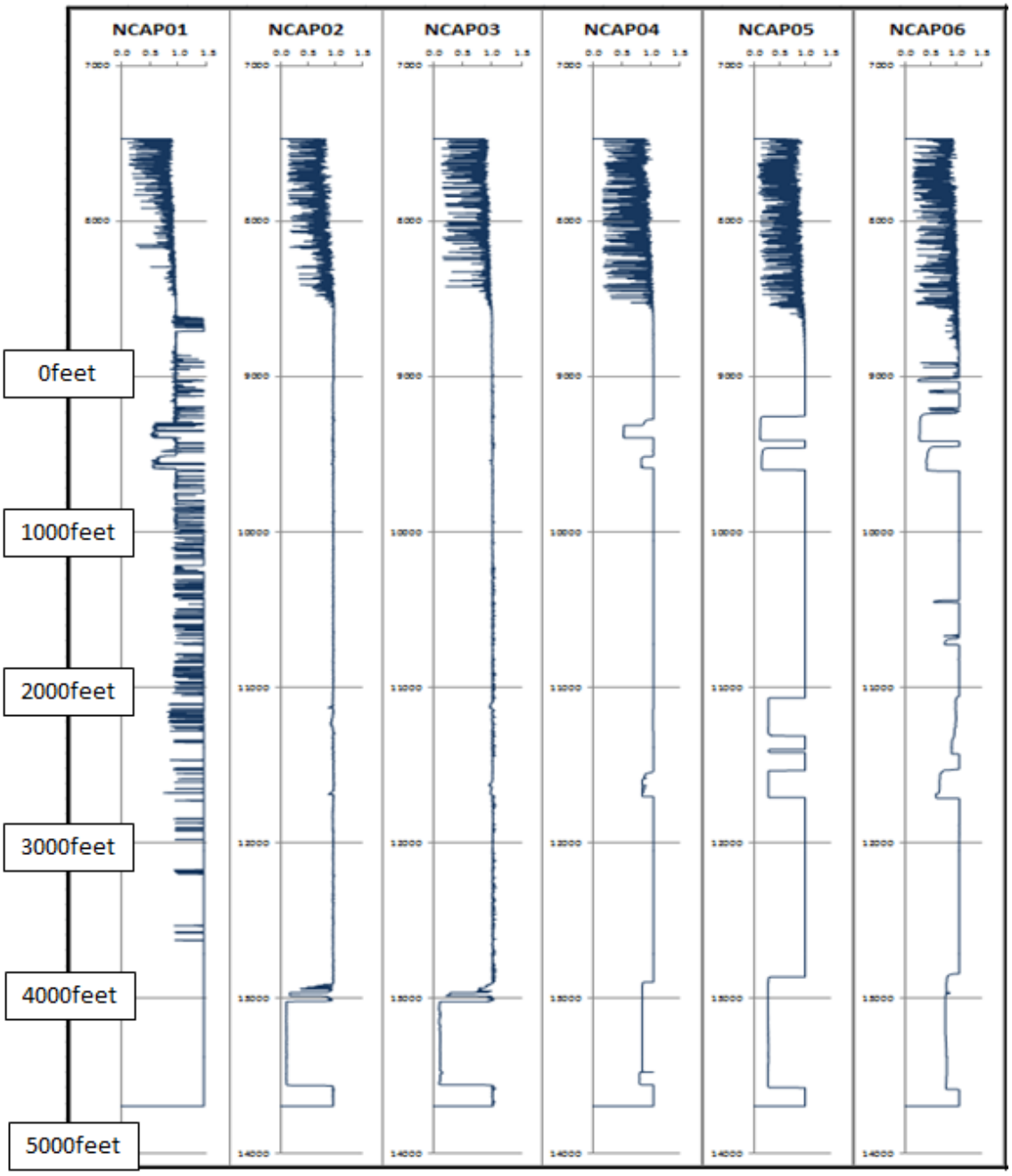

Fig. 3.31—Raw log data for capacitance array tool of Well 3 (CAT01-CAT06)

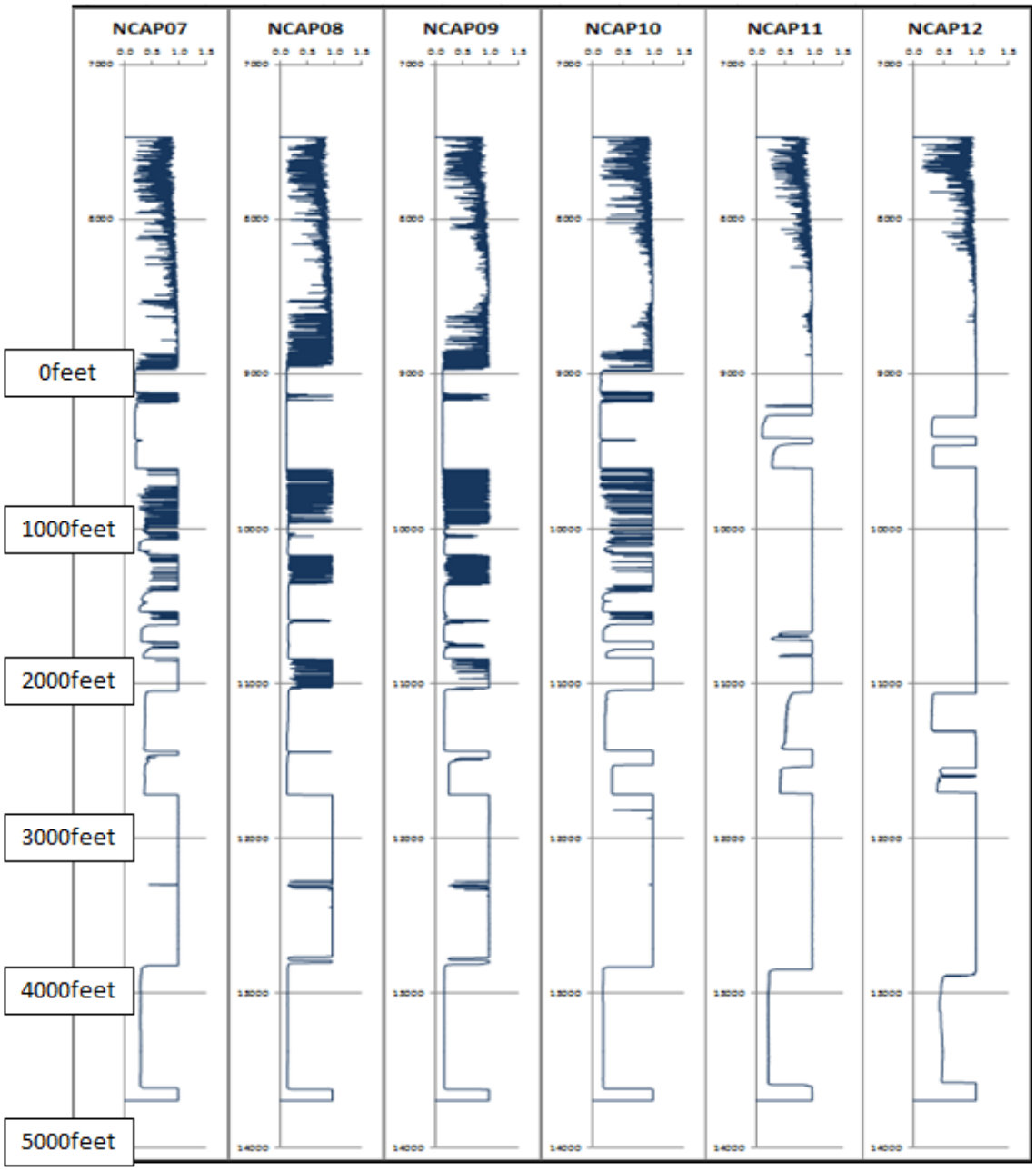

Fig. 3.32—Raw log data for capacitance array tool of Well 3 (CAT07-CAT12)

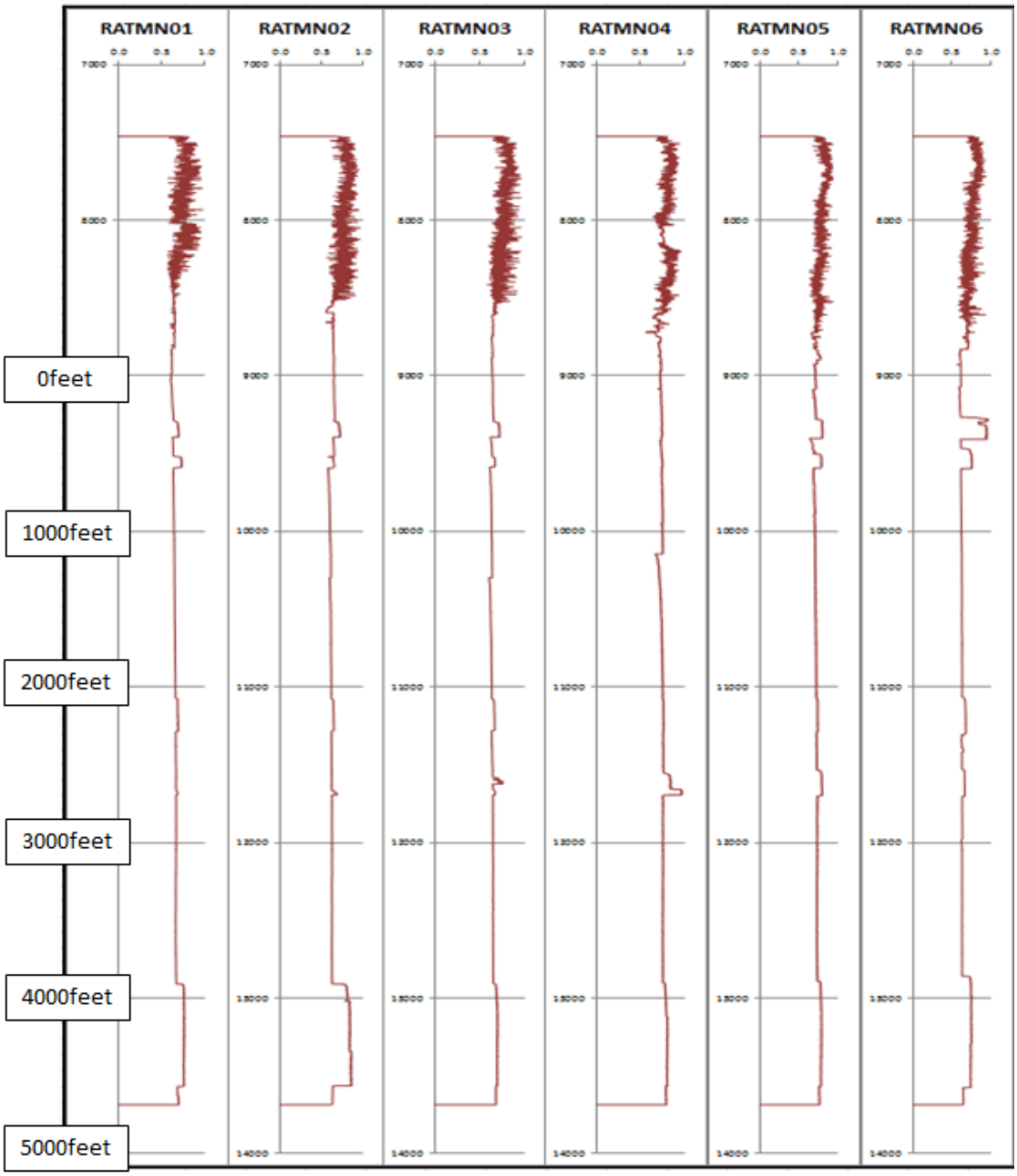

Fig. 3.33—Raw log data for resistivity array tool of Well 3 (RAT01-RAT06)

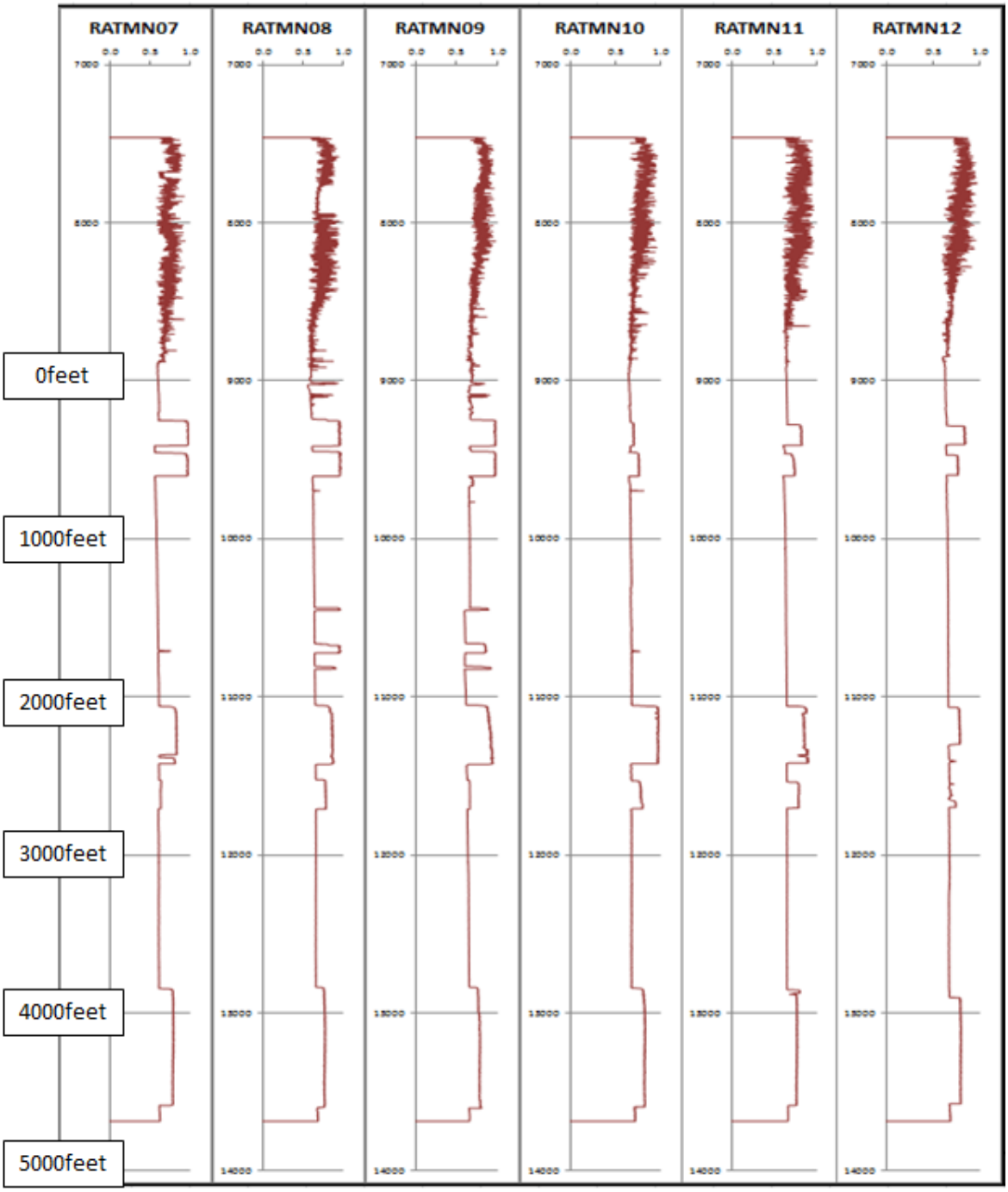

Fig. 3.34—Raw log data for resistivity array tool of Well 3 (RAT07-RAT12)

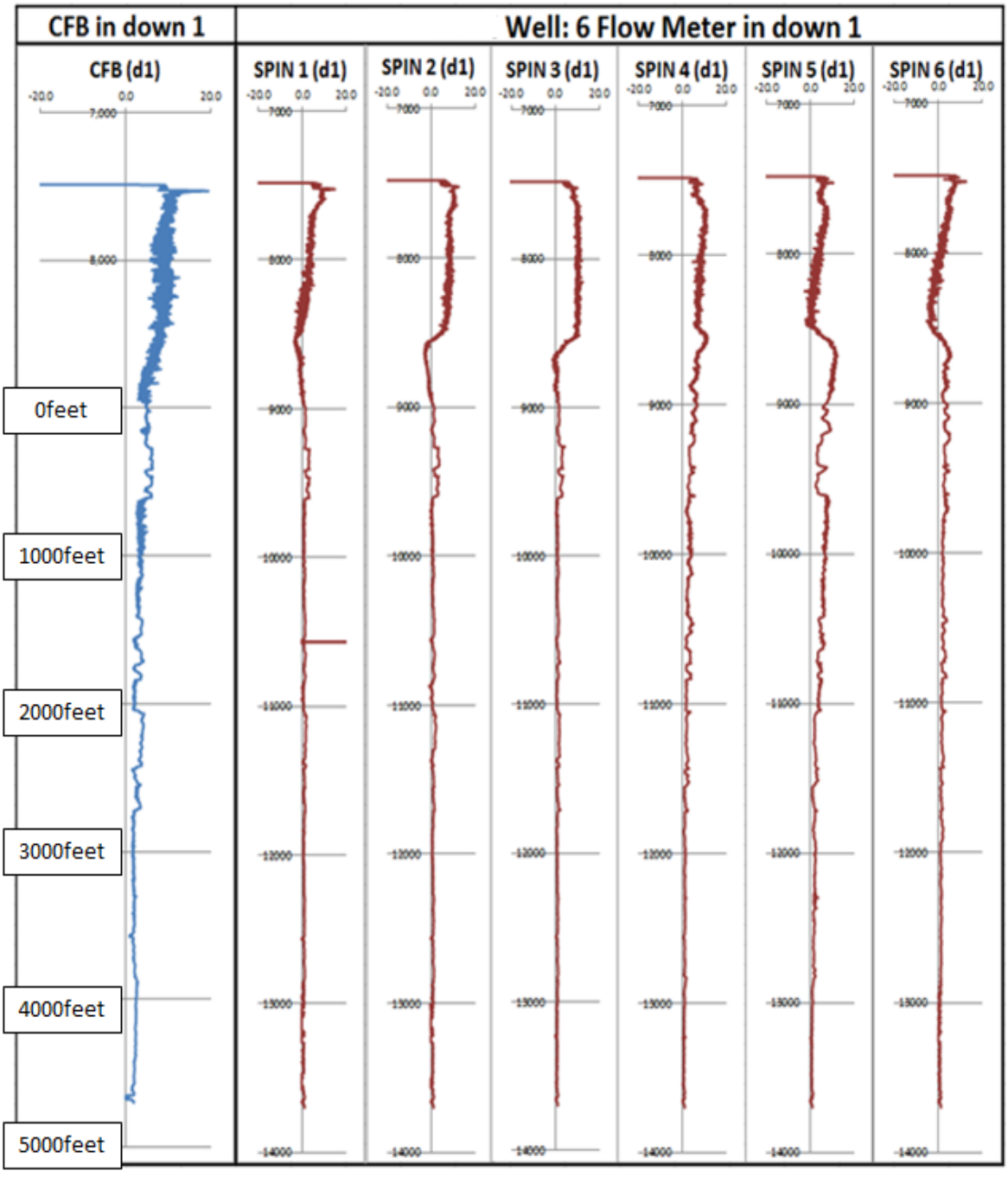

Fig. 3.35—Raw log data for spinner array tool of Well 3

In the inflow rate determination, we match the data from tools with the simulation results given by a certain set of inflow rate distribution. In the data matching, we used the mixture velocity profile given by SAT, the gas holdup given by CAT and RAT, the gas and water holdups given by CWH and GHT and the density profile. As shown in **Fig. 3.36**, the water holdup given by CAT and RAT has inconsistent trend with the other measurements (e.g. density log), the data is not used in the determination of inflow profile. The generated inflow distributions are shown in **Fig. 3.37**. In the estimation of inflow profiles, the surface production rate is used as the constraint of the problem.

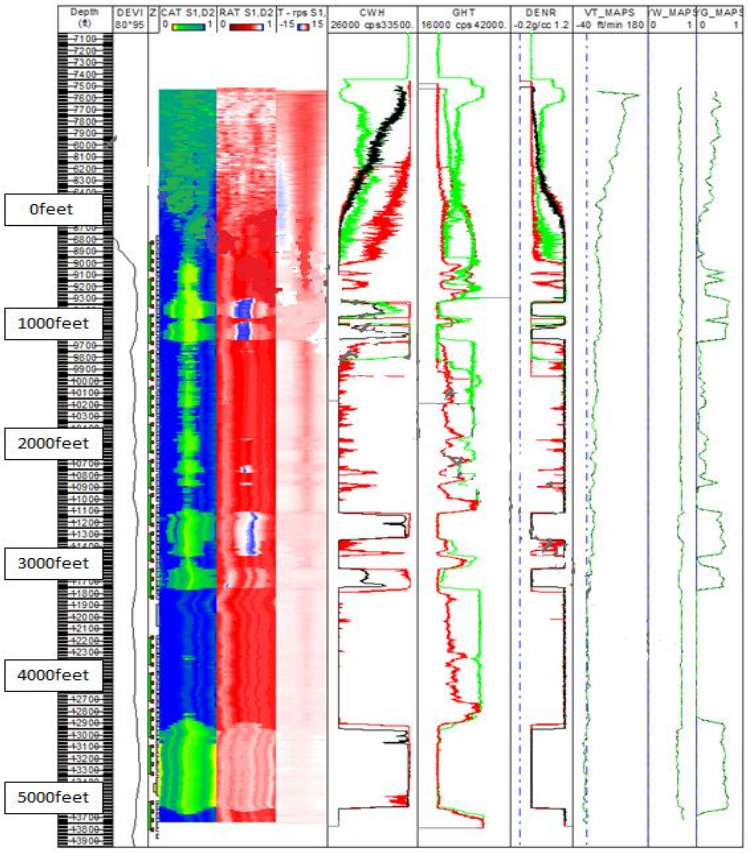

Fig. 3.36—Physical interpretation wellbore flow condition of Well 3

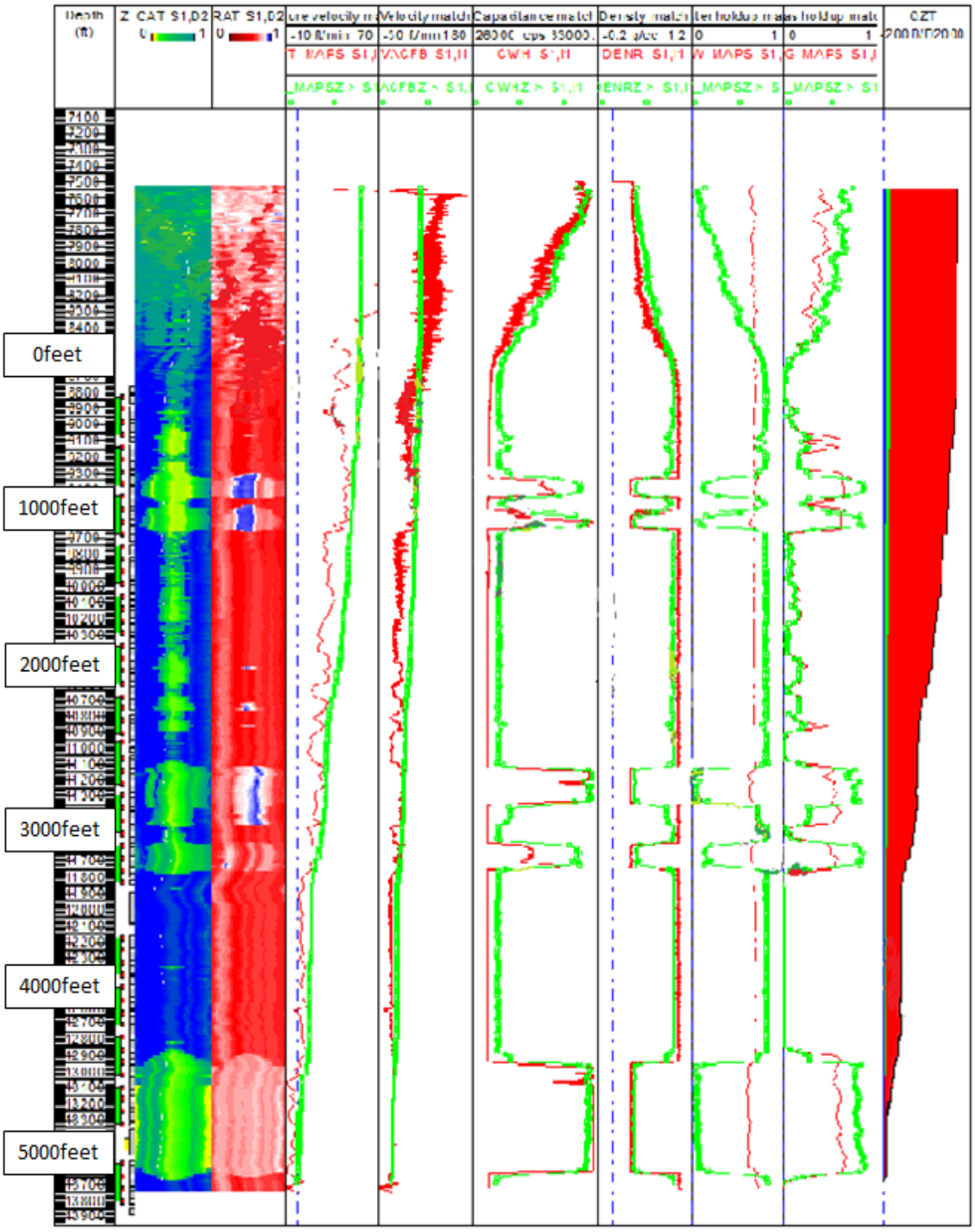

Fig. 3.37—Inflow rate prediction using multiple probe tools of Well 3

3.3.4 Comparison with the result from new method

Fig. 3.38 shows the gas flow rate, the results by Halliburton and the results given by Emeraude have good agreement in the global trend though the result by the new method shows lower flow rate in the middle region (500 feet – 1,500 feet).

For oil **Fig. 3.39** and water flow **Fig. 3.40** rate, the results given by the Emeraude and the new method show good agreement with each other and with surface production rate. Though the Halliburton interpretation considers the surface production as constraints, their interpretation has difference from the surface production they used.

Cumulative liquid volume (oil and water) of each method near the heel is almost the same as calculated from surface conditions, though the inflow trend of the liquid phase is different between Halliburton results and ours (Emeraude and new method) because they used zone inflow calculation to avoid unrealistic results and extreme computational time in their interpretation.

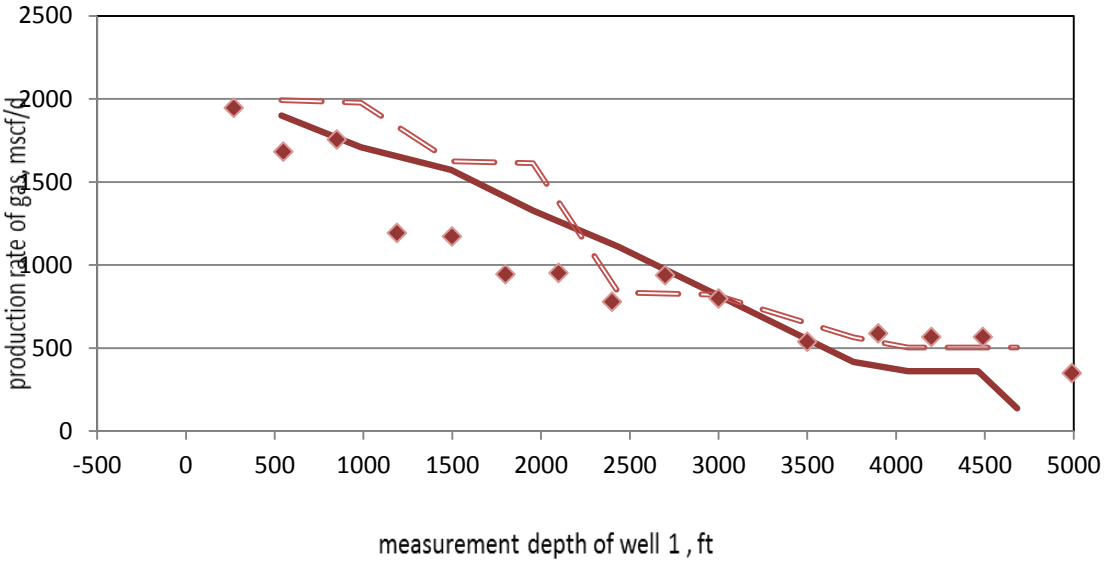

Fig. 3.38—Gas production rate in Well 3

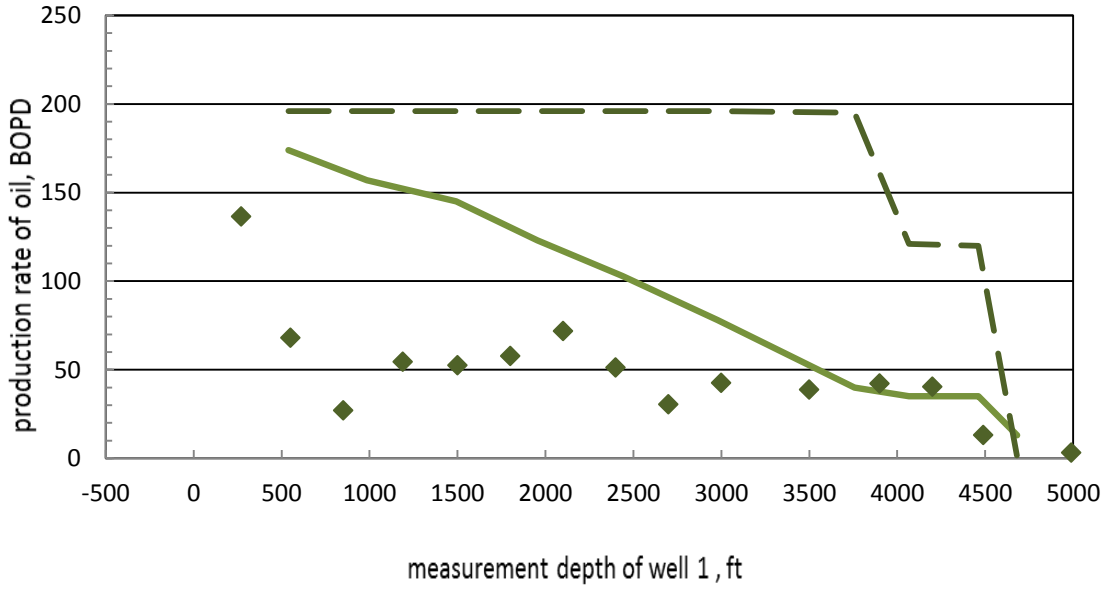

Fig. 3.39—Oil production rate in Well 3

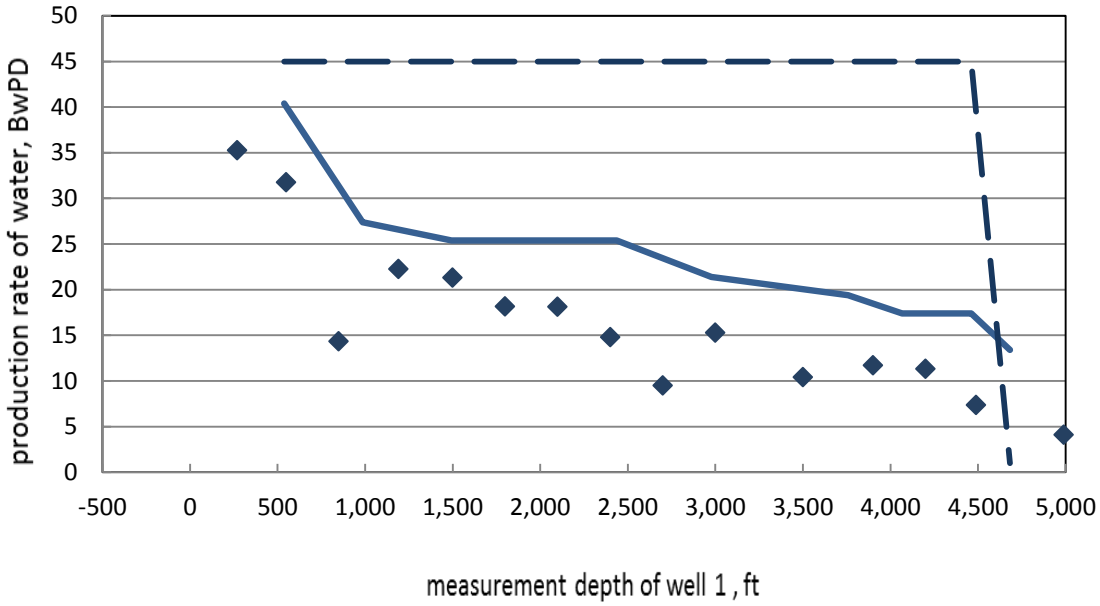

Fig. 3.40—Water production rate in Well 3

4. SUMMARY AND CONCLUSIONS

We have developed a method to interpret array production logging tools to interpret the flow rate profiles of multiple phases. In this method, array spinner flowmeters are calibrated for their response to each phase by synchronizing the response at a heel location to the known surface volumetric flow rates of individual phases.

- In highly deviated and horizontal wells, traditional PL sensors may not prove the most accurate data as a result of the wellbore and well flowing conditions. A sample and effective calibration of SAT response at a heel location was presented in this report.
- Comparing with commercial software, a reasonable gas flow profile was obtained.
- While the water flow profile was jeopardized by low water flow rates and well inclination effects and the big difference occurred between commercial software and new method also showed this situation.
- In the following work, we could consider about calculation of multiphase under downhole conditions by using multi-pass method.

REFERENCES

Al-Belowi, A. R et al. (2010). "Production Logging in Horizontal Wells: Case Histories from Saudi Arabia Utilizing Different Deployment and Data Acquisition Methodologies in Open Hole and Cased Completions." Abu Dhabi International Petroleum Exhibition and Conference. Abu Dhabi, UAE, Society of Petroleum Engineers.

Curtis, M. R. (1967). "Flow Analysis in Producing Wells." Member AIME, Schlumberger Well Services, Houston, Texas. Annual Fall Meeting of the Society of Petroleum Engineers of AIME, Houston. Tex.

Dale, C. R (1949). "Bottom Hole Flow Surveys for Determination of Fluid and Gas Movements in Wells." *Trans.*, AIME **186**, 205-10.

Hill, A. D (1900): *Production Logging – Theoretical and Interpretive Elements*, SPE Monogragh, Vol.14, Society of Petroleum Engineers.

Leach, B. D. et al. (1974). "The Full Bore Flowmeter." Fall Meeting of the Society of Petroleum Engineers of AIME, Houston.

McCain, J. W. D., et al. (2011). "Petroleum Reservoir Fluid Property Correlations." Tulsa, Okalahoma, Penn Well Publishing Company.

Millikan. C. (1941). "Temperature Surveys in Oil Wells." Trans., AIME 142: 15-23.

Peebler, B. (1982): "Multipass Interpretation of the Full Bore Spinner." Schlumberger, Houston.

Riddle, G. (1962). "Acoustic Wave Propagation in Bonded and Unbonded Oil Well Casing." Fall Meeting of the Society of Petroleum Engineers of AIME, Los Angeles.

Riordan, M. (1951). "Surface Indicating Pressure, Temperature and Flow Equipment." *Trans.*, AIME **192**, 257-62.

Schlumberger, M., et al. (1937): "Temperature Measurements in Oil Wells." *J. Inst. Pet. Technologists* **23**, No. 159.

Zett. A., et al. (2011). "New Sensor Development Helps Optimise Production Logging Data Acquisition in Horizontal Wells." Society of Petrophysicists and Well Log Analysts, Colorado Springs.

APPENDIX

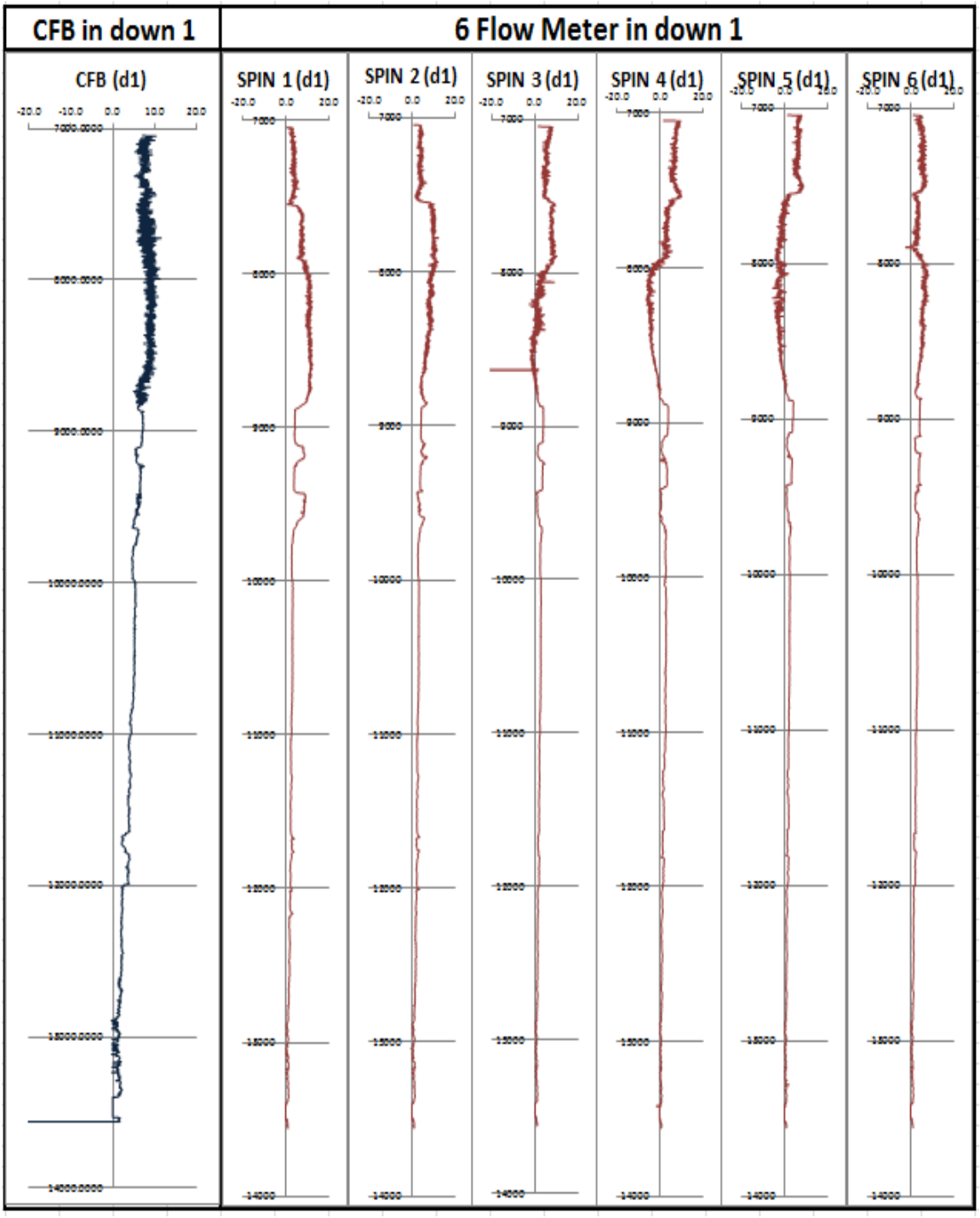

Appendix.1 SAT data of down 1 pass of well 2

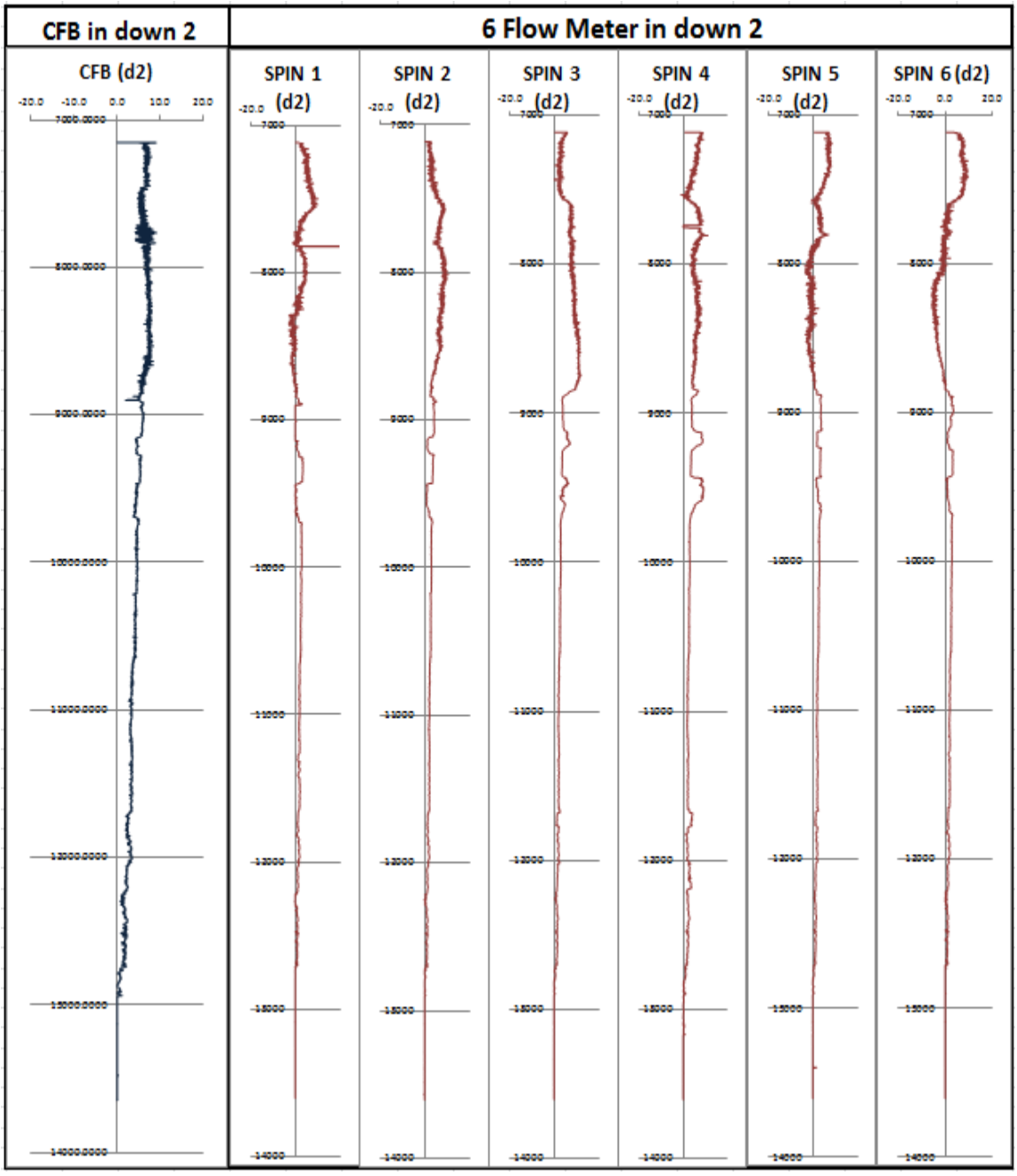

Appendix.2 SAT data of down 2 pass of well 2

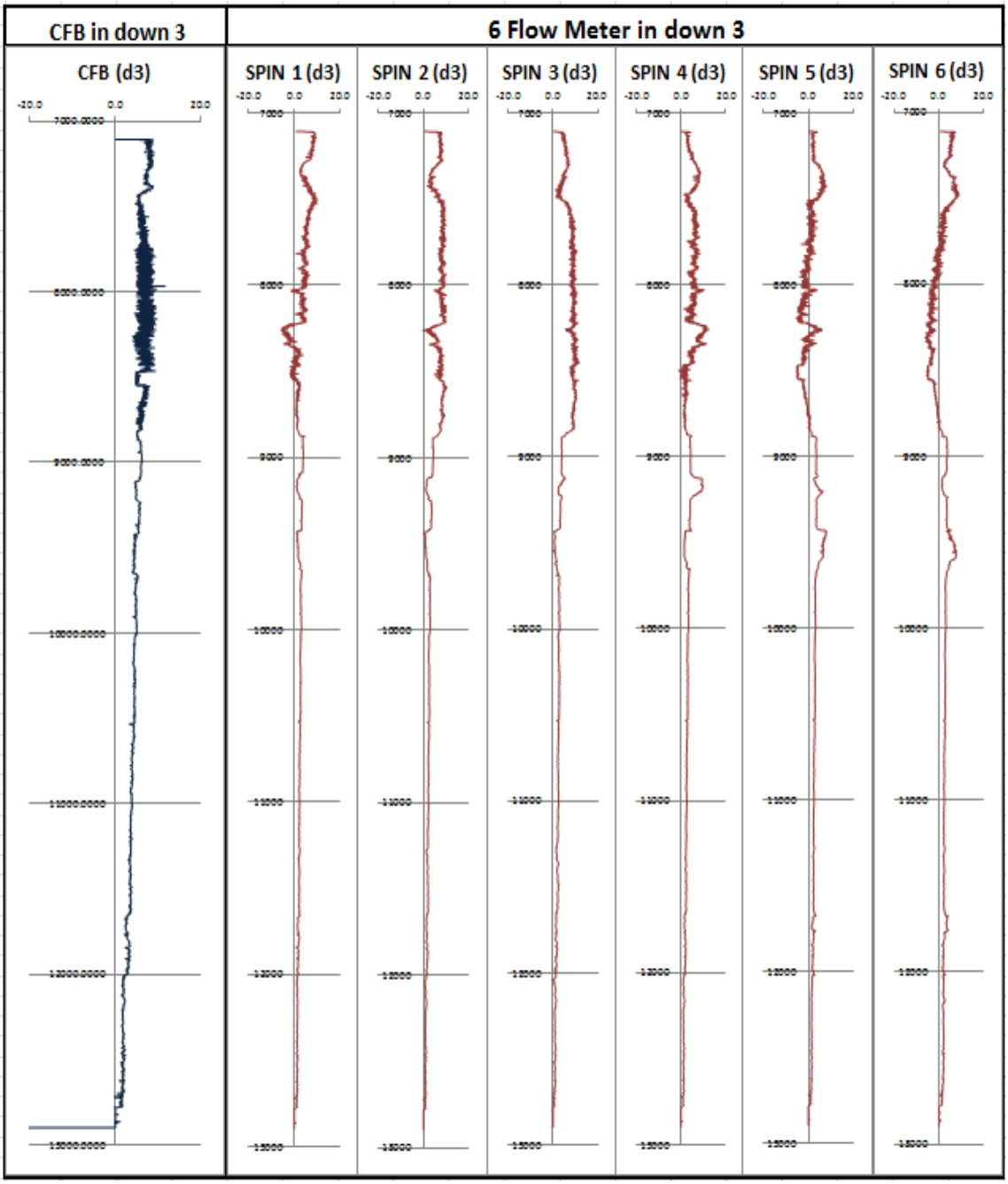

Appendix.3 SAT data of down 3 pass of well 2

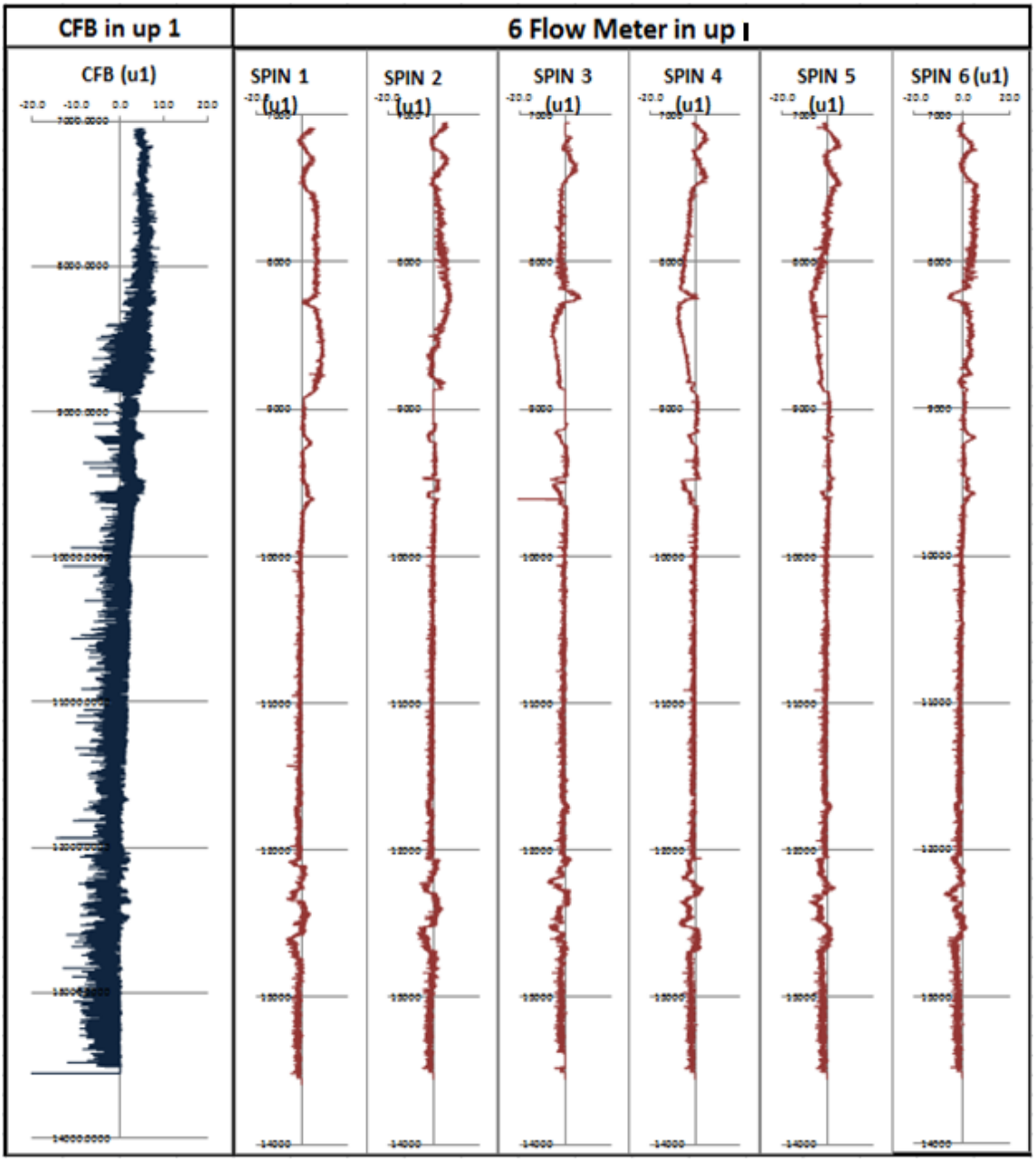

Appendix.4 SAT data of up 1 pass of well 2

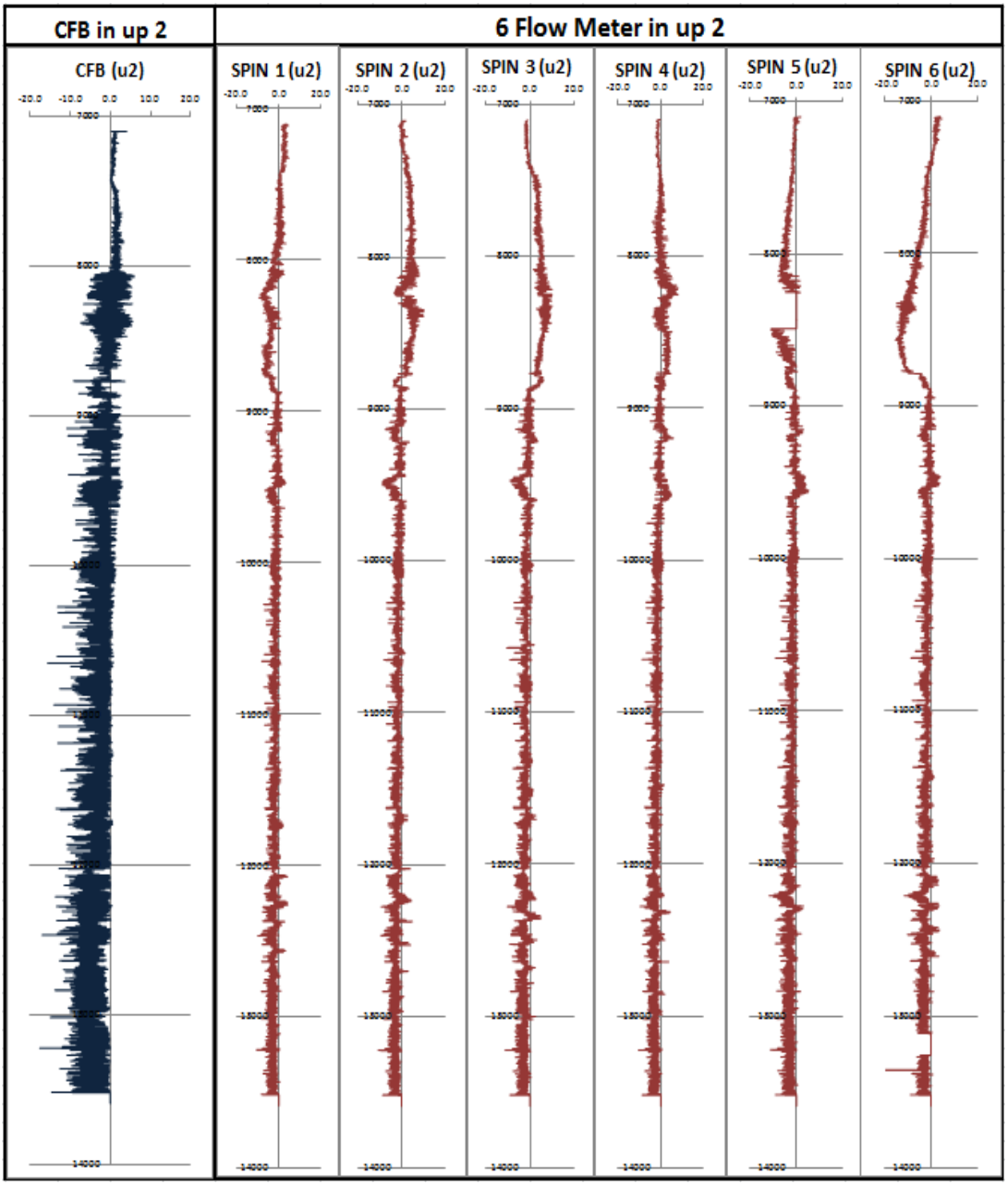

Appendix.5 SAT data of up 2 pass of well 2

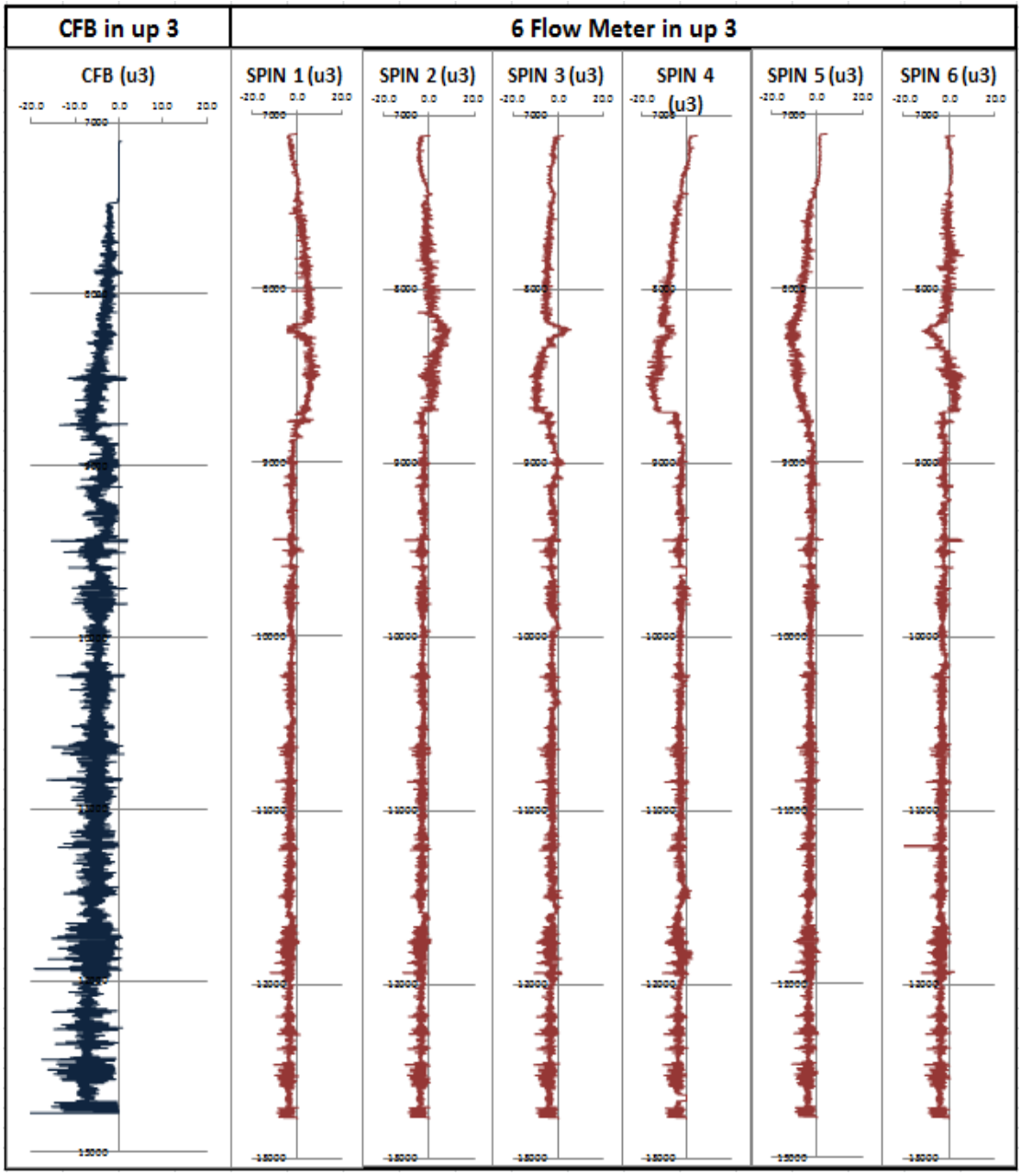

Appendix.6 SAT data of up 3 pass of well 2

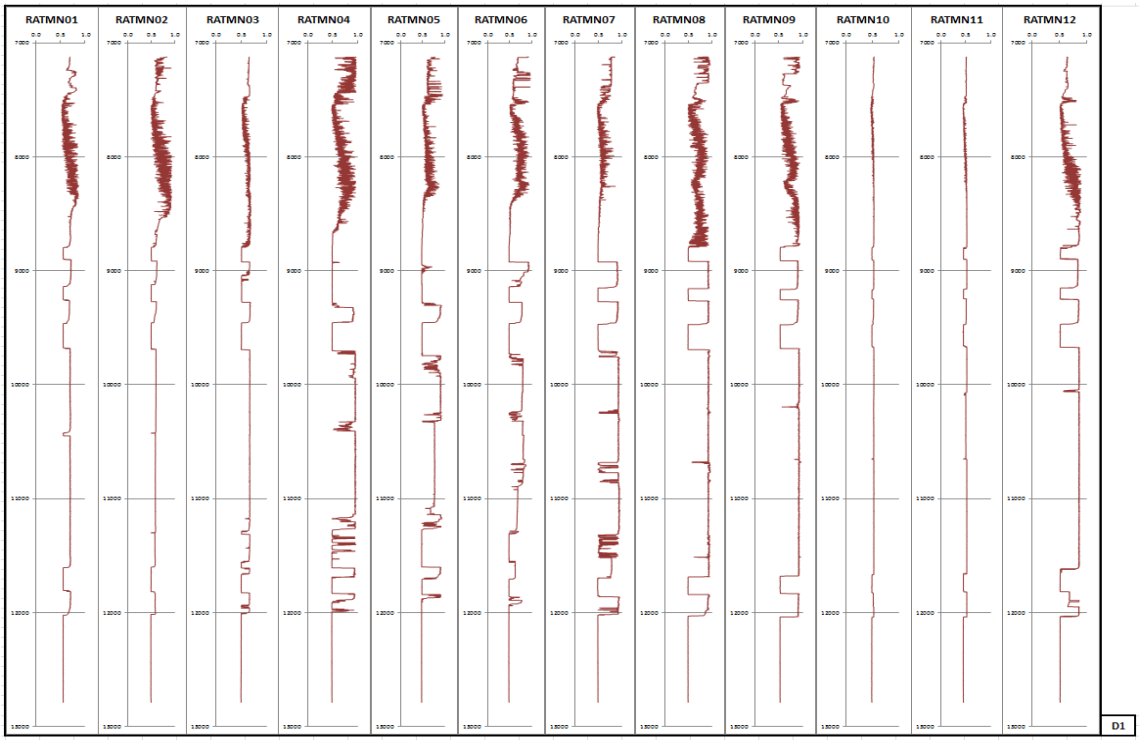

Appendix.7 RAT data of down 1 pass of well 2

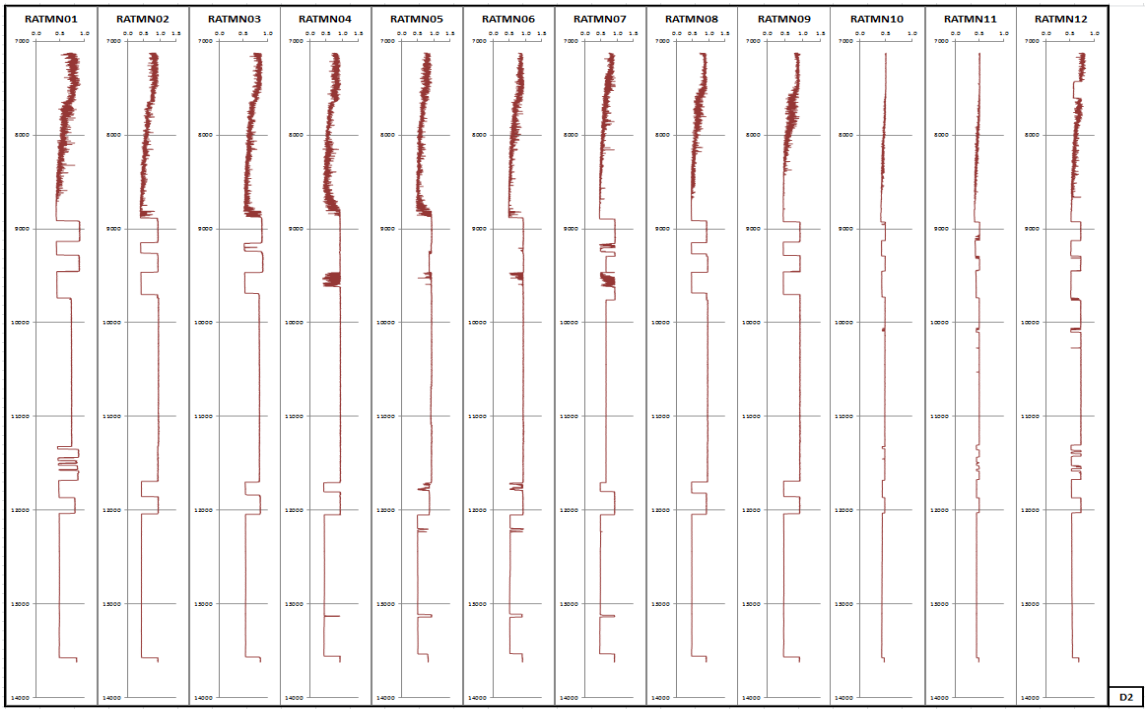

Appendix.8 RAT data of down 2 pass of well 2

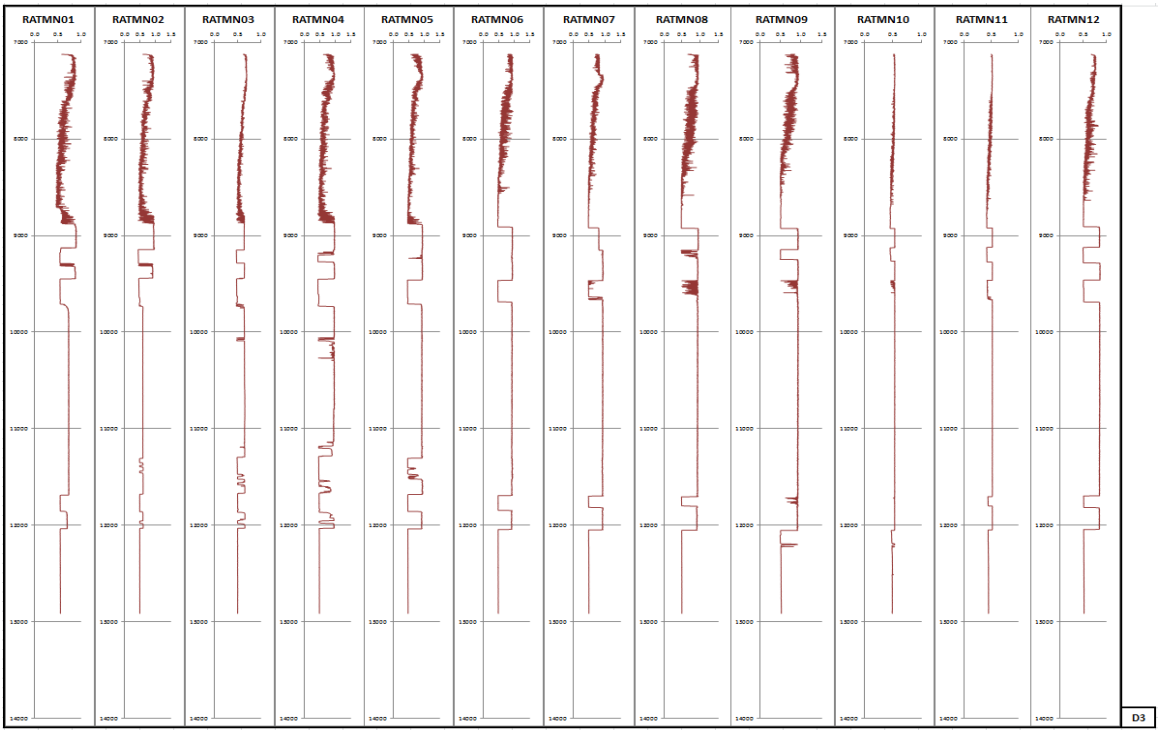

Appendix.9 RAT data of down 3 pass of well 2

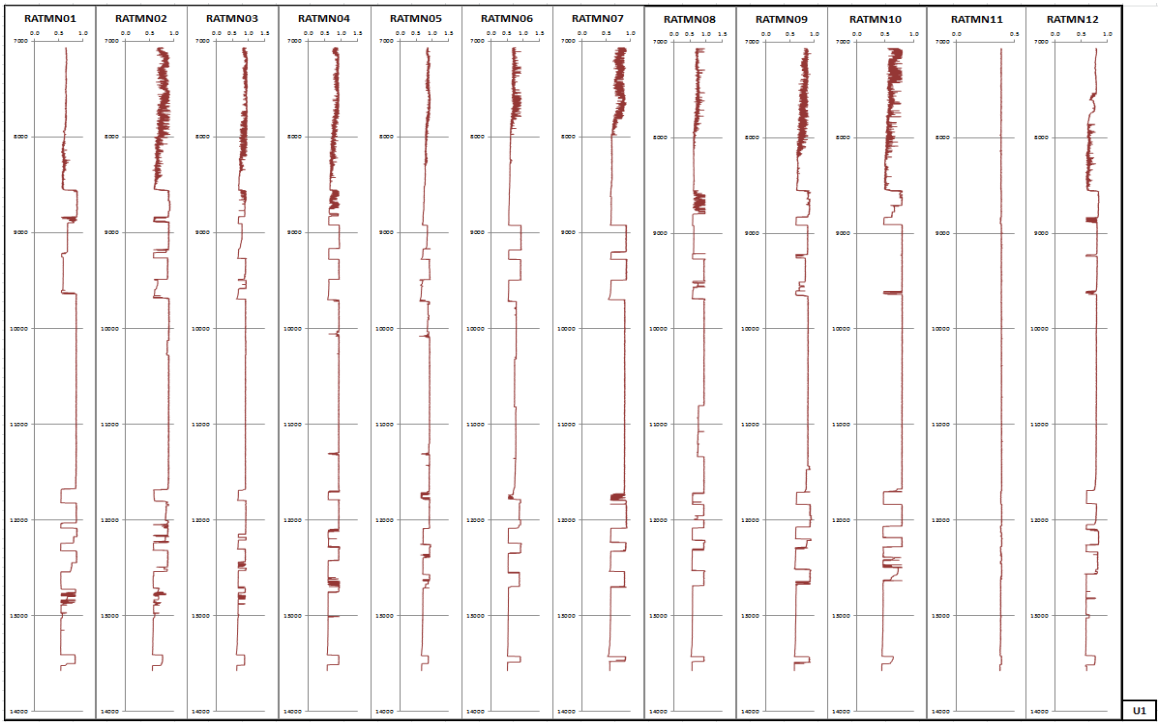

Appendix.10 RAT data of up 1 pass of well 2

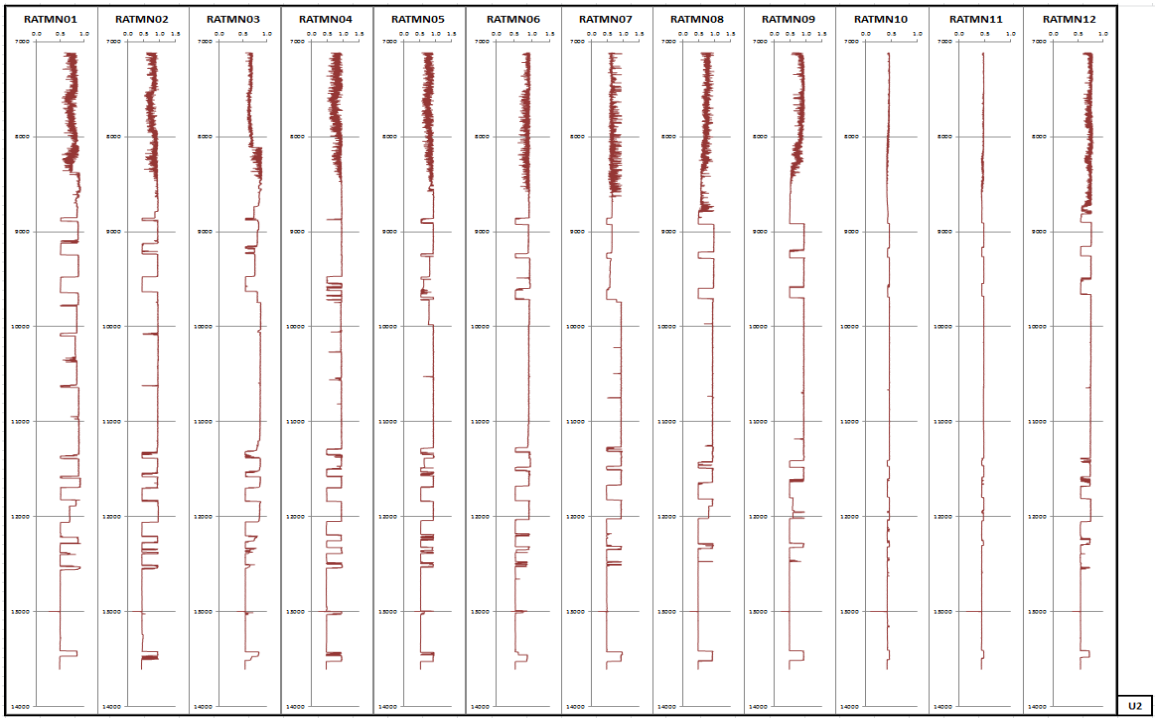

Appendix.11 RAT data of up 2 pass of well 2

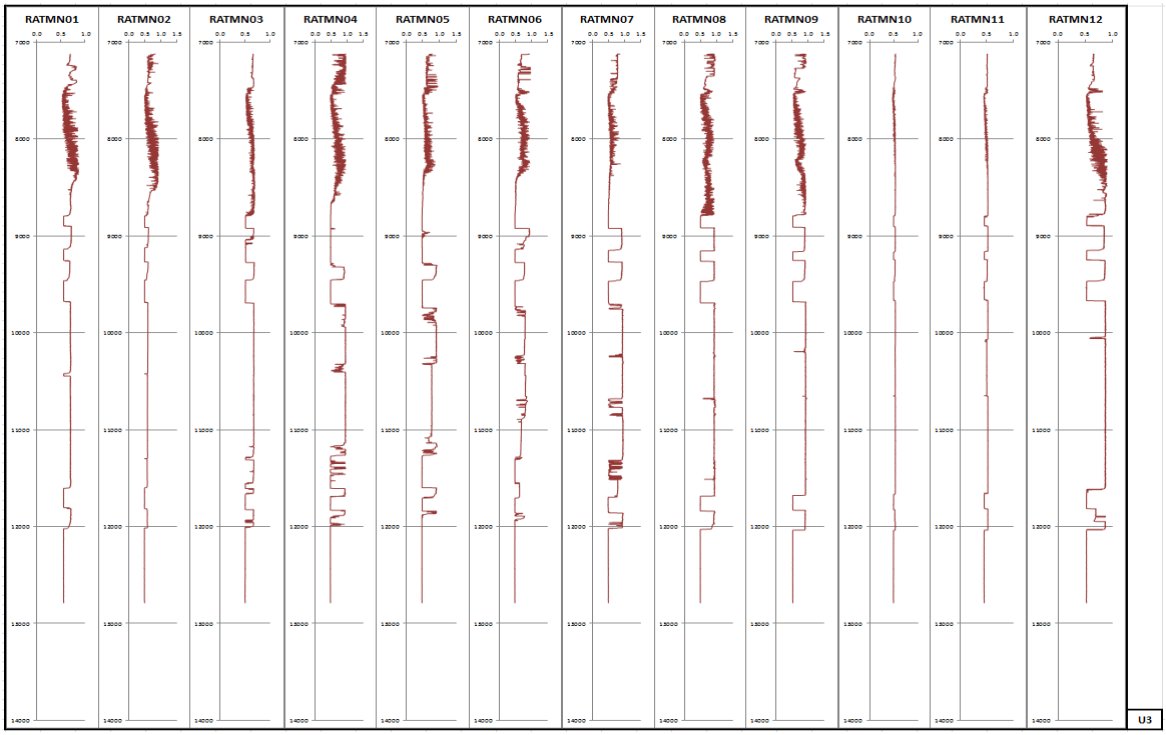

Appendix.12 RAT data of up 3 pass of well 2

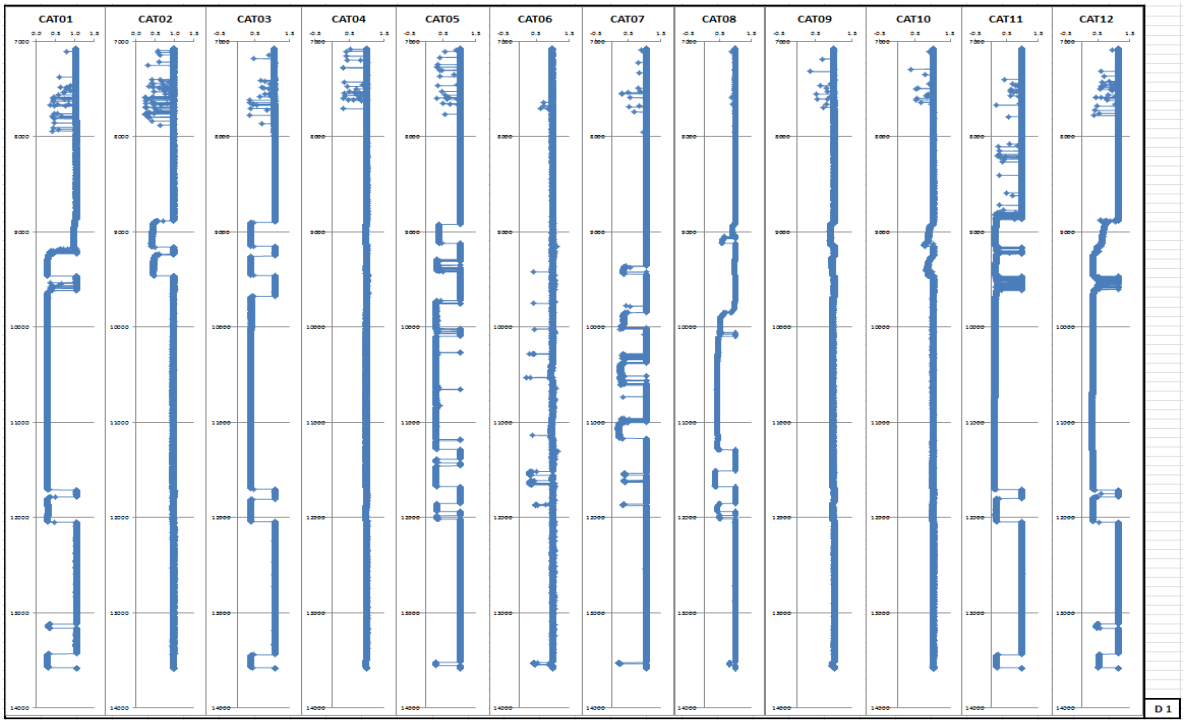

Appendix.13 CAT data of down 1 pass of well 2

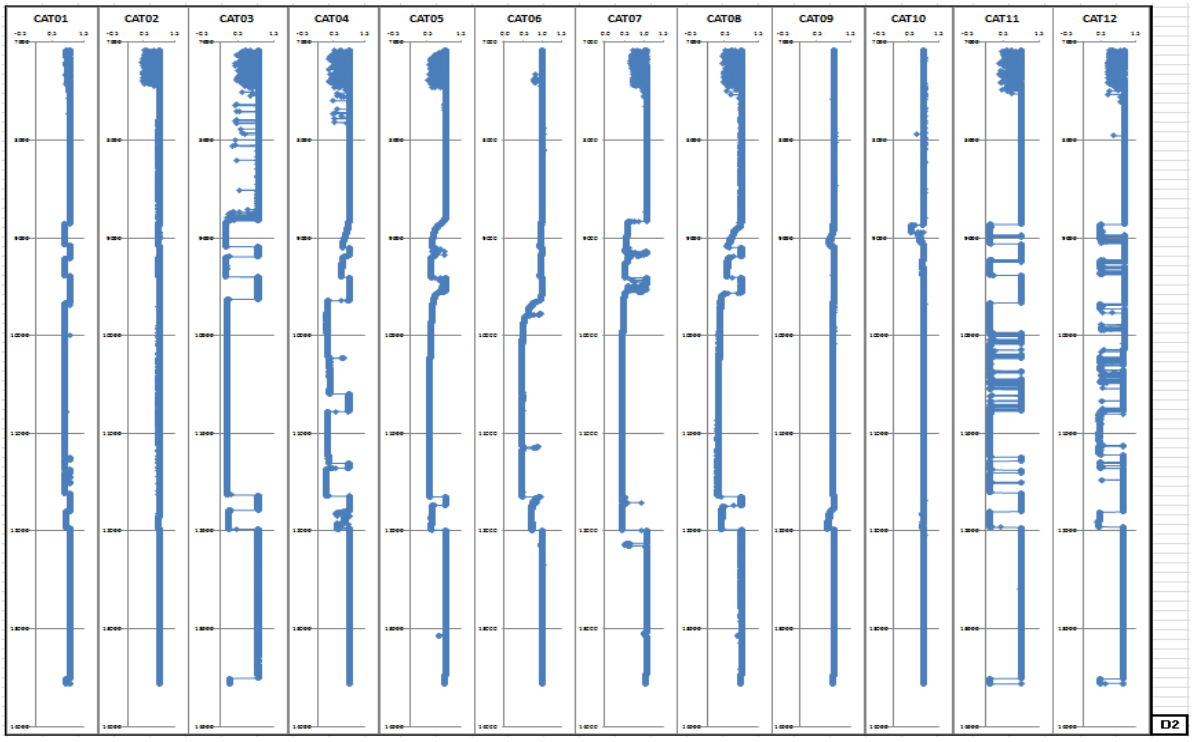

Appendix.14 CAT data of down 2 pass of well 2

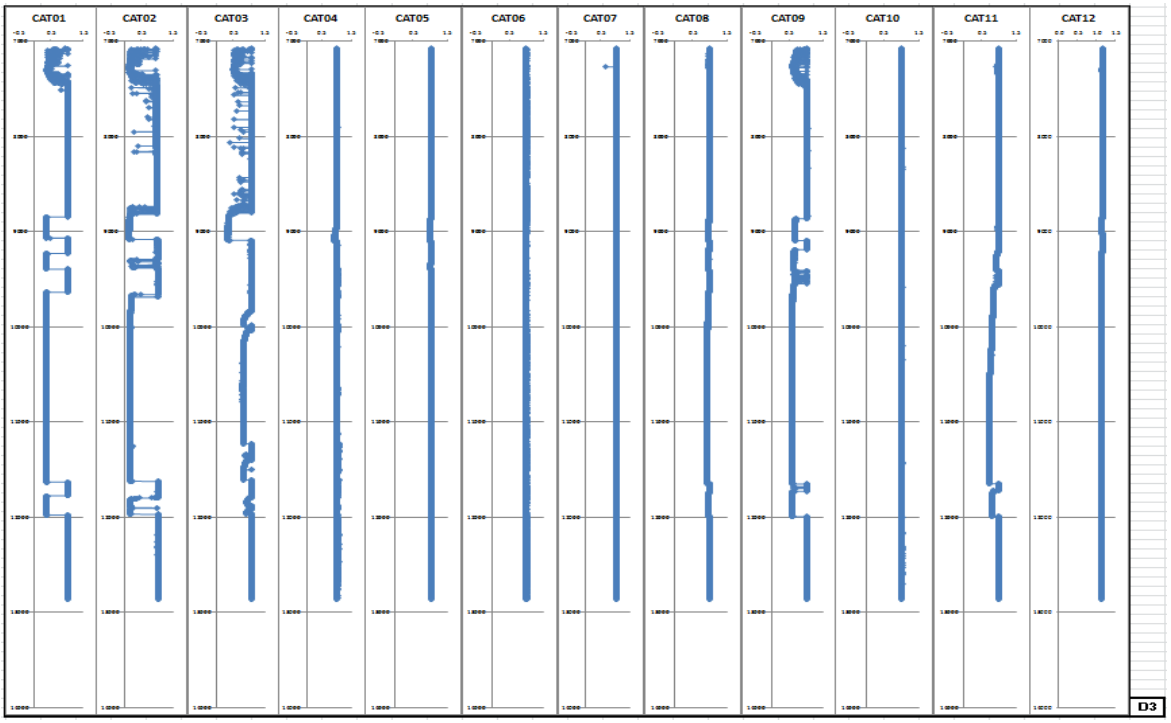

Appendix.15 CAT data of down 3 pass of well 2

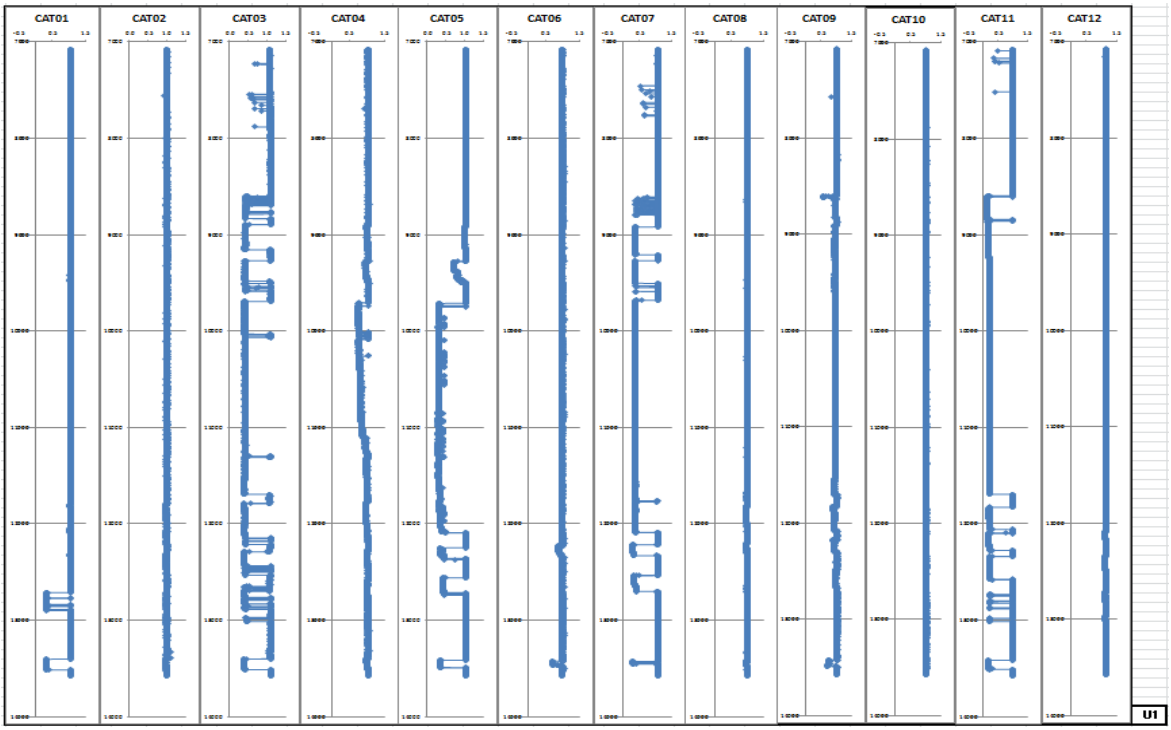

Appendix.16 CAT data of up 1 pass of well 2

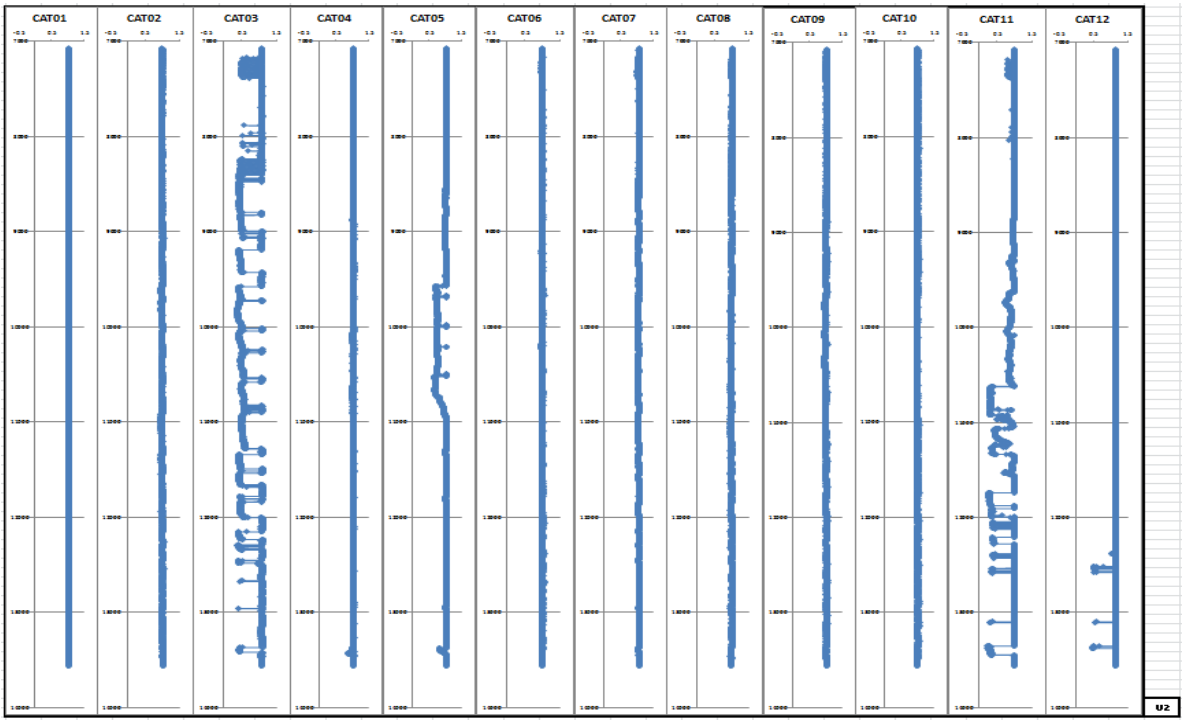

Appendix.17 CAT data of up 2 pass of well 2

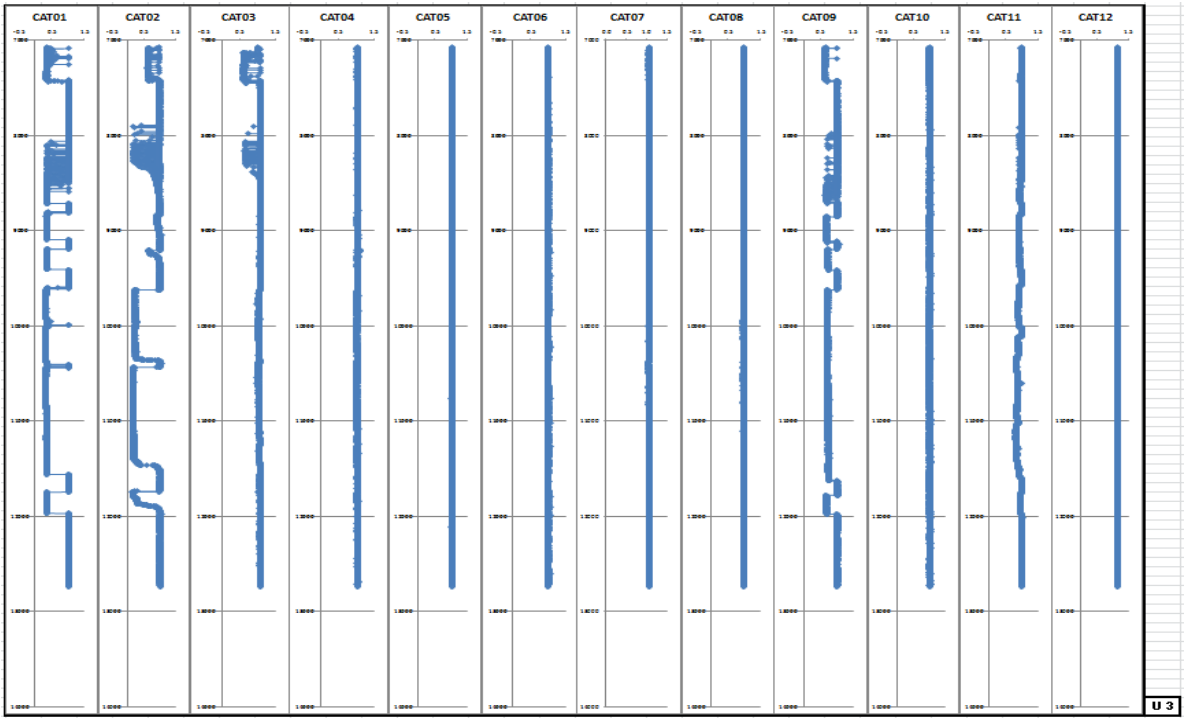

Appendix.18 CAT data of up 3 pass of well 2

TABLE 1 SAT DATA IN DOWN 1 OF WELL 2								
Station	DEPT	CFB	SPIN1	SPIN2	SPIN3	SPIN4	SPIN5	SPIN6
15	5	7.328	4.2189	4.2925	3.8278	4.0181	4.1065	4.2581
14	315	6.6175	4.1344	4.1425	3.5445	3.2916	3.6087	3.927
13	625	5.1929	7.4574	4.16	1.404	0	1.4114	2.1959
12	935	4.742	2.9174	2.9245	2.4954	2.8746	2.5297	2.9354
11	1245	5.2623	3.2361	3.1964	2.7373	2.9762	2.4609	3.1676
10	1545	5.0029	3.15	3.2688	2.6224	3.0086	2.3989	3.1329
9	1855	4.8028	2.8275	2.8821	2.4541	2.6756	2.1333	2.9061
8	2165	4.0867	2.4438	2.449	2.0747	2.5568	1.8471	2.4553
7	2465	3.762	2.2307	2.3316	1.8465	1.8183	1.7588	2.2424
6	2775	2.2126	2.8929	2.3051	1.3834	1.3743	1.3331	1.5743
5	3085	2.2353	2.3098	2.2069	1.2135	1.0397	0.9495	1.37
4	3395	2.0316	2.028	1.8562	1.2224	0.989	1.0123	1.372
3	3705	1.3571	1.4277	1.4352	0.9816	0.9482	0.9056	1.1335
2	4005	1.3006	1.1082	1.1668	0.7732	0.7653	0.8255	0.9201
1	4315	1.5177	1.2613	1.2219	0.8725	0.8637	0.81	1.0652

TABLE 2 SAT DATA IN DOWN 1 OF WELL 3								
Station	DEPT	CFB	SPIN1	SPIN2	SPIN3	SPIN4	SPIN5	SPIN6
	feet	Flow meter res/min						
1	4990	1.9009	0.8634	0.8011	0.5896	0.0509	0.5973	0.6708
2	4490	2.4038	1.4621	1.1662	0.9366	0.8011	1.0376	1.0534
3	4200	1.8628	1.7858	1.2408	1.1229	1.0402	1.1334	1.2941
4	3900	1.8862	1.6152	1.4976	1.1912	1.1390	1.2309	1.2409
5	3500	1.6092	2.4337	1.3831	0.7440	0.6524	0.8266	0.9540
6	3000	1.9096	3.2152	2.2175	1.1689	1.0773	1.1795	1.3255
7	2700	3.8259	2.1670	1.8536	1.6641	1.3680	1.8512	1.8732
8	2400	1.9434	4.3333	2.1029	0.4342	0.2708	0.7662	1.5448
9	2100	2.702	6.1312	1.9326	0.9599	0.8323	0.8337	2.3120
10	1800	2.6968	5.8354	1.9748	1.1502	1.0967	1.0994	1.8405
11	1500	2.9645	6.9238	4.3063	0.6192	0.5375	0.8909	1.5784
12	1190	3.1418	7.3157	2.1610	1.2355	0.2650	0.7998	3.2941
13	850	5.9851	3.4516	3.4623	3.2730	2.9395	3.0891	3.6212
14	550	4.5885	8.1662	4.4216	1.7286	1.3511	1.6116	2.9603
15	270	4.9058	11.1967	6.8719	-0.3242	-1.3257	0.7571	4.5581